STIC-ILL NPL

From: Sullivan, Daniel
Sent: Tuesday, October 22, 2002 2:19 PM
T : STIC-ILL
Subject: Request

Please send the following:

Nat Biotechnol. 1998 Sep;16(9):857-61.

Proc Natl Acad Sci U S A. 1997 Sep 30;94(20):10699-704.

Nat Med. 1998 Dec;4(12):1449-52.

Immunity. 1998 Jan;8(1):57-65.

J Immunol. 1999 May 1;162(9):5205-11.

J Immunol Methods. 1998 Mar 1;212(1):41-8.

Nat Biotechnol. 1998 May;16(5):440-3.

Cell. 1997 Jan 24;88(2):223-33.

Biochem Biophys Res Commun. 1993 Jul 30;194(2):876-84.

Proc Natl Acad Sci U S A. 1994 Jan 18;91(2):664-8.

J Cell Biol. 1995 Mar;128(5):919-27.

FEBS Lett. 1998 May 8;427(2):203-8.

Nat Med. 1999 Jan;5(1):29-33.

Thank you.

Daniel M. Sullivan
Examiner AU 1636
Room: 12D12
Mail Box: 11E12
Tel: 703-305-4448

09937837

Proc. Natl. Acad. Sci. USA
Vol. 94, pp. 10699–10704, September 1997
Cell Biology

Hypo-phosphorylation of the retinoblastoma protein (pRb) by cyclin D:Cdk4/6 complexes results in active pRb

SERGEI A. EZHEVSKY*, HIKARU NAGAHARA*, ADITA M. VOCERO-AKBANI, DAVID R. GIUS, MICHAEL C. WEI, AND STEVEN F. DOWDY†

Howard Hughes Medical Institute and Division of Molecular Oncology, Departments of Pathology and Medicine, Washington University School of Medicine, St. Louis, MO 63110

Communicated by Robert A. Weinberg, Whitehead Institute for Biomedical Research, Cambridge, MA, July 11, 1997 (received for review March 15, 1997)

ABSTRACT **In cycling cells, the retinoblastoma protein (pRb) is un- and/or hypo-phosphorylated in early G_1 and becomes hyper-phosphorylated in late G_1. The role of hypo-phosphorylation and identity of the relevant kinase(s) remains unknown. We show here that hypo-phosphorylated pRb associates with E2F *in vivo* and is therefore active. Increasing the intracellular concentration of the Cdk4/6 specific inhibitor $p15^{INK4b}$ by transforming growth factor β treatment of keratinocytes results in G_1 arrest and loss of hypo-phosphorylated pRb with an increase in unphosphorylated pRb. Conversely, $p15^{INK4b}$-independent transforming growth factor β-mediated G_1 arrest of hepatocellular carcinoma cells results in loss of Cdk2 kinase activity with continued Cdk6 kinase activity and pRb remains only hypo-phosphorylated. Introduction of the Cdk4/6 inhibitor $p16^{INK4a}$ protein into cells by fusion to a protein transduction domain also prevents pRb hypo-phosphorylation with an increase in unphosphorylated pRb. We conclude that cyclin D:Cdk4/6 complexes hypo-phosphorylate pRb in early G_1 allowing continued E2F binding.**

Progression of normal human cells into malignant ones involves the genetic alteration of several classes of genes, including protooncogenes (positive regulators), tumor suppressor genes (negative regulators), and DNA damage repair genes. Alteration of these genes appears to result in the loss of negative control of the late G_1 restriction point and, hence, uncontrolled proliferation (1–3). Recent work has pieced together an important G_1 phase cell cycle regulatory pathway involving the INK4 kinase inhibitors, $p15^{INK4b}$, $p16^{INK4a}$, $p18^{INK4c}$, and $p19^{INK4d}$, that negatively regulate complexes of cyclin D1, D2, and D3 bound to Cdk4 or Cdk6 (referred to herein as cyclin D:Cdk4/Cdk6 complexes) that phosphorylate the retinoblastoma tumor suppressor gene product (pRb) (2–4). pRb is an active transcriptional repressor when bound to transcription factors, such as members of the E2F family (5–10). Inactivation of pRb by hyper-phosphorylation in late G_1 phase causes the release of E2F, allowing transcription of genes important for DNA synthesis (11). Genetic alteration of this pathway, such as inactivation of either $p16^{INK4a}$ or pRb, or amplification of cyclin D1 or Cdk4, occurs in a large number of human malignancies (12). However, there appears to be no oncogenic selective advantage in mutating any two of these genes, suggesting the involvement of these genes in a linear pathway (3, 12). Therefore, it is critical to understand the exact physiological functioning of these gene products in this pathway.

pRb exists in three general forms: unphosphorylated pRb, present in G_0 cells and when pRb is newly synthesized; hypo-phosphorylated pRb, present in contact-inhibited cells and in early G_1; and hyper-phosphorylated pRb, that is inactive and present in late G_1, S, G_2, and M phases of cycling cells (13, 14). Thus in cycling cells, pRb alternates between a hypo-phosphorylated form present in early G_1 to a hyper-phosphorylated form after passage through the restriction point in late G_1 and continued through S, G_2, M, phases. The role of hypo-phosphorylated pRb in early G_1 has not been determined. In addition, the identity of the cyclin:Cdk complex(es) that converts unphosphorylated pRb to hypo-phosphorylated pRb has not yet been determined. Although the presence of cyclin D:Cdk4/6 complexes in early G_1 of cycling cells suggests that these complexes are likely candidates to hypo-phosphorylate pRb (14–16), reports based on overexpression systems and *in vitro* kinase assays have been interpreted to conclude that cyclin D:Cdk4/6 complexes are responsible for inactivating pRb by hyper-phosphorylation in late G_1. However, these overexpression conditions are not necessarily reflective of physiological levels and/or activities of cyclin D:Cdk4/6 complexes *in vivo*.

We chose to investigate the role of pRb hypo-phosphorylation and to identify the physiologically relevant cyclin:Cdk complex(es) utilizing pRb as an *in vivo* substrate. We manipulated the cellular environment by addition of transforming growth factor β (TGF-β) to cycling and contact inhibited cells and by a novel method of transducing full length $p16^{INK4a}$ protein directly into cells. We report here that cyclin D:Cdk4/6 complexes hypo-phosphorylate pRb and that hypo-phosphorylated pRb associates with E2F transcription factors.

MATERIALS AND METHODS

Cell Culture and Flow Cytometry Analysis. HaCaT human keratinocytes and HepG2 human hepatocellular carcinoma cells (ATCC) were maintained in α-minimal essential medium (MEM), and Jurkat T cells (ATCC) in RPMI 1640 medium plus 10% bovine fetal serum, penicillin, and streptomycin in 5% CO_2 at 37°C. TGF-β (R & D Systems) was added to a final concentration of 10 ng/ml to low density (2×10^6) or high density (8×10^6 cells per 10-cm dish) cultures. Cells were washed with PBS(−), fixed in −20°C 70% ethanol, and rehydrated with PBS(−) containing 0.1% BSA, RNase A (1 μg/ml), and propidium iodide (10 μg/ml) for 20 min prior to analysis on FACScan (Becton Dickinson). Cells (1×10^4) were counted and analyzed for cell cycle position using MODFIT LT software.

Labeling and Immunoprecipitations. Cells were labeled in the presence of TGF-β or TAT-p16 proteins for 5 hr with 3–5 mCi (1 Ci = 37 GBq) [^{32}P]orthophosphate (ICN) per 10-cm dish in 3.5 ml phosphate-free MEM supplemented with 10% dialyzed serum or with 250 μCi [^{35}S]methionine (NEN) in 3.5 ml methionine minus MEM with 10% dialyzed serum. Cells were lysed in situ by the addition of 1 ml of E1A lysis buffer [ELB: 50 mM Hepes, pH 7.2/250 mM NaCl/2 mM EDTA/0.1% Nonidet P-40/1 mM DTT/1 μg/ml aprotinin (Sigma)/1 μg/ml leupeptin (Sigma)/50

The publication costs of this article were defrayed in part by page charge payment. This article must therefore be hereby marked "*advertisement*" in accordance with 18 U.S.C. §1734 solely to indicate this fact.

Abbreviations: pRb, retinoblastoma protein; TGF-β, transforming growth factor β; GST, glutathione *S*-transferase; FACS, fluorescence-activated cell sorter; MEM, minimal essential medium.

*S.A.E. and H.N. contributed equally to this work.
†To whom reprint requests should be addressed.

μg/ml phenylmethylsulfonyl fluoride (Sigma)/0.5 mM NaP_2O_7/0.1 mM $NaVO_4$/5.0 mM NaF]. Cellular lysates were precleared with killed *Staphylococcus aureus* cells (Zymed), and pRb was immunoprecipitated by addition of 5 μl G99–549 anti-pRb antibodies (PharMingen) that recognize only the fast migrating, un- and hypo-phosphorylated forms of pRb (17) or 400 μl of anti-E2F-4 monoclonal antibody tissue culture supernatant (K. Moberg and J. A. Lees, Massachusetts Institute of Technology). A total of 0.5 μg polyclonal rabbit anti-Cdk6 and anti-p16 antibodies (Santa Cruz Biotechnology) were used under the same conditions. Immune complexes were collected on protein A Sepharose (Pharmacia), washed three times with 1 ml ELB, boiled in SDS buffer, resolved by SDS/PAGE, transferred to nitrocellulose filters, exposed to storage PhosphorImager screens (Kodak), and analyzed on a Storm PhosphorImager (Molecular Dynamics). For secondary immunoprecipitation, samples were cooled after boiling, diluted 1:30 with ELB, clarified of protein A Sepharose beads, and immunoprecipitated as described above using twice the amount of antibodies. Nitrocellulose filters after exposure to PhosphorImager screen were blocked in 5% nonfat milk in PBS(−)/0.2% Tween for 30 min and incubated with monoclonal anti-pRb antibodies G3–349 (PharMingen) for 2 hr, washed three times in PBS(−)/0.2% Tween, probed with secondary rabbit anti-mouse horseradish peroxidase-conjugated antibodies (The Jackson Laboratories) for 1 hr, washed, and developed by addition of ECL reagent (Amersham).

Kinase Assay and Reverse Transcription–PCR. Anti-Cdk2 or anti-Cdk6 immunoprecipitates were washed three times with ELB followed by final wash with kinase buffer (50 mM Hepes, pH 7.0/10 mM $MgCl_2$/1 mM DTT/1 μM unlabeled ATP) and suspended in 25 μl of kinase buffer plus 100 μCi of [γ-^{32}P]ATP (Amersham; 6,000 Ci/mmol) and 2 μg of freshly prepared (C. Sherr, personal communication) glutathione *S*-transferase (GST)–C′–pRb [residues 792–928 (18)] for Cdk6 kinase reaction, 10 μCi of [γ-^{32}P]ATP and 2 μg of histone H1 (Sigma) for Cdk2 kinase reaction. Reactions were incubated for 30 min at 30°C, stopped by addition of 2× SDS buffer, separated on SDS/PAGE, and analyzed by PhosphorImager screen (Kodak) exposure and analysis (Molecular Dynamics). Equal amounts of rabbit anti-mouse antibodies were used as negative controls.

cDNA synthesis from total RNA was performed using Perkin–Elmer RT-PCR kit with oligo(dT) primers. Amplification of p15 and cyclin E cDNA was performed in 50 μl reaction using 1 μg of cDNA and 20 pmol of p15-5′ (5′-GGAAGAGTGTCGTTAAGTTTACG-3′)/p15-3′ (5′-GTTGGCAGCCTTCATCGAAT-3′) primers and cyclin E-5′ (5′-GCAGGATCCAGATGAAGA-3′)/cyclin E-3′ (5′-CTTGTGTCGCCATATACCGGTC-3′) in 50 mM KCl, 10 mM Tris·HCl (pH 8.3), 200 μM dNTPs, 2 mM $MgCl_2$, 10% dimethyl sulfoxide, and 2.5 units *Taq* polymerase (Perkin–Elmer) for 35 cycles at 94°C for 1 min, 49°C for 1 min, and 72°C for 1 min. A final extension of 5 min was carried out at 72°C. PCR products were resolved on a 2% agarose gel and visualized with ethidium bromide staining.

Two-Dimensional Phosphopeptide Map Analysis. pRb was immunoprecipitated with G-99 antibodies from [^{32}P]orthophosphate-labeled control or TGF-β-treated HaCaT cells, separated by SDS/PAGE, and transferred to a nitrocellulose membrane, and the ^{32}P-labeled pRb band was visualized by ARG film (Kodak). The ^{32}P-labeled pRb section was digested with trypsin essentially as described (19). Phosphopeptides were loaded onto thin-layer cellulose (TLC) plates (Baker-flex/VWR Scientific), separated in the first dimension by electrophoresis on a Multiphor II (Pharmacia), followed by second dimension separation TLC for ≈7 hr in TLC buffer (75 ml *n*-butanol/50 ml pyridine/15 ml glacial acetic acid/60 ml H_2O). TGF-β and control samples were loaded based on approximately equal cpm of ^{32}P and not moles of pRb.

Plasmid Construction and Protein Expression. pTAT-p16 wild-type and mutant (R87P) vectors were generated by inserting a *NcoI–EcoRI* fragment from p16 cDNAs obtained from Parry and Peters (20) into the pTAT vector (A.V.A. and S.F.D., unpublished data). TAT-p16 proteins were purified by sonication of high-expressing BL21(DE3)pLysS (Novagen) cells from a 1 liter culture in 10 ml of buffer A (8 M urea/20 mM Hepes. pH 7.0/100 mM NaCl). Cellular lysates were resolved by centrifugation, loaded onto a 5 ml Ni-NTA column (Qiagen, Chatsworth, CA) in buffer A containing 20 mM imidazole and eluted by increasing imidazole concentration followed by dialysis against 20 mM Hepes/150 mM NaCl. Purified TAT-p16 protein was added to a final concentration of 100–300 nM to cells in complete medium. Fluorescein isothiocyanate-labeled TAT-p16 proteins were generated by fluorescein labeling (Pierce), followed by gel purification on a S-12 column attached to FPLC (Pharmacia).

RESULTS

Hypo-phosphorylated pRb Interacts with E2F *in Vivo*. To understand the physiological role of hypo-phosphorylated pRb, we first sought to determine if hypo-phosphorylated pRb associated with cellular transcription factors, such as members of the E2F family. Previous work has shown that pRb forms physical complexes with E2F (5–9); however, it has not been shown if E2F family members interact with un- and/or hypo-phosphorylated pRb. To do so, 1×10^8 cycling HaCaT cells were labeled with 100 mCi of [^{32}P]orthophosphate for 5 hr, E2F-4:pRb complexes were immunoprecipitated from cellular lysates with anti-E2F-4 antibodies (90% of total lysate) (21) and pRb (10% of total lysate) was immunoprecipitated by using conformation-dependent anti-pRb antibodies (G99) that selectively recognize un- and hypo-phosphorylated pRb that represent the fastest migrating form of pRb on SDS/PAGE (Fig. 1*A*, lane 2) (17). The primary immune complexes were washed, boiled, diluted, and re-immunoprecipitated with polyclonal anti-pRb antibodies. Secondary immune complexes were resolved by SDS/PAGE, transferred to a filter, and analyzed for ^{32}P content (Fig. 1*B*). To normalize for pRb protein levels between anti-E2F-4 and anti-pRb immunoprecipitates, the same filter was then probed with anti-pRb antibodies (Fig. 1*C*).

The coimmunoprecipitation of ^{32}P-labeled hypo-phosphorylated pRb with E2F-4 was readily detectable (Fig. 1*B*) whereas nonspecific control antibodies failed to immunoprecipitate pRb (Fig. 1*A*). Approximately 5% of the total amount of hypo-phosphorylated pRb found in anti-pRb immunoprecipitates was present in these E2F-4:pRb complexes (Fig. 1*C*). The ratio of ^{32}P content to pRb protein was not altered between direct anti-pRb immunoprecipitates and anti-E2F-4 coimmunoprecipitated pRb. This finding indicates that E2F-4 does not selectively interact with a subset of hypo-phosphorylated pRb forms containing a different molar ratio of phosphate per molecule of pRb compared with the total hypo-phosphorylated pRb forms. In addition, we detect ^{32}P-labeled hypo-phosphorylated pRb in complex with E2F-1 from HaCat, HT1080 fibrosarcoma cells, and leukemic Jurkat T cells (data not shown). Moreover, this finding is consistent with the observation that viral oncoproteins such as simian virus 40 T Ag and adenovirus E1A sequester ^{32}P-labeled hypo-phosphorylated pRb (ref. 22; unpublished data). These results demonstrate for the first time that hypo-phosphorylated pRb interacts with members of the E2F transcription factor family *in vivo* and support the notion that hypo-phosphorylated pRb is active.

pRb Hypo-phosphorylation Is Inhibited in TGF-β-Treated Cells. Given the importance of E2F:pRb complexes in regulation of G_1 to S phase cell cycle progression, we next sought to uncover the *in vivo* cyclin:Cdk complex(es) that hypo-phosphorylate pRb. TGF-β treatment of HaCaT keratinocytes has previously been shown to result in a G_1-specific arrest, induction of the Cdk4/6 inhibitor $p15^{INK4b}$, loss of hyper-phosphorylated pRb, and appearance of the fastest migrating

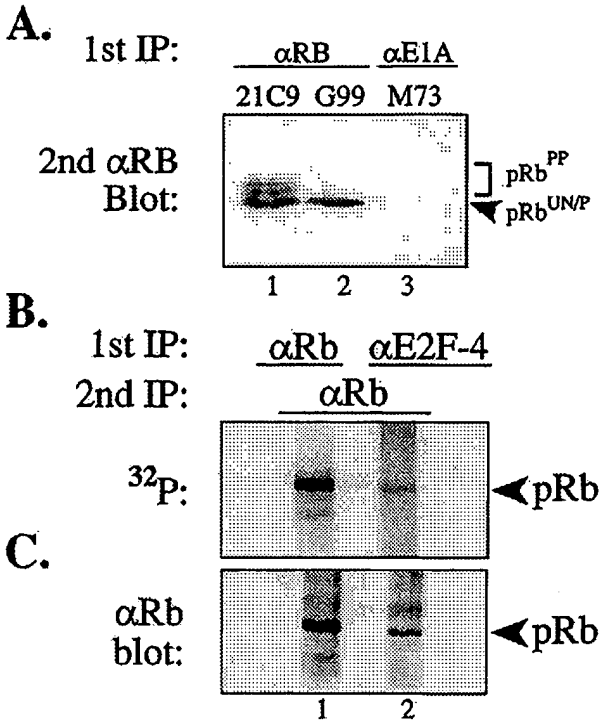

FIG. 1. E2F-4 interacts with hypo-phosphorylated pRb *in vivo*. (*A*) Antibody controls of immunoprecipitated and immunoblotted pRb from asynchronously cycling HaCat cells using 21C9 anti-pRb antibodies that recognize all forms of pRb (lane 1), conformational specific G99 anti-pRb antibodies that recognize only the fastest migrating, un- and hypo-phosphorylated pRb forms (lane 2), and nonspecific control M73 anti-E1A antibodies (lane 3). Please note the complete absence of immunoprecipitated pRb in lane 3 (HaCaT cells do not express E1A). (*B* and *C*) HaCaT human keratinocytes (1×10^8) were labeled with 100 mCi [^{32}P]orthophosphate and primary immunoprecipitation was performed with either anti-E2F-4 (90% of total lysate) or with G99 anti-pRb (10% of total lysate) antibodies followed by secondary immunoprecipitation with rabbit anti-pRb antibodies, resolved by SDS/PAGE, transferred to a filter, and analyzed for ^{32}P content (*B*) and then probed with anti-pRb antibodies to normalize for pRb protein levels (*C*).

form of pRb on SDS/PAGE (23, 24). However, due to the comigration of un- and hypo-phosphorylated pRb species as the fastest form on SDS/PAGE, the phosphorylation status of pRb in TGF-β-treated cells was not determined. Therefore, we treated cells with TGF-β, labeled pRb *in vivo* with [^{32}P]orthophosphate, and immunoprecipitated pRb with G99 conformation-dependent anti-pRb antibodies. This approach allowed for the comparison of pRb hypo-phosphorylation levels in untreated, proliferating control cells (that contain hypo- and hyper-phosphorylated forms of pRb) to cells treated with TGF-β. A gradual reduction in pRb hypo-phosphorylation and an accumulation of cells in G_1 was observed in untreated cultures with decreasing serum concentration (Fig. 2 *A* and *C*), consistent with the previously reported growth factor dependency of cyclin D1 expression (25). However, we observed a dramatic reduction in pRb hypo-phosphorylation in TGF-β-treated cells, whereas pRb protein levels remained relatively constant between TGF-β-treated and control cultures. These results suggested a TGF-β-dependent negative regulation of pRb hypo-phosphorylating cyclin:Cdk complex-(es).

To ascertain whether loss of pRb hypo-phosphorylation was specific to TGF-β signaling or merely an outcome of G_1 phase arrest, we labeled with [^{32}P]orthophosphate contact-inhibited, G_1-arrested HaCaT cells in 10% fetal bovine serum and immunoprecipitated pRb with G99 antibodies. Despite the equality of G_1-arrested HaCaT cells, a further reduction in pRb hypo-phosphorylation in TGF-β-treated cells compared with untreated control cells was observed (Fig. 2*D*). pRb contains 16 putative Cdk consensus phosphorylation sites (26). To examine whether TGF-β-dependent loss of pRb hypo-phosphorylation was restricted to a limited number of phosphorylation sites or if it was a global loss, immunoprecipitated pRb from ^{32}P-labeled lysates of TGF-β treated and control HaCaT cells were analyzed by two-dimensional tryptic phosphopeptide mapping (18). Comparison of the pRb phosphopeptide maps from control and TGF-β-treated HaCaT cells from cycling or contact inhibited cells revealed the apparent loss of a single tryptic phosphopeptide species (see arrow) in TGF-β-treated cells (Fig. 3; data not shown). In addition, the G99 immunoprecipitated pRb phosphopeptide maps from cycling and contact inhibited cells are nearly identical (data not shown). The loss of this single pRb tryptic phosphopeptide species, although interesting *per se*, cannot account for the observed overall reduction of pRb hypo-phosphorylation in TGF-β treated cells. Thus, loss of hypo-phosphorylated pRb is specific to TGF-β signaling and not merely an outcome of G_1 phase cell cycle arrest.

Direct Transduction of p16 Protein into Cells Inhibits pRb Hypo-phosphorylation. TGF-β treatment of responsive cells results in a wide array of effects (27); therefore, to focus on cyclin D:Cdk4/6 functioning *in vivo* and exclude additional TGF-β-regulated pathways, we chose to inactivate cyclin D:Cdk4/6 complexes directly by transduction of full-length $p16^{INK4a}$ protein into cells. Both $p15^{INK4b}$ and $p16^{INK4a}$ have previously been shown to bind specifically to Cdk4/6 (28). Several groups have

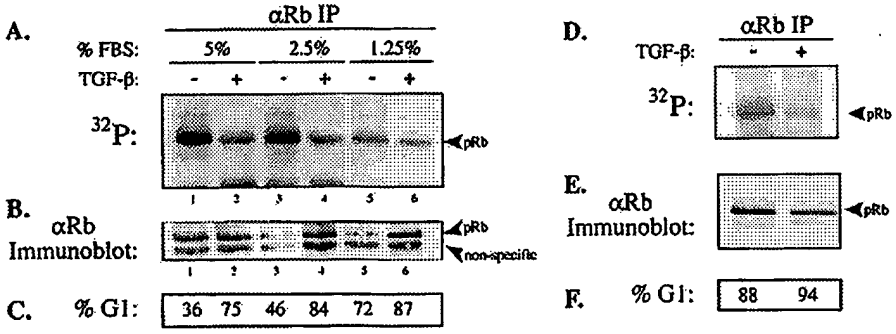

FIG. 2. TGF-β treatment of cycling and contact inhibited G_1-arrested HaCaT cells results in a reduction in the amount of *in vivo* hypo-phosphorylation of pRb. (*A–C*) Low-density asynchronous cycling and (*D–F*) high density contact-inhibited G_1-arrested HaCaT cells were treated with TGF-β for 36 hr, labeled with [^{32}P]orthophosphate, and immunoprecipitated with G99 anti-pRb antibodies that recognize the fastest migrating forms of pRb. Immune complexes were resolved by SDS/PAGE, transferred to a filter, and analyzed for ^{32}P content (*A* and *D*) and then the same filter was probed with anti-pRb antibodies (*B* and E) to normalize for pRb protein levels as indicated. (*C* and *F*) Percentage of cells in G_1 determined by FACS analysis.

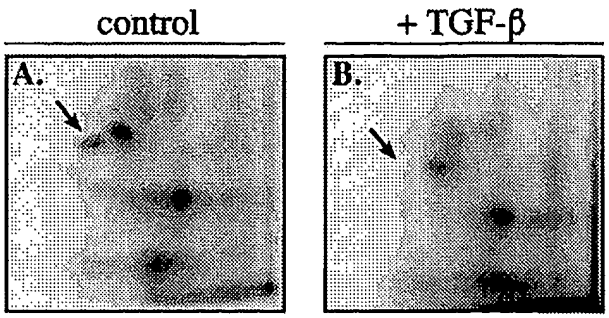

FIG. 3. TGF-β treatment of HaCaT cells results in the loss of a single tryptic phosphopeptide species detected on the remaining low level of hypo-phosphorylated pRb species. Two-dimensional tryptic phosphopeptide mapping of *in vivo* [^{32}P]orthophosphate-labeled pRb from G99 anti-pRb immune complexes from low density control (*A*) and TGF-β-treated (*B*) cultures of HaCaT cells. Arrow indicates the loss of a phosphorylated pRb tryptic peptide. TGF-β and control samples were loaded based on approximately equal cpm of ^{32}P and not moles of pRb

described the ability of HIV-1 Tat protein to transduce into cells by crossing the cell membrane (29, 30) and Fawell *et al.* (31) expanded on its utility. However, no in-frame expression system to produce and transduce full-length proteins utilizing this technology has been subsequently developed. Therefore, we constructed a bacterial expression vector containing the minimal 11 amino acid Tat protein transduction domain, named pTAT, and fused it in-frame to wild-type and mutant (R87P) human p16^{INK4a} cDNAs. pTAT-p16$^{WT/MUT}$ vectors allow for the production and purification of full-length TAT-p16 fusion proteins from bacteria (Fig. 4*A*). Addition of fluorescein isothiocyanate-conjugated wild-type and mutant TAT-p16 protein to p16(−) Jurkat T cells demonstrated the rapid entry into greater than 99% of cells, achieving maximum intracellular concentrations within 30 min as measured by fluorescence-activated cell sorter (FACS) analysis and confocal microscopy (unpublished data).

Transient transfection of proliferating cells with p16^{INK4a} encoding expression plasmids has been shown to result in G_1 arrest and loss of pRb hyper-phosphorylation (32–34). To test the ability of TAT-p16 protein to elicit a G_1-specific arrest, contact-inhibited HaCaT cells in 10% fetal bovine serum were replated at low density in the presence of 300 nM wild-type or mutant TAT-p16 protein and analyzed for cell cycle progression by FACS analysis at 30 hr postreplating (Fig. 4*B*). Untreated control and mutant TAT-p16 protein-treated HaCaT cells progressed into S phase; however, the addition of wild-type TAT-p16 protein to cells resulted in a G_1 arrest. To analyze the ability of wild-type TAT-p16 to bind Cdk6, we treated p16^{INK4a}(−) Jurkat T cells with either wild-type or mutant TAT-p16 and labeled with [^{35}S]methionine. Cellular lysates were prepared and TAT-p16 immunoprecipitated with anti-p16 antibodies followed by boiling in SDS buffer, dilution, and re-immunoprecipitation with anti-Cdk6 antibodies (Fig. 4*C*). The results showed that wild-type but not mutant TAT-p16 was capable of forming complexes with Cdk6 *in vivo*. Thus, bacterially produced wild-type and mutant TAT-p16 fusion proteins of ≈20 kDa can efficiently transduce into >99% of target cells and bind its cognate intracellular target.

To analyze the influence of accumulated TAT-p16 protein on pRb hypo-phosphorylation, contact inhibited HaCaT cells in 10% FBS were pretreated with wild-type or mutant TAT-p16 protein for 1 hr, followed by addition of [^{32}P]orthophosphate for 4 hr. pRb was immunoprecipitated from cellular lysates with G99 anti-pRb antibodies, resolved by SDS/PAGE, transferred to a filter, and analyzed for pRb ^{32}P content (Fig. 4*D*) and then normalized for pRb protein levels (Fig. 4*E*). Transduction of TAT-p16 wild-type protein into cells resulted in a dramatic reduction in pRb hypo-phosphorylation compared with cells treated with TAT-p16 mutant protein whereas pRb protein levels remained relatively constant. The further increased loss of pRb hypo-phosphorylation observed in cells transduced with TAT-p16 protein compared with TGF-β treatment likely reflects the ability to achieve a higher intracellular concentration of Cdk4/6 inhibitor TAT-p16 versus TGF-β induction of p15^{INK4b} protein. Taken together, these results support the notion that cyclin D:Cdk4/6 complexes hypo-phosphorylate pRb *in vivo*.

p15^{INK4b}-Independent, TGF-β-Mediated G_1 Arrest Does Not Alter pRb Hypo-phosphorylation. To further analyze the involvement of cyclin D:cdk4/6 complexes in hypo-phosphorylating pRb, we searched for a TGF-β-responsive cell line that arrests in G_1, inactivates Cdk2, but retains Cdk6 kinase activity. We hypothesized that in such a cell type, pRb would remain hypo-phosphorylated upon TGF-β treatment. To this end, we found that treatment of human HepG2 hepatocellular carcinoma cells

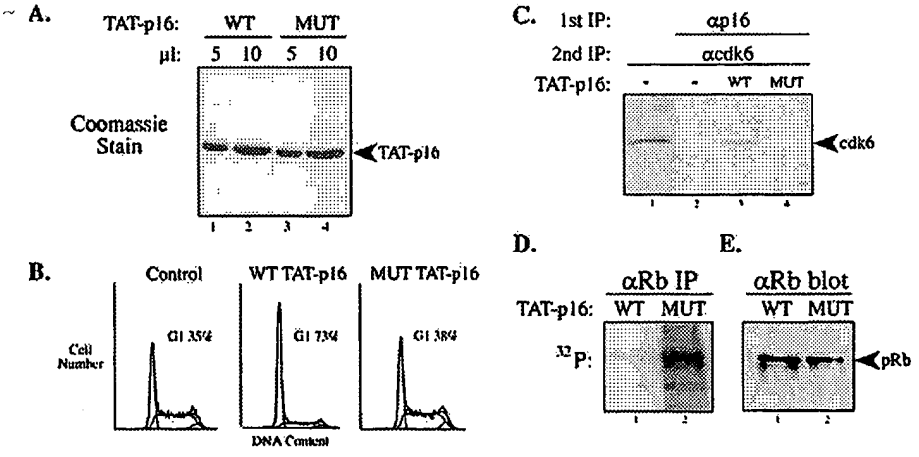

FIG. 4. Transduction of full-length p16 protein directly into cells results in loss of pRb hypo-phosphorylation. (*A*) Comparison of purity and concentration of bacterially expressed wild-type and mutant TAT-p16 purified fusion proteins by Coomassie blue staining. (*B*) High-density 36-hr contact-inhibited HaCaT cells were replated at low density and treated with either wild-type or mutant TAT-p16 protein at a final concentration of 300 nM. Cells were analyzed for cell cycle position by FACS at 30-hr postreplating. (*C*) p16^{INK4a}(−) Jurkat T cells were transduced with either wild-type or mutant TAT-p16 protein, labeled with [^{35}S]methionine, and immunoprecipitated with anti-p16 antibodies, then re-immunoprecipitated with anti-Cdk6 antibodies and resolved by SDS/PAGE. The position of Cdk6 is indicated. (*D* and *E*) Wild-type and mutant TAT-p16 proteins were added to high density 36-hr contact-inhibited HaCaT cells for 1 hr and then [^{32}P]orthophosphate labeled for 5 hr in the presence of TAT-p16. Cellular lysates were prepared and pRb was immunoprecipitated with G99 anti-pRb antibodies, transferred to a filter, exposed to a PhosphorImager screen for ^{32}P content (*D*), and then the same filter was probed with anti-pRb antibodies (*E*) to normalize for pRb protein levels.

with TGF-β results in a G_1 arrest as measured by propidium iodide staining and FACS analysis (Fig. 5*A*). Immunoblotting analysis of HepG2 cells treated with TGF-β revealed a loss of hyper-phosphorylated forms of pRb and the appearance of the fastest migrating pRb species, potentially consisting of both un- and hypo-phosphorylated forms (Fig. 5*B*).

We next measured the effect of TGF-β signaling on Cdk2 and Cdk6 kinase activity in HepG2 cells. Anti-Cdk2 and anti-Cdk6 immunoprecipitation-kinase assays were performed on cellular lysates from control and TGF-β-treated HepG2 cells using histone H1 or GST–C′ terminus Rb as *in vitro* substrates, respectively (Fig. 5 *C* and *D*). Cdk2 activity was markedly diminished following 48 hr of TGF-β treatment in agreement with loss of pRb hyper-phosphorylation. In contrast, Cdk6 activity was not affected by TGF-β signaling (Fig. 4*D*). The continued Cdk6 activity in TGF-β-treated HepG2 cells is consistent with the failure of these cells to induce the Cdk4/6-specific inhibitor $p15^{INK4b}$ as measured by anti-p15 immunoprecipitation and p15 reverse transcription–PCR analyses (H.N. & S.F.D, unpublished data).

Finally, we analyzed the effect of TGF-β signaling on pRb hypo-phosphorylation in HepG2 cells. HepG2 cells were treated with TGF-β for 48 hr and labeled with [^{32}P]orthophosphate, and pRb was immunoprecipitated from cellular lysates using G99 anti-pRb antibodies. The immune complexes were resolved by SDS/PAGE, transferred to a filter, and analyzed for pRb ^{32}P content and then pRb protein levels (Fig. 5 *E* and *F*). The results showed no change in pRb hypo-phosphorylation levels between TGF-β-treated and control HepG2 cells. In addition, no changes were observed between the tryptic phosphopeptide maps of hypo-phosphorylated pRb obtained from control or TGF-β-treated HepG2 cells (data not shown).

Thus, in HepG2 cells, TGF-β can effect a G_1 arrest by a previously unknown 15^{INK4b}-independent pathway that retains cyclin D:Cdk6 kinase activity but negatively regulates Cdk2 kinase activity and pRb remains hypo-phosphorylated. This observation is consistent with a role for cyclin D:Cdk4/6 complexes in only hypo-phosphorylating pRb and not in its hyper-phosphorylation.

DISCUSSION

The loss of negative regulation of G_1 phase cell cycle progression by inactivating mutation of $p16^{INK4a}$ or RB, or amplification of cyclin D1 or Cdk4 is a critical step in human oncogenesis and has therefore become an intense area of investigation. The previously held notion that cyclin D:Cdk4/6 complexes inactivate pRb by hyper-phosphorylation was based largely on cyclin D overexpression experiments, serum deprivation-addition experiments, and *in vitro* kinase assays using fragments of pRb as a substrate. Although these experiments are informative and reproducible, they do not appear to reflect the physiological roles of these complexes *in vivo*.

To solve this paradox and avoid potential artifacts from overexpression of activators like cyclin D1, we utilized pRb as an *in vivo* substrate and manipulated the activity of cyclin D:Cdk4/6 complex(es) by increasing the intracellular concentrations of cyclin D:Cdk4/6-specific inhibitors: $p15^{INK4b}$ through TGF-β treatment or p16 by direct transduction of TAT-p16 protein. We conclude that cyclin D:Cdk4/6 complexes only hypo-phosphorylate pRb and that hypo-phosphorylated pRb actively associates with E2F family members *in vivo* and is not "partially" inactive. Thus, given the role of cyclin D:Cdk4/6 complexes in hypo-phosphorylating pRb, we suggest it unlikely that cyclin D:Cdk4/6 complexes perform both the hypo-phosphorylation and the inactivating hyper-phosphorylation of pRb observed in late G_1 that likely occurs by cyclin E:Cdk2 complexes (Fig. 6). Indeed, the presence of only hypo-phosphorylated pRb in TGF-β-treated HepG2 cells that contain active cyclin D:Cdk6 complexes but inactive cyclin E:Cdk2 complexes further solidifies this notion. Furthermore, the idea that cyclin D:Cdk4/6 complexes hyper-phosphorylate pRb would predict that in p16(−) tumor cells should contain inappropriately, constitutively hyper-phosphorylated pRb; however, pRb continues to alternate between hypo-phosphorylated in early G_1 to hyper-phosphorylated forms in late G_1, S, G_2, and M phases in both p16(−) leukemic Jurkat T cells and p16(−) HT1080 fibrosarcoma cells, and continues to associate with E2F-1 and E2F-4 (ref. 14; unpublished observation).

Hypo-phosphorylation of pRb may serve the cell several purposes. First, hypo-phosphorylated pRb appears to be comprised of multiple isoforms that individually contain a combination of one or two phosphates on the 16 putative Cdk consensus sites (refs. 22, 35, and 36; unpublished observation). The generation of multiple isoforms of active hypo-phosphorylated pRb may target subsets of pRb to specific transcription factors and, hence, regulate specific promoters. As an example, *in vitro* mixing

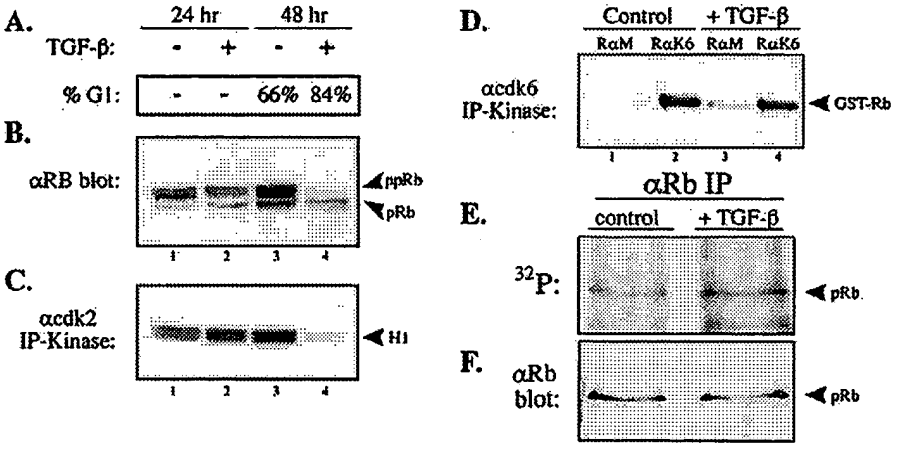

FIG. 5. HepG2 hepatocellular carcinoma cells that arrest in G_1 with TGF-β treatment in a $p15^{INK4b}$-independent manner do not alter the *in vivo* hypo-phosphorylation of pRb. (*A*) DNA content by FACS analysis of asynchronous HepG2 cells treated with TGF-β for 48 hr. (*B*) Anti-pRb immunoblot analysis of control and TGF-β treated HepG2 cellular lysates with anti-pRb antibodies at 24 and 48 hr. (*C*) Anti-cdk2 and (*D*) anti-cdk6 and control rabbit anti-mouse IgG (RαM) immunoprecipitation-kinase assay from control and TGF-β treated HepG2 lysates using histone H1 and GST–RB–C′ as *in vitro* substrates, respectively. (*E* and *F*) Asynchronous HepG2 cells were treated with TGF-β for 48 hr, labeled *in vivo* with [^{32}P]orthophosphate, and immunoprecipitated with G99 anti-pRb antibodies that recognize the fastest migrating forms of pRb. Immune complexes were resolved by SDS/PAGE, transferred to a filter, and analyzed for ^{32}P content (*E*) and then the same filter was probed with anti-pRb antibodies (*F*) to normalize for pRb protein levels as indicated.

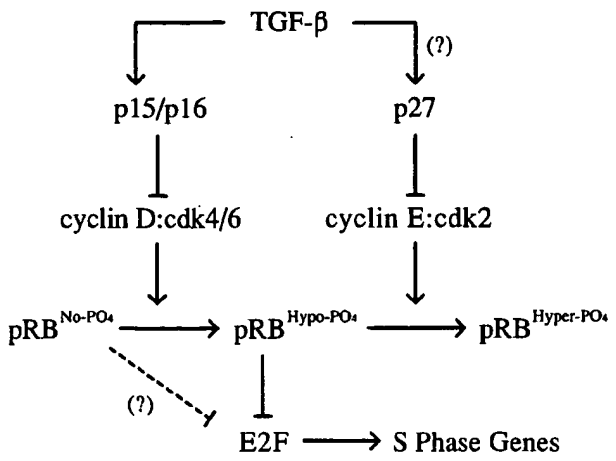

FIG. 6. Model of p15/16, cyclin D:Cdk4/6, pRb, E2F pathway. Cyclin D:Cdk4/6 complexes associate with pRbs pocket domain and then proceed to hypo-phosphorylate pRb in early G_1, and likely throughout the entire cell cycle. Hypo-phosphorylated pRb is active and binds to transcription factors, such as E2Fs. The initial hyper-phosphorylating inactivator of pRb is likely cyclin E:Cdk2 complexes expressed and activated at a position congruent with the passage through the late G_1 restriction point. Hyper-phosphorylation of pRb results in the dissociation of E2Fs and subsequent activation of E2F-specific promoters, such as genes required for DNA synthesis. The presence of unphosphorylated pRb in TGF-β-treated wild-type cells and the apparent requirement of cyclin E:cdk complexes for prior hypo-phosphorylated pRb as an *in vivo* substrate (37) suggests that TGF-β signaling drives the cell further into a G_0-like state.

experiments of baculovirus produced hypo-phosphorylated pRb with E1A or E2F-1:DP-1 complexes demonstrates that E1A interacts with a larger subset of hypo-phosphorylated pRb isoforms then E2F-1:DP-1 complexes do as ascertained by two-dimensional phosphopeptide mapping (R. R. Latek and S.F.D., unpublished observation). Second, prior pRb hypo-phosphorylation by cyclin D1 appears required for subsequent pRb hyper-phosphorylation by cyclin E as has been shown in genetically engineered yeast cells (37). Thus, TGF-β-dependent loss of pRb hypo-phosphorylation may further remove pRb from becoming a substrate for inactivating hyper-phosphorylation by cyclin E:Cdk2 and thereby potentiate a stronger TGF-β-dependent G_1 arrest, driving cells into G_0.

The data presented here demonstrate that cyclin D:Cdk4/6 complexes perform the hypo-phosphorylation of pRb *in vivo* and thereby leaves open the question of how p16 or cyclin D1 genetic alterations contribute to oncogenic progression. Three mutually inclusive hypo-theses emerge. First, dysregulated cyclin D:Cdk4/6 complexes may place an inappropriate key phosphate(s) on pRb that inactivates its transcriptional repression abilities while allowing continued E2F association. Second, dysregulated cyclin D:Cdk4/6 complexes may prevent the appearance of unphosphorylated pRb and thereby prohibit the cell from entering a true G_0 state, dependent on the presence of unphosphorylated pRb. Lastly, dysregulated cyclin D:Cdk4/6 complexes in tumors may lead to inappropriate phosphorylation of other (unknown) target protein substrates or activation of proteins by amplified cyclin D1 in a kinase-independent fashion (38). Future work on the types of pRb hypo-phosphorylated isoforms present in p16(−) or cyclin D1-amplified tumors compared with normal cells should serve to address these questions and help understand the involvement of these gene products in human oncogenesis.

We thank P. Boukamp and N. Fusenig (German Cancer Research Center) for HaCaT cells, K. Moberg and J. Lees (Massachusetts Institute of Technology) for anti-E2F-4 antibodies, G. Peters (Imperial Cancer Research Fund) for p16 cDNAs, M. Dustin (Washington University) for confocal microscopy, T. Dixon for clerical help, and O. Kanagawa and the members of the Dowdy lab for critical input. D.A.G. was supported by an ASTRO fellowship. M.C.W. was supported by a National Institutes of Health Medical Scientist Training Program Training Grant (5 T32 GM07200). S.F.D. is an Assistant Investigator of the Howard Hughes Medical Institute.

1. Pardee, A. B. (1974) *Proc. Natl. Acad. Sci. USA* **71,** 1286–1290.
2. Weinberg, R. A. (1995) *Cell* **81,** 323–330.
3. Sherr, C. J. (1996) *Science* **274,** 1672–1677.
4. Sherr, C. J. & Roberts, J. M. (1995) *Genes Dev.* **9,** 1149–1163.
5. Bagchi, S., Weinmann, R. & Raychaudhuri, P. (1991) *Cell* **65,** 1063–1072.
6. Chellappan, S. P., Hiebert, S., Mudryj, M., Horowitz, J. M. & Nevins, J. R. (1991) *Cell* **65,** 1053–1061.
7. Helin, K., Lees, J. A., Vidal, M., Dyson, N., Harlow, E. & Fattaey, A. (1992) *Cell* **70,** 337–350.
8. Kaelin, W., Jr., Krek, W., Sellers, W. R., DeCaprio, J. A., Ajchenbaum, F., Fuchs, C. S., Chittenden, T., Li, Y., Farnham, P. J., Blanar, M. A., Livingston, D. M. & Flemington, E. K. (1992) *Cell* **70,** 351–364.
9. Lees, E. M. & Harlow, E. (1993) *Mol. Cell. Biol.* **13,** 1194–1201.
10. Weintraub, S. J., Prater, C. A. & Dean, D. C. (1992) *Nature (London)* **358,** 259–261.
11. La Thangue, N. B. (1994) *Trends Biochem. Sci.* **19,** 108–114.
12. Hall, M. & Peters, G. (1996) *Adv. Cancer Res.* **68,** 67–108.
13. DeCaprio, J. A., Ludlow, J. W., Lynch, D., Furukawa, Y., Griffin, J., Piwnica-Worms, H., Huang, C. M. & Livingston, D. M. (1989) *Cell* **58,** 1085–1095.
14. Dowdy, S. F., VanDyk, G. H. & Schreiber (1997) in *Human Genome Methods*, ed. Adolph K. (CRC, Boca Raton, FL), in press.
15. Won, K. A., Xiong, Y., Beach, D. & Gilman, M. Z. (1992) *Proc. Natl. Acad. Sci. USA* **89,** 9910–9914.
16. Ajchenbaum, F., Ando, K., DeCaprio, J. A. & Griffin, J. D. (1993) *J. Biol. Chem.* **268,** 4113–4119.
17. Dunaief, J. L., Strober, B. E., Guha, S., Khavari, P. A., Alin, K., Luban, J., Begemann, M., Crabtree, G. R. & Goff, S. P. (1994) *Cell* **79,** 119–130.
18. Meyerson, M. & Harlow, E. (1994) *Mol. Cell. Biol.* **14,** 2077–2086.
19. Nagahara, H., Latek, R. R., Ezhevsky, S. A. and Dowdy, S. F. (1997) in *Methods in Molecular Biology: 2-D Protein Gel Electrophoresis Protocols*, ed. Link, A. J. (Humana, Clifton, NJ), in press.
20. Parry, D. & Peters, G. (1996) *Mol. Cell. Biol.* **16,** 3844–3852.
21. Moberg, K., Starz, M. A. & Lees, J. A. (1996) *Mol. Cell. Biol* **16,** 1436–1449.
22. Mittnacht, S., Lees, J. A., Desai, D., Harlow, E., Morgan, D. O. & Weinberg, R. A. (1994) *EMBO J.* **13,** 118–127.
23. Hannon, G. J. & Beach, D. (1994) *Nature (London)* **371,** 257–261.
24. Reynisdottir, I., Polyak, K., Iavarone, A. & Massague, J. (1995) *Genes Dev.* **9,** 1831–1845.
25. Matsushime, H., Quelle, D. E., Shurtleff, S. A., Shibuya, M., Sherr, C. J. & Kato, J. Y. (1994) *Mol. Cell. Biol.* **14,** 2066–2076.
26. Lee, W. H., Shew, J. Y., Hong, F. D., Sery, T. W., Donoso, L. A., Young, L. J., Bookstein, R. & Lee, E. Y. (1987) *Nature (London)* **329,** 642–645.
27. Polyak, K. (1996) *Biochim. Biophys. Acta* **1242,** 185–199.
28. Hall, M., Bates, S. & Peters, G. (1995) *Oncogene* **11,** 1581–1588.
29. Green, M. & Loewenstein, P. M. (1988) *Cell* **55,** 1179–1188.
30. Frankel, A. D. & Pabo, C. O. (1988) *Cell* **55,** 1189–1193.
31. Fawell, S., Seery, J., Daikh, Y., Moore, C., Chen, L. L., Pepinsky, B. & Barsoum, J. (1994) *Proc. Natl. Acad. Sci USA* **91,** 664–668.
32. Koh, J., Enders, G. H., Dynlacht, B. D. & Harlow, E. (1995) *Nature (London)* **375,** 506–510.
33. Lukas, J., Parry, D., Aagaard, L., Mann, D. J., Bartkova, J., Strauss, M., Peters, G. & Bartek, J. (1995) *Nature (London)* **375,** 503–506.
34. Medema, R. H., Herrera, R. E., Lam, F. & Weinberg, R. A. (1995) *Proc. Natl. Acad. Sci USA* **92,** 6289–6293.
35. Mittnacht, S. & Weinberg, R. A. (1991) *Cell* **65,** 381–393.
36. Dowdy, S. F., Hinds, P. W., Louie, K., Reed, S. I., Arnold, A. & Weinberg, R. A. (1993) *Cell* **73,** 499–511.
37. Hatakeyama, M., Brill, J. A., Fink, G. R. & Weinberg, R. A. (1994) *Genes Dev.* **8,** 1759–1771.
38. Zwijsen, R. M., Wientjens, E., Klompmaker, R., van der Sman, J., Bernards, R. & Michalides, R. J. (1997) *Cell* **88,** 405–415.

STIC-ILL

QP501.F4
Adams

Fr m: Sullivan, Daniel
Sent: Tuesday, October 22, 2002 2:19 PM
To: STIC-ILL
Subject: Request

Please send the following:

Nat Biotechnol. 1998 Sep;16(9):857-61.

Proc Natl Acad Sci U S A. 1997 Sep 30;94(20):10699-704.

Nat Med. 1998 Dec;4(12):1449-52.

Immunity. 1998 Jan;8(1):57-65.

J Immunol. 1999 May 1;162(9):5205-11.

J Immunol Methods. 1998 Mar 1;212(1):41-8.

Nat Biotechnol. 1998 May;16(5):440-3.

Cell. 1997 Jan 24;88(2):223-33.

Biochem Biophys Res Commun. 1993 Jul 30;194(2):876-84.

Proc Natl Acad Sci U S A. 1994 Jan 18;91(2):664-8.

J Cell Biol. 1995 Mar;128(5):919-27.

FEBS Lett. 1998 May 8;427(2):203-8.

Nat Med. 1999 Jan;5(1):29-33.

Thank you.

Daniel M. Sullivan
Examiner AU 1636
Room: 12D12
Mail Box: 11E12
Tel: 703-305-4448

09937837

FEBS 20192

FEBS Letters 427 (1998) 203–208

Features of replicative senescence induced by direct addition of antennapedia-p16^{INK4A} fusion protein to human diploid fibroblasts

Daishiro Kato[a,b], Kazuhiro Miyazawa[a,b], Marugarida Ruas[c], Maria Starborg[c], Ikuo Wada[b], Takahiro Oka[b], Toshiyuki Sakai[a], Gordon Peters[c], Eiji Hara[a,*]

[a] *Department of Preventive Medicine, Kyoto Prefectural University of Medicine, Kawaramachi-Hirokoji, Kamigyo-ku, Kyoto 602-0841, Japan*
[b] *Second Department of Surgery, Kyoto Prefectural University of Medicine, Kawaramachi-Hirokoji, Kamigyo-ku, Kyoto 602-0841, Japan*
[c] *Imperial Cancer Research Fund Laboratories, 44 Lincoln's Inn Fields, London WC2A 3PX, UK*

Received 23 March 1998

Abstract The p16^{INK4A} cyclin-dependent kinase (Cdk) inhibitor is now recognized as a major tumor suppressor that is inactivated by a variety of mechanisms in a wide range of human cancers. It is also implicated in the mechanisms underlying replicative senescence since p16^{INK4A} RNA and protein accumulate as cells approach their proscribed limit of population doublings in tissue culture. To obtain further evidence of its role in senescence, we have sought ways of overexpressing p16^{INK4A} in primary human diploid fibroblasts (HDF). To circumvent the low transfection efficiency of primary cells we have exploited a recombinant form of the full-length p16^{INK4A} protein fused to a 16 amino acid peptide from the *Drosophila* antennapedia protein. This peptide has the capacity to cross both cytoplasmic and nuclear membranes allowing the direct introduction of the active protein to primary cells. Here, we show that antennapedia-tagged wild-type p16^{INK4A} protein, but not a functionally compromised tumor-specific variant, causes G1 arrest in early passage HDFs by inhibiting the phosphorylation of the retinoblastoma protein. Significantly, the arrested cells display several phenotypic features that are considered characteristic of senescent cells. These data support a role for p16^{INK4A} in replicative senescence and raise the possibility of using the antennapedia-tagged protein therapeutically.

Key words: p16^{INK4A}; Antennapedia; Cellular senescence; Cell cycle

1. Introduction

p16^{INK4A} (also known as the tumor suppressor gene, MTS1) is a G1 specific cell cycle inhibitor which negatively regulates the cyclin-dependent kinases (Cdk) Cdk4 and Cdk6 by binding in competition with D-type cyclins [1–3]. Cdk4 and Cdk6 kinases are important for the phosphorylation and inactivation of the retinoblastoma susceptibility gene product, pRB [4,5]. Therefore, p16^{INK4A} plays a critical role in blocking the G1/S transition by preventing the inactivation of pRB [6,7]. There are at present two different classes of Cdk inhibitors (CdkI): the KIP/CIP family (p21, p27 and p57) and the INK4 family (p15^{INK4B}, p16^{INK4A}, p18^{INK4C} and p19^{INK4D}) [8]. In contrast to the KIP/CIP family, which inhibits a broad range of Cdks, the INK4 family is specific for Cdk4 and Cdk6. The INK4 proteins, which contains four or more ankyrin repeats, are expressed in distinct tissue-specific patterns, suggesting that, although they have essentially indistinguishable biochemical properties [9], they are not strictly redundant [10]. Among these CdkI genes, p16^{INK4A} is the only gene which is frequently mutated and/or deleted in human cancer cell lines and, to lesser extent, in primary tumors [2,3,11].

Cellular senescence is considered to be genetically programmed and induced by the expression of dominant-acting growth suppressor(s) [12,13]. There are also evidence that tumorigenesis entails, at least in part, mechanisms that permit cells to escape senescence [13]. Therefore, cellular senescence could be a mechanism for tumor suppression. Several lines of evidence suggest that two well-recognized tumor suppressors, the p53 and Rb genes, appear to be critical for the senescence of human diploid fibroblasts (HDF) [14,15]. In the case of Rb, the growth suppressive (unphosphorylated) form of the protein accumulates in senescent cells, due to the loss of phosphorylation by Cdks [16]. The observation that p16^{INK4A} levels rise as cells senesce suggest that p16^{INK4A} may be an inducer of cellular senescence, whose expression may record the number of cell divisions completed and subsequently promote cell cycle exit [17,18]. Moreover, mice carrying a targeted deletion of the p16^{INK4A} locus develop spontaneous tumors at an early age and mouse primary embryo fibroblasts (MEF) grow for multiple passages apparently without undergoing senescence or passing through a characteristic crisis [19]. These data suggest the possibility that p16^{INK4A} acts as a tumor suppressor by the induction of cellular senescence. This may explain why the p16^{INK4A} gene, but not other cdkI genes, is frequently mutated in immortalized cancer cell lines. However, a recent report by Kamijo and coworkers argues for this possibility [20]. They report that much of the phenotype ascribed to p16^{INK4A}-null mice may in fact be attributed to disruption of p19^{ARF}, an alternative spliced transcript whose product is completely distinct from p16^{INK4A} in its sequence and functional properties [20].

To resolve this controversy, we have introduced a large amount of p16^{INK4A} protein into early passage HDF and determined whether cells acquire a senescent phenotype. Because of the low transfection efficiency typically achieved in primary cells, we employed a technique to deliver the p16^{INK4A} protein into the cells. A 16 amino acid peptide derived from the third antennapedia homeodomain (ant tag) has been shown to allow the intracellular delivery of antisense oligonucleotides or biologically active peptides to the nucleus [21]. Interestingly, this ant-tagged peptide is efficiently translocated through the plasma membrane and into the nucleus in the absence of

*Corresponding author. Fax: (81) (75) 241-0792.
E-mail: ehara@basic.kpu-m.ac.jp

Abbreviations: Cdk, cyclin-dependent kinase; HDF, human diploid fibroblasts; Rb, retinoblastoma susceptibility gene; MEF, mouse embryo fibroblasts; β-gal, β-galactosidase; HTLV-1, human T-cell leukemia virus type 1; GST, glutathione *S*-transferase

PII S0014-5793(98)00426-8

exogenously provided energy [21]. This kind of carrier peptide has recently become a popular tool for introducing synthetic peptides into cells [22–24]. However, synthetic peptides retain only a part of the function of an intact protein. In order to retain the full range of $p16^{INK4A}$ biological activities, we engineered an intact $p16^{INK4A}$ protein with an ant tag at its N-terminus. The modified $p16^{INK4A}$ gene was cloned into a bacterial expression vector. A histidine tag (his tag) was added to the N-terminus of the ant-tagged $p16^{INK4A}$ protein, which allows the one step purification of the bacterially expressed recombinant protein [25].

In the present study, we introduced the bacterially expressed ant-tagged full-sized $p16^{INK4A}$ protein into early passage HDF by simple addition of the recombinant protein to the tissue culture medium. The ant-tagged $p16^{INK4A}$ protein efficiently inhibited cell growth. This growth inhibition was accompanied by a change in phenotype resembling that of senescent cells. These data support a role for $p16^{INK4A}$ in cellular senescence, and raise the possibility that recombinant penetrative full-sized proteins prepared in bacteria offer a novel therapeutic approach towards tumor suppression.

2. Materials and methods

2.1. Plasmid construction and preparation of recombinant protein

The DNA fragment encoding the 16 amino acids (aa 43–58) of the antennapedia homeodomain (ant tag) was cloned into the multi-cloning site of the his tag expression plasmid, pRSETa (Invitrogen), then the DNA fragment encoding wild-type or R87P mutant of the $p16^{INK4A}$ coding region was subcloned under the ant tag. The recombinant proteins were expressed in 4 l of *Escherichia coli* BL21 (DE3) pLysE culture and recovered from the soluble fraction of bacterial lysate using non-denaturing condition for his-tagged protein purification [25]. The purified proteins were dialyzed to remove imidazole and concentrated by the Selective absorbent (ATTO #AB-1100 Japan).

2.2. In vitro binding assay

[^{35}S]Methionine-labeled Cdk2 and Cdk4 were synthesized by coupled transcription and translation of plasmid DNAs using TNT expression system (Promega). Samples (5 μl) of reaction products were mixed with 50 ng of bacterially expressed his-tagged $p16^{INK4A}$ proteins and incubated for 30 min at 30°C. After the incubation, the mixtures were analyzed as described previously [26].

2.3. Cell culture and [^{3}H]thymidine labeling

Normal human diploid fibroblasts, TIG-3 (obtained from the Japanese Cancer Research Resources Bank, Tokyo, Japan) were cultured as described previously [17]. Sparse cells ($1–5\times10^3$ per cm^2) were given 10 μCi of [^{3}H]thymidine (Amersham TRK686) per ml for 2 h, washed in phosphate-buffered saline (PBS), rinsed twice in methanol, and processed for autoradiography, as described [27].

2.4. β-Galactosidase (β-gal) staining

Cells were washed in PBS, fixed for 3–5 min in 2% formaldehyde/0.2% glutaraldehyde, washed, and incubated at 37°C (no CO_2) with freshly prepared senescence-associated β-Gal (SA-β-Gal) staining solution [27]: 1 mg of 5-bromo-4-chloro-3-indolyl β-D-galactoside (X-Gal) per ml/40 mM citric acid/40 mM sodium phosphate, pH 6.0/5 mM potassium ferrocyanide/5 mM potassium ferricyanide/150 mM NaCl/2 mM $MgCl_2$. Staining was evident in 2–6 h and maximal in 16 h.

3. Results

3.1. Construction of antennapedia-tagged $p16^{INK4A}$ proteins

Published results have established that the chemical conjugation of an antennapedia homeodomain-derived peptide extending from amino acids 43–58 facilitated the cellular internalization of synthetic peptides [21], such as 20 amino acids derived from $p16^{INK4A}$ [22], p53 [23] and DP-1 [24]. However, 20 amino acid residues rarely if ever exhibit all the activities of an intact protein. This is especially true in the case of proteins that have multi-functional domains, or whose functional domain is unknown. Therefore, it would be of interest to develop a system to produce penetrative full-sized proteins. For this purpose, we constructed a recombinant full-size $p16^{INK4A}$ protein with a his tag and ant tag at its N-terminus (H-ant-p16wt). The recombinant protein was expressed and purified from bacteria using non-denaturing conditions and Ni-affinity chromatography, as described by Hoffmann and Roeder [25]. To more critically examine the internalization and biological activities of the ant-tagged $p16^{INK4A}$ protein, we also constructed two other recombinant his-tagged $p16^{INK4A}$ proteins: one lacks the ant tag (H-p16wt), and the other (H-ant-p16mut) has a loss-of-function mutation (R87P) in the $p16^{INK4A}$ coding region associated with familial melanoma [26]. Because the $p16^{INK4A}$ protein tends to aggregate, we used only freshly prepared proteins for all experiments. The quality of the freshly prepared $p16^{INK4A}$ proteins (H-p16wt, H-ant-p16wt and H-ant-p16mut) was confirmed by SDS-PAGE stained by Coomassie brilliant blue, and also by Western blotting using an anti-his-tag antibody (Fig. 1A) and anti-$p16^{INK4A}$ antibody (data not shown). To confirm the activity of these recombinant proteins, an in vitro binding assay was performed using in vitro translated Cdk2 and Cdk4 proteins. Equal amounts of $p16^{INK4A}$ proteins were mixed with ^{35}S-labeled Cdk2 or Cdk4 proteins, immunoprecipitated with the anti-his-tag antibody, and analyzed by SDS-PAGE. Although the amount of input Cdk2 protein is slightly less than that of Cdk4 (Fig. 1B), both wild-type $p16^{INK4A}$ proteins (H-p16wt and H-ant-p16wt) specifically bound to Cdk4 and

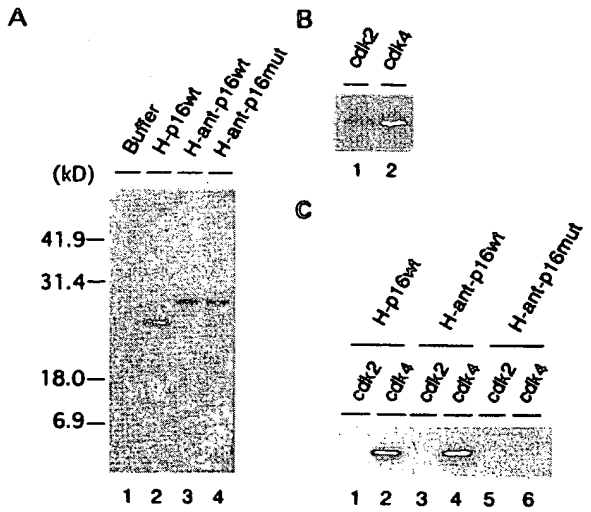

Fig. 1. The activity of recombinant $p16^{INK4A}$ protein. Histidine-tagged $p16^{INK4A}$ proteins prepared from bacteria were fractionated by SDS-PAGE in a 12% gel and immunoblotted with a monoclonal antibody against the his tag. Immune complexes were detected with enhanced chemiluminescence (ECL) (Amersham) (A). Human Cdk2 and Cdk4 were radiolabeled by in vitro translation (B) and mixed with 50 ng of bacterially expressed his-tagged $p16^{INK4A}$ proteins, H-p16wt (C, lanes 1, 2), H-ant-p16wt (C, lanes 3, 4), H-ant-p16mut (lanes 5, 6). The samples were analyzed either directly (B) or after immunoprecipitation with anti-$p16^{INK4A}$ antibody (C). The proteins were then fractionated by SDS-PAGE in a 12% gel and the labeled Cdks were detected by autoradiography.

did not bind to Cdk2 (Fig. 1C, lanes 1–4). The R87P mutant (H-ant-p16mut) did not bind either Cdk2 or Cdk4, as expected (Fig. 1C, lanes 5, 6) and previously reported [26]. These data demonstrated that bacterially expressed wild-type $p16^{INK4A}$ proteins have the expected binding activity in vitro.

3.2. Internalization of recombinant proteins

To confirm intracellular penetration, three his-tagged $p16^{INK4A}$ proteins were added to the tissue culture medium of early passage (35PDL) human diploid fibroblasts, TIG-3 (20 μM final concentration). The presence of roughly equal amounts of his-tagged proteins in the tissue culture medium was confirmed by Western blotting (Fig. 2A). Twelve hours after addition, the cells were harvested, nuclear extracts were prepared to avoid the contamination of the $p16^{INK4A}$ protein stuck to the surface of the cell membrane and subjected to Western blotting using anti-his-tag antibody (Fig. 2B). Both ant-tagged proteins (H-ant-p16wt and H-ant-p16mut) were detected in the nuclear extracts (Fig. 2B, lanes 3, 4). However, the his-tagged p16 protein lacking the ant tag (H-p16wt) was not observed in the nuclear extracts (Fig. 2B, lane 2). We observed the same results using the anti-$p16^{INK4A}$ antibody to detect the proteins in the nuclear extracts (data not shown). These data demonstrated that the ant tag efficiently delivered full-length $p16^{INK4A}$ protein to the nucleus, whereas the his-tagged $p16^{INK4A}$ protein by itself did not translocate to the nucleus. These results were confirmed by immunofluorescence (data not shown). Therefore, the ant tag is essential for the internalization of $p16^{INK4A}$ protein.

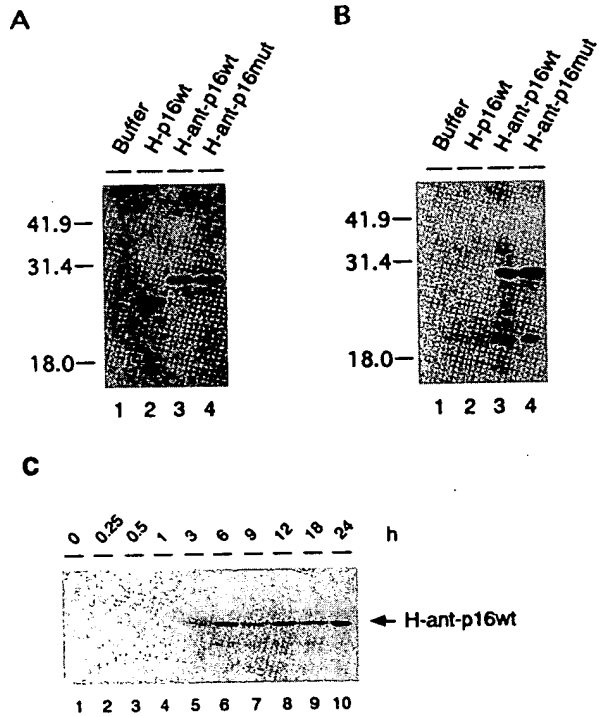

Fig. 2. Internalization of recombinant $p16^{INK4A}$ proteins. Recombinant $p16^{INK4A}$ proteins (20 μM concentration) were added to the tissue culture medium of early passage (35PDL) TIG-3 cells (lane 1: mock, buffer alone; lane 2: H-p16wt; lane 3: H-ant-p16wt; lane 4: H-antp16mut). 5 μl of each medium was subjected to SDS-PAGE in a 12% gel and immunoblotted with monoclonal antibody against the his tag. Immune complexes were detected with ECL (A). Nuclear extracts prepared from the treated cells were fractionated by SDS-PAGE in a 12% gel and immunoblotted with monoclonal antibody against the his tag. Immune complexes were detected with ECL (B). Nuclear extracts were prepared from the cells treated with H-ant-p16wt for 0, 15, and 30 min, 1, 3, 6, 9, 12, 18 and 24 h. Each sample was subjected to Western blotting using the monoclonal antibody against $p16^{INK4A}$ (C).

We next determined the time required for internalization of the ant-tagged $p16^{INK4A}$ protein. Early passage (35PDL) TIG-3 cells were incubated with 20 μM H-ant-p16wt protein for 15 and 30 min, 1, 3, 6, 9, 12, 18 and 24 h. Nuclear extracts were then prepared and subjected to Western blotting using the anti-$p16^{INK4A}$ antibody. As shown in Fig. 2C, H-ant-p16wt protein was detectable in the nucleus within 3 h, reaching a maximal level in 6 h. These results suggest that it takes about 3 h for the internalization of ant-tagged $p16^{INK4A}$ protein in TIG-3 cells.

3.3. Cell growth inhibition by antennapedia-tagged $p16^{INK4A}$ protein

$p16^{INK4A}$ is thought to be a strong inhibitor of the G1/S transition. Therefore, we have examined the activity of ant-tagged $p16^{INK4A}$ proteins by [^{3}H]thymidine incorporation, which measures DNA synthesis. Asynchronously growing early passage (35PDL) TIG-3 cells were incubated with recombinant $p16^{INK4A}$ proteins (20 μM) for 48 h, and [^{3}H]thymidine incorporation during 2 h was then measured as described in Section 2. As shown in Fig. 3A,B, an equal percentage (approximately 40%) of cells incorporated [^{3}H]thymidine in mock (Fig. 3A) and H-p16wt (Fig. 3B) treated cells. This result is consistent with our earlier results showing that H-p16wt does not internalize (Fig. 2B, lane 2) and thus the his-tagged $p16^{INK4A}$ protein has little or no effect on S phase entry in TIG-3 cells. The same experiment was done using penetrative $p16^{INK4A}$ proteins (H-ant-p16wt, H-ant-p16mut). Although the H-ant-p16mut protein slightly inhibited [^{3}H]thymidine incorporation (Fig. 3D), these effects were negligible. However, Fig. 3C clearly shows that the both number of cells and [^{3}H]thymidine incorporation are significantly decreased in H-ant-p16wt treated cells. Similar results were obtained using synchronized TIG-3 cells (Fig. 3E–H). Serum-starved TIG-3 cells reached mid-S-phase around 16 h after the addition of serum. Therefore, serum-starved early passage TIG-3 cells were treated with recombinant proteins for 2 days, then the cells were stimulated with serum for 16 h and examined for [^{3}H]thymidine incorporation. [^{3}H]Thymidine incorporation was drastically reduced in H-ant-p16wt treated cells. In synchronized cells, a lower concentration (10 μM) of H-ant-p16wt protein was sufficient to inhibit cell growth (Fig. 3G). These data clearly suggest that we can deliver a functional full length $p16^{INK4A}$ protein into cells and inhibit S-phase entry by using the antennapedia tag.

3.4. Inhibition of pRB phosphorylation and induction of a phenotype resembling that of cellular senescence by antennapedia-tagged $p16^{INK4A}$ protein

To confirm that the $p16^{INK4A}$-induced growth arrest (Fig. 3C,G) is caused by inhibition of Cdk activity, we examined the phosphorylation status of pRB. Serum-starved early passage TIG-3 cells were treated with either H-ant-p16wt or H-ant-p16mut for 2 days, then the cells were stimulated with serum. At the indicated times thereafter, whole cell extracts were prepared and subjected to Western blotting using an anti-RB antibody. As shown in Fig. 4, pRB is phosphoryl-

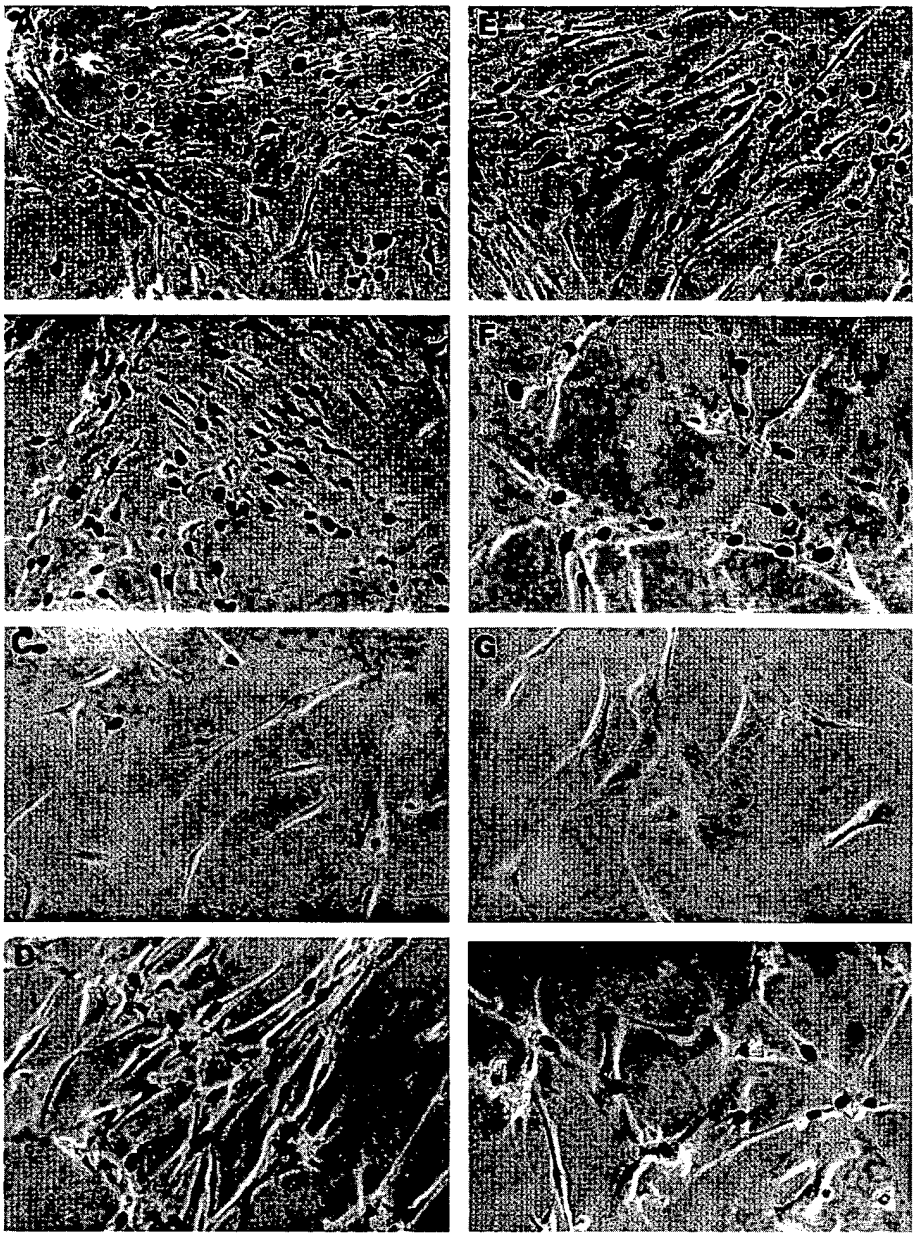

Fig. 3. [^{3}H]Thymidine incorporation. Asynchronously growing early passage TIG-3 cells were incubated with a buffer (A), H-p16wt (B), H-ant-p16wt (C), H-ant-p16mut (D) for 48 h and labeled with [^{3}H]thymidine. Serum-starved TIG-3 cells were incubated with just a buffer (E), H-p16wt (F), H-ant-p16wt (G), H-ant-p16mut (H) for 48 h and labeled with [^{3}H]thymidine. Cells were fixed and visualized by autoradiogaphy.

ated following serum stimulation in cells treated (Fig. 4, lanes 5, 6) or untreated (data not shown) with the H-ant-p16mut protein. However, pRB phosphorylation was not observed in cells treated with the H-ant-p16wt protein (Fig. 4, lanes 2, 3). These data confirm that the penetrative $p16^{INK4A}$ protein inhibits cell growth by inhibiting pRB phosphorylation.

We next asked whether cells arrested by the H-ant-p16wt protein displayed any characteristics of senescent cells. Asynchronously growing early passage TIG-3 cells were incubated with H-ant-p16wt protein (20 μM) for 7 days. The cells were then fixed and stained for SA-β-gal, described to be expressed by senescent cells [27]. The enlarged growth-arrested cells gave a positive staining reaction (Fig. 5B). As described elsewhere, untreated early passage TIG-3 cells were negative for SA-β-gal staining (Fig. 5A), but late passage TIG-3 cells, which had lost growth potential, showed significant SA-β-gal activity (Fig. 5C) [27–29]. Moreover, the treated cells do not return to the cell cycle, but rather remain growth arrested and retain the SA-β-gal activity even 7 days after removal of ant-tagged $p16^{INK4A}$ protein (Fig. 5D). We confirmed that the H-ant-p16wt protein level decreased to the background level by 7 days after removal of the protein from tissue culture medium (data not shown). This result is consistent with several other reports suggesting that cellular senescence is an essentially irreversible phenotype [13,28]. These results demonstrated that ectopic expression of $p16^{INK4A}$ protein in early passage human primary fibroblasts caused the rapid appearance of three phenotypes associated with senescence: growth arrest in G1, accumulation of unphosphorylated pRB, and expression of SA-β-gal.

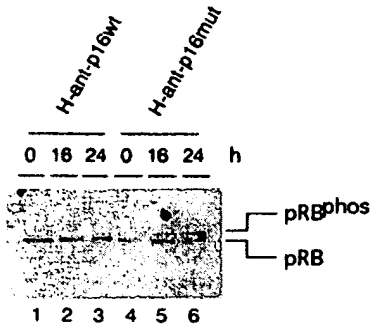

Fig. 4. Inhibition of phosphorylation of pRB by penetrative $p16^{INK4A}$ protein. Serum-starved early passage TIG-3 cells were incubated with H-ant-p16wt (lanes 1–3) or H-ant-p16mut (lanes 4–6) for 48 h, then cells were treated with a medium containing 20% fetal bovine serum with ant-tagged p16 proteins. Cell lysates were fractionated by SDS-PAGE in a 8% gel and immunoblotted with monoclonal antibody against pRB. Immune complexes were detected with ECL. pRB: hypophosphorylated form of RB protein. pRB^{phos}: hyperphosphorylated form of RB protein.

4. Discussion

In this study, we delivered the full-length $p16^{INK4A}$ protein into primary human cells using an antennapedia tag. We developed a system to produce a penetrative $p16^{INK4A}$ protein by a one step purification from bacteria. Because bacterially expressed his-tagged $p16^{INK4A}$ proteins aggregate in a relatively short time, all experiments were done using freshly prepared recombinant $p16^{INK4A}$ proteins. Antennapedia-tagged $p16^{INK4A}$ proteins, both wild-type and mutant $p16^{INK4A}$, were efficiently taken up by cells from the tissue culture medium (Fig. 2). In general, the transfection efficiency of plasmid DNA into primary cells is extremely low. Therefore, antennapedia-tagged proteins provide many advantages for biological studies and clinical applications.

Addition of the antennapedia-tagged wild-type $p16^{INK4A}$ protein into the tissue culture medium efficiently inhibited the phosphorylation of pRB (Fig. 4) and caused growth arrest (Fig. 3) of early passage human diploid fibroblasts. This was not the case when we added the antennapedia-tagged mutant $p16^{INK4A}$ protein, or the simply histidine-tagged $p16^{INK4A}$ protein. Moreover, the morphological change that occurred when $p16^{INK4A}$ protein was introduced into the early passage cells led us to investigate the possibility that these early passage cells might have been induced to enter senescence. Introduction of the $p16^{INK4A}$ protein induced cell enlargement and the inability to proliferate at subconfluent cell densities despite the presence of serum. Using SA-β-gal staining, which has been shown to be expressed by senescent cells [27], we subsequently showed a high degree of SA-β-gal in the early passage TIG-3 cells treated with antennapedia-tagged $p16^{INK4A}$ protein (Fig. 5B). These results are consistent with recent reports suggesting that $p16^{INK4A}$ might be a key factor in the block to phosphorylation of the RB protein in senescent cells. The level of $p16^{INK4A}$ protein is very low in presenescent growing cells [30], but is elevated at the end of the replicative life span [17,18]. In addition, targeted deletion of the $p16^{INK4A}$ gene causes many type of cancer in mice, and primary fibroblasts from these mice do not senesce in culture [19]. Although another cdk inhibitor, $p21^{CIP1/WAF1/SDI1}$, is also known as a gene whose expression is increased as cells senesce [31], it is rarely mutated in cancer cell lines. Moreover, $p21^{CIP1/WAF1/SDI1}$ knock out mice develop normally and primary fibroblasts from these mice senesce as expected [32,33]. Therefore, expression of $p21^{CIP1/WAF1/SDI1}$ may not be required for the senescence of fibroblasts [34]. Although $p19^{ARF}$, an alternative reading frame protein encoded by the INK4A locus, seems also to be important for cell senescence [20], our data presented here, and the evidence that overexpression of $p16^{INK4A}$ induces cell senescence in human glioma cells [35], strongly suggest that $p16^{INK4A}$ plays an important role in cel-

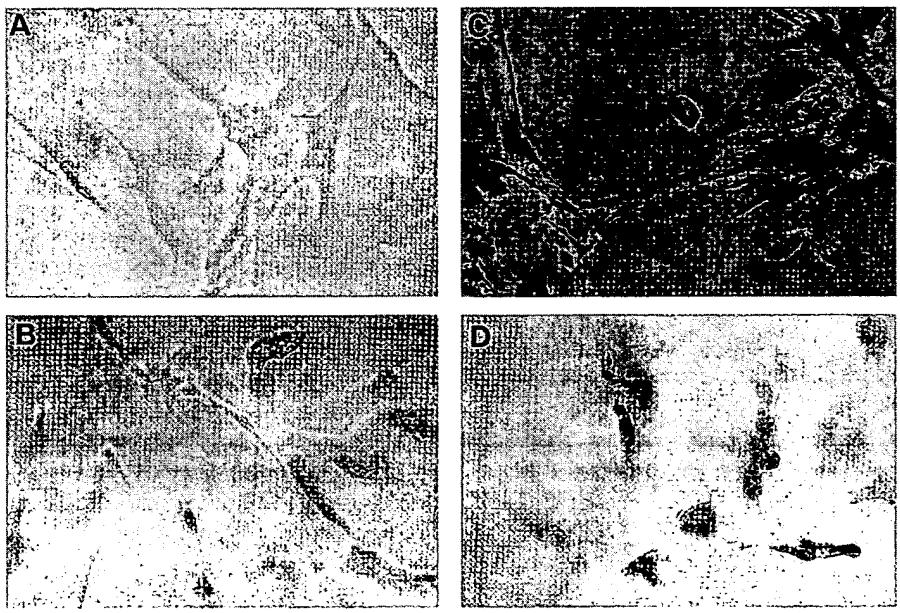

Fig. 5. Senescence-associated β-galactosidase (SA-β-gal) staining of TIG-3 cells. Early passage TIG-3 cells were treated with buffer (mock) (A) or H-ant-p16wt (B) for 7 days and stained for SA-β-gal activity. As positive control, late passage TIG-3 cells (C) were stained for SA-β-gal activity. H-ant-p16wt treated cells were washed with PBS and incubated with the tissue culture medium without H-ant-p16wt protein for a further 7 days. Then cells were stained for SA-β-gal activity (D).

lular senescence. Furthermore, recent findings suggest that the functional inactivation of $p16^{INK4A}$ by Tax oncoprotein of human T-cell leukemia virus type 1 (HTLV-1) through protein-protein interaction contributes to cellular immortalization induced by HTLV-1 infection [36]. Taking these evidences together, $p16^{INK4A}$ acts as a tumor suppressor which prevent cellular immortalization.

Our work presented here also raises the possibility that bacterially produced penetrative tumor suppressor proteins offer a novel therapeutic approach towards controlling aberrant cellular proliferation. In our hands, histidine-tagged $p16^{INK4A}$ protein prepared from bacteria aggregate rapidly, specially at high concentrations. Therefore, we are currently trying further application to increase the solubility of antennapedia-tagged $p16^{INK4A}$ protein. Our recent observation suggests that glutathione *S*-transferase (GST)-tagged $p16^{INK4A}$ protein is much more soluble than his-tagged $p16^{INK4A}$ protein and is efficiently internalized by the addition of the ant tag (Kato and Hara, unpublished results).

Acknowledgements: We are grateful to our many colleagues, particularly Naoya Tanida, Naoko Ohtani-Fujita, Takeshi Nakamura and Shinichiro Niwa for their technical support and valuable suggestions. We are also indebted to Michel Volovitch for his useful information about the antennapedia tag. Judith Campisi provided helpful comments on the manuscript. This work was supported by Sumitomo Electric Industries and the Imperial Cancer Research Fund.

References

[1] Serrano, M., Hannon, G.J. and Beach, D. (1993) Nature 366, 704–707.
[2] Kamb, A., Gruis, N.A., Weaver-Feldhaus, J., Liu, Q., Harshman, K., Tavtigian, S.V., Stockert, E., Day, R.S., Johnson, B.E. and Skolnick, M.H. (1994) Science 264, 436–440.
[3] Nobori, T., Miura, K., Wu, D.J., Lois, A., Takabayashi, K. and Carson, D.A. (1994) Nature 368, 753–756.
[4] Sherr, C.J. (1994) Cell 79, 551–555.
[5] Hunter, T. and Pines, J. (1994) Cell 79, 573–582.
[6] Lukas, J., Parry, D., Aagaard, L., Mann, D.J., Bartkova, J., Strauss, M., Peters, G. and Bartek, J. (1995) Nature 375, 503–506.
[7] Koh, J., Enders, G.H., Dynlacht, B.D. and Harlow, E. (1995) Nature 351, 506–510.
[8] Sherr, C.J. and Roberts, J.M. (1995) Genes Dev. 9, 1149–1163.
[9] Hirai, H., Roussel, M.F., Kato, J.Y., Ashmun, R.A. and Sherr, C.J. (1995) Mol. Cell. Biol. 15, 2672–2681.
[10] Sherr, C.J. (1996) Science 274, 1672–1677.
[11] Okamoto, A., Demetrick, D.J., Spillare, E.A., Hagiwara, K., Hussain, S.P., Bennett, W.P., Forrester, K., Gerwin, B., Serrano, M., Beach, D.H. and Harris, C.C. (1994) Proc. Natl. Acad. Sci. USA 91, 11045–11049.
[12] Lumpkin Jr., C.K., McClung, J.K., Pereira-Smith, O.M. and Smith, J.R. (1986) Science 232, 393–395.
[13] Campisi, J., Dimiri, G. and Hara, E. (1996) Handbook of the Biology of Aging, 4th edn., pp. 121–149, Academic Press, New York.
[14] Shay, J.W., Pereira-Smith, O.M. and Wright, W.E. (1991) Exp. Cell Res. 196, 33–39.
[15] Hara, E., Tsurui, H., Shinozaki, A., Nakada, S. and Oda, K. (1991) Biochem. Biophys. Res. Commun. 179, 528–534.
[16] Stein, G.H., Beeson, M. and Gordon, L. (1990) Science 249, 666–669.
[17] Hara, E., Smith, R., Parry, D., Tahara, H., Stone, S. and Peters, G. (1996) Mol. Cell. Biol. 16, 859–867.
[18] Alcorta, D.A., Xiong, Y., Phelps, D., Hannon, G., Beach, D. and Barrett, J.C. (1996) Proc. Natl. Acad. Sci. USA 93, 13742–13747.
[19] Serrano, M., Lee, H., Chin, L., Cordon-Cardo, C., Beach, D. and DePinho, R.A. (1996) Cell 85, 27–37.
[20] Kamijo, T., Zindy, F., Roussel, M.F., Quell, D.E., Downing, J.R., Ashmun, R.A., Grosveld, G. and Sherr, C.J. (1997) Cell 91, 649–654.
[21] Derossi, D., Chassaing, G. and Prochiantz, A. (1998) Trends Cell Biol. 8, 84–87.
[22] Fahraeus, R., Paramio, J.M., Ball, K.L., Lain, S. and Lane, D.P. (1996) Curr. Biol. 6, 84–91.
[23] Selivanova, G., Iotsova, V., Okan, I., Fritsche, M., Strom, M., Groner, B., Grafstrom, R.C. and Wiman, K.G. (1997) Nature Med. 3, 632–638.
[24] Bandara, L.R., Girling, R. and La Thangue, N.B. (1997) Nature Biotechnol. 15, 896–901.
[25] Hoffmann, A. and Roeder, R.G. (1991) Nucleic Acids Res. 19, 6337–6338.
[26] Parry, D. and Peters, G. (1996) Mol. Cell. Biol. 16, 3844–3852.
[27] Dimri, G.P., Lee, X., Basile, G., Acosta, M., Scott, G., Roskelley, C., Medrano, E.E., Linskens, M., Rubelj, I., Pereira-Smith, O., Peacocke, M. and Campisi, J. (1995) Proc. Natl. Acad. Sci. USA 92, 9363–9367.
[28] Ogryzko, V.V., Hirai, T.H., Russanova, V.R., Barbie, D.A. and Howard, B.H. (1996) Mol. Cell. Biol. 16, 5210–5218.
[29] Serrano, M., Lin, A.W., McCurrach, M.E., Beach, D. and Lowe, S.W. (1997) Cell 88, 593–602.
[30] Quelle, D.E., Ashmun, R.A., Hannon, G.J., Rehberger, P.A., Trono, D., Richter, K.H., Walker, C., Beach, D., Sherr, C.J. and Serrano, M. (1995) Oncogene 11, 635–645.
[31] Noda, A., Ning, Y., Venable, S.F., Pereira-Smith, O.M. and Smith, J.R. (1994) Exp. Cell Res. 211, 90–98.
[32] Deng, C., Zhang, P., Harper, J.W., Elledge, S.J. and Leder, P. (1995) Cell 82, 675–684.
[33] Brugarolas, J., Chandrasekaran, C., Gordon, J.I., Beach, D., Jacks, T. and Hannon, G.J. (1995) Nature 377, 552–557.
[34] Medcalf, A.S.C., Klein-Szanto, A.J.P. and Cristofalo, V.J. (1996) Cancer Res. 56, 4582–4585.
[35] Uhrbom, L., Nister, M. and Westermark, B. (1997) Oncogene 15, 505–514.
[36] Suzuki, T., Kitao, S., Matsushime, H. and Yoshida, M. (1996) EMBO J. 15, 1607–1614.

STIC-ILL

From: Sullivan, Daniel
Sent: Tuesday, October 22, 2002 2:19 PM
To: STIC-ILL
Subject: Request

Please send the following:

Nat Biotechnol. 1998 Sep;16(9):857-61.

Proc Natl Acad Sci U S A. 1997 Sep 30;94(20):10699-704.

Nat Med. 1998 Dec;4(12):1449-52.

Immunity. 1998 Jan;8(1):57-65.

J Immunol. 1999 May 1;162(9):5205-11.

J Immunol Methods. 1998 Mar 1;212(1):41-8.

Nat Biotechnol. 1998 May;16(5):440-3.

Cell. 1997 Jan 24;88(2):223-33.

Biochem Biophys Res Commun. 1993 Jul 30;194(2):876-84.

Proc Natl Acad Sci U S A. 1994 Jan 18;91(2):664-8.

J Cell Biol. 1995 Mar;128(5):919-27.

FEBS Lett. 1998 May 8;427(2):203-8.

Nat Med. 1999 Jan;5(1):29-33.

Thank you.

Daniel M. Sullivan
Examiner AU 1636
Room: 12D12
Mail Box: 11E12
Tel: 703-305-4448

09937837

Transduction of full-length TAT fusion proteins into mammalian cells: TAT-p27^{Kip1} induces cell migration

HIKARU NAGAHARA, ADAMINA M. VOCERO-AKBANI, ERIC L. SNYDER, ALAN HO, DAWN G. LATHAM, NATALIE A. LISSY, MICHELLE BECKER-HAPAK, SERGEI A. EZHEVSKY & STEVEN F. DOWDY

Howard Hughes Medical Institute and Division of Molecular Oncology, Depts of Pathology and Medicine, Washington University School of Medicine, St. Louis, MO 63110, USA

H.N. & A.M.V.-A. contributed equally

Correspondence and requests for materials should be addressed to S.F.D. e-mail: dowdy@pathology.wustl.edu

Cellular manipulation by transfection or viral introduction of cDNA expression vectors and microinjection of proteins into cells presents various difficulties, including massive overexpression, broad cell-to-cell intracellular concentration ranges of expressed proteins and low percentage of cells targeted[1,2]. Moreover, use of antisense approaches to manipulate intracellular processes have both specific gene and cell-type restrictions. Thus, the ability to manipulate cellular processes by the introduction of full-length proteins in a concentration-dependent fashion into 100% of cells would alleviate these technological problems.

In 1988, Green[3] and Frankel[4] independently discovered HIV TAT protein is able to cross cell membranes. In 1994, Fawell *et al.*[5] demonstrated that chemically cross-linking a 36-amino acid domain of TAT to heterologous proteins conferred the ability to transduce into cells. Other transduction domains were identified that reside in the Antennapedia (Antp) protein from *Drosophila*[6] and HSV VP22 protein from HSV (ref. 7). Although the exact mechanism of transduction across cellular membranes remains unclear, small Antp peptides have been shown to transduce into cells at 4 °C in a receptorless fashion[8], indicating that all cell types potentially can be targeted by this method.

Although TAT-mediated protein transduction was first discovered in 1988, no method to 'harness' this technological potential has been devised. We describe here the development of a full-length protein transduction method using urea-denatured, genetic in-frame TAT fusion proteins, which can be applied to a broad spectrum of proteins regardless of size or function. As an example, we focus on a newly discovered biological property of the p27^{kip1} Cdk inhibitor protein to elicit cell migration in hepatocellular carcinoma cells.

Generation of denatured full-length TAT fusion proteins

Rather than depending on the uncertainties and inefficiencies of chemically cross-linking proteins, we constructed a bacterial expression vector, pTAT-HA, to produce genetic in-frame TAT fusion proteins (Fig. 1*a*). The vector pTAT-HA has an N-terminal 6-histidine leader followed by the 11-amino-acid TAT protein transduction domain[3] flanked by glycine residues (for free bond rotation of the domain), a hemaglutinin (HA) tag and a polylinker. We analyzed transduction of cell-cycle regulatory proteins, including the Cdk inhibitor p27^{kip1} protein[9] and a dominant-negative form of Cdk2 (ref. 10). We generated pTAT-HA vectors expressing the full-length, wild-type p27^{kip1} protein (TAT-p27^{wt}; 30 kDa), a functional truncated N-terminal protein (TAT-p27^{t}; 20 kDa), an inactive p27 point mutant protein (TAT-p27^{kk}; ref. 9), a dominant-negative form of Cdk2 protein (TAT-Cdk2^{dn}; 36 kDa; ref. 10) and a control HSV thymidine kinase protein (TAT-TK; 42 kDa)(Fig. 1*b*).

The exact mechanism of transduction across bilipid membranes is unknown at present; however, because of reduced structural constraints, high energetic (ΔG), denatured proteins may transduce more efficiently into cells than low energetic, correctly folded proteins. Once inside the cell, transduced denatured proteins may be correctly refolded by chaperones[11] such as HSP90 (ref. 12). Therefore, we devised a urea-denaturing protein purification protocol (Fig. 1*c*). Recombinant TAT fusion proteins were denatured and solubilized in 8 M urea then placed into aqueous buffer on an ionic exchange column by doing a single urea 'step' from 4 M to 0 M. Less efficient means of removing the urea include rapid dialysis or the use of desalting columns (Fig. 1*c*). In addition, sonication in 8 M urea allows for the isolation of insoluble recombinant protein present in bacterial inclusion bodies. Moreover, by using single 'steps' to change buffers, the procedure can be done in the absence of an FPLC/HPLC system by using commonly available gravity flow columns.

Transduction of denatured TAT fusion proteins into cells

To analyze the ability of TAT fusion proteins to transduce into cells, TAT-p27^{wt} fusion protein was conjugated to fluorescein (FITC), added to the culture media of Jurkat T cells and analyzed by fluorescence activated cell sorting (FACS)(Fig. 2*a*, left panel). TAT-p27^{wt}–FITC protein rapidly transduced into ~100% of cells, achieving maximum intracellular concentration in less than 10 min. There was a narrow intracellular concentration range of the transduced protein within the population, as indicated by the nar-

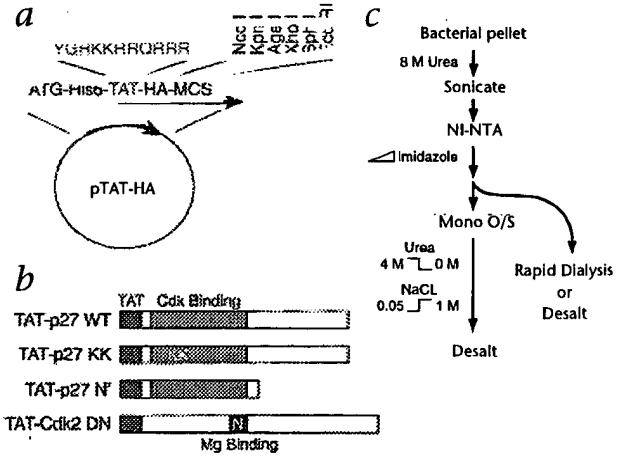

Fig. 1 The pTAT-HA vector and purification protocol. ***a***, pTAT-HA expression vector. ***b***, TAT fusion proteins used here. KK and N indicate point mutations in the Cdk binding and Mg^{2+} coordinating domains, respectively[9,10]. ***c***, Denaturation and TAT fusion protein purification protocol.

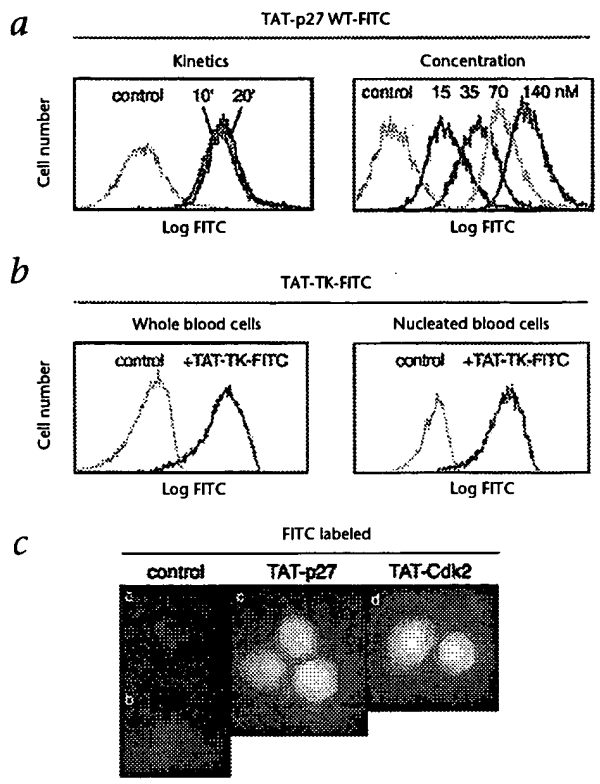

row FACS peak width between control and transduced cells. FACS analysis 1 h after addition (steady-state levels) of cells treated with 10, 35, 70 or 140 nM TAT-p27^{WT}–FITC protein demonstrated a concentration dependency for protein transduction and, thus, the ability to modulate intracellular concentrations (Fig. 2*a*, right panel). TAT-p27$^{KK/N'}$ TAT-Cdk2^{DN} and TAT-TK proteins all behaved similarly (data not shown). In addition to established cell lines, TAT fusion proteins readily transduced into all cells present in whole blood, including both nucleated and enucleated cells (Fig. 2*b*). Moreover, we have transduced TAT fusion proteins into a variety of cell types, including peripheral blood lymphocytes (PBLs), diploid human fibroblasts, keratinocytes, bone marrow stem cells, osteoclasts, fibrosarcoma cells, osteosarcoma, glioma, hepatocellular carcinoma, renal carcinoma and NIH 3T3 cells (data not shown). Confocal microscopy analysis of transduced TAT-p27–FITC and TAT-Cdk2^{DN}–FITC proteins demonstrated both cytoplasmic and nuclear localization, and not just attachment to cellular membranes (Fig. 2*c*).

The protein p27^{kip1} binds and inactivates cyclin E:Cdk2 complexes[9]. Therefore, to determine the *in vivo* biochemical function of transduced TAT-p27 proteins, we treated Jurkat T cells with 100 nM of TAT-p27^{WT}, TAT-p27$^{N'}$ or TAT-TK fusion proteins during concomitant ^{35}S-methionine labeling of cellular proteins. TAT fusion proteins were immunoprecipitated with anti-HA antibodies (Fig. 3*a*). Transduced TAT-p27^{WT} and TAT-p27$^{N'}$ proteins bound Cdk2 *in vivo*, but TAT-TK protein did not. Consistent with TAT-p27^{WT} binding Cdk2 *in vivo*, anti-Cdk2 immunoprecipitation-kinase assays from cells transduced with TAT-p27^{WT} showed loss of Cdk2 kinase activity compared to controls (Fig. 3*b*). p27^{kip1} and Cdk2^{DN} arrest cells in the G_1 phase of the cell cycle[9,10]; therefore, we did a cell-cycle-arrest, dose-dependent analysis of the transduced TAT-27 and TAT-Cdk2^{DN} proteins. Treatment of cells with 200, 100 or 50 nM TAT-p27^{WT} protein resulted in a substantial G_1-phase cell-cycle arrest (Fig. 3*c*), whereas 25 nM and 12 nM had decreasing abilities to effect an arrest, and mutant TAT-p27^{KK} and TAT-TK proteins did not arrest cells (Table 1*a*). TAT-Cdk2^{DN} protein also effectively arrested cells in G_1 and dropped in ability linearly as the concentration was decreased (Fig. 3*d*).

These observations demonstrate that misfolded TAT fusion proteins efficiently transduce into ~100% of cells in a rapid, concentration-dependent manner, are refolded *in vivo* and retain known biological and biochemical activities. In addition, we have transduced more than 40 full-length proteins (Table 1*b*), indicating that the urea denaturation protocol may be applicable to a broad spectrum of proteins regardless of size or function.

Fig. 2 Analysis of transduced proteins. ***a***, FACS kinetic analysis of FITC-labeled TAT-p27^{WT} protein added to Jurkat T cells at 0, 10 or 20 min (left panel) and dose-dependent analysis of 10, 35, 70 or 140 nM TAT-p27^{WT}–FITC protein at 1 h after addition (right panel). ***b***, FACS analysis of human whole blood cells 1 h after addition of FITC-labeled TAT-TK protein. ***c***, Confocal microphotograph sections (original magnification, ×1,000) of cells treated with control (PBS), or TAT-p27^{WT}–FITC or TAT-Cdk2^{DN}–FITC proteins.

Transduction of TAT-p27^{kip1} fusion protein elicits cell migration

As an example of manipulating cellular biology by transduction of full-length proteins, we focused on cell migration. Treatment of human HepG2 hepatocellular carcinoma cells with hepatocyte growth factor/scatter factor (HGF) results in G_1 cell-cycle arrest and induction of cell migration or a 'scattering' phenotype[13,14]. In searching for specific intracellular targets of HGF signaling associ-

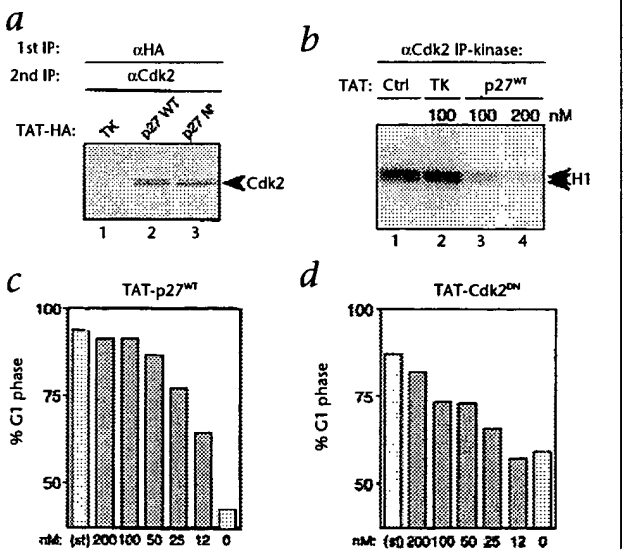

Fig. 3 *In vivo* biochemical and biological properties of transduced proteins. ***a***, Formation of *in vivo* complexes of transduced TAT-p27 proteins with endogenous Cdk2. 100 nM TAT-p27^{WT}, TAT-p27$^{N'}$ or control TAT-HSV TK proteins were transduced into Jurkat T cells during concomitant ^{35}S-methionine labeling of cellular proteins and immunoprecipitated with anti-HA antibodies followed by re-immunoprecipitation with anti-Cdk2 antibodies. ***b***, Anti-Cdk2 immunoprecipitation-kinase assay from cells transduced with TAT-TK or TAT-p27^{WT} proteins. ***c*** and ***d***, HaCat keratinocytes were arrested in G_1 phase by contact inhibition, then replated at low density, transduced with varying concentrations TAT-p27^{WT} (*c*) or TAT-Cdk2^{DN} proteins (*d*) and analyzed for cell-cycle position at 30 h post-replating. Percentage of cells in G_1 at start (st) and at 30 h after replating (0) are shown.

ated with cell scattering, we found that cyclin E:Cdk2 complexes were specifically inactivated (Fig. 4*a*). Consistent with loss of cyclin E:Cdk2 activity, we observed an induction of $p27^{kip1}$ protein levels in response to HGF signaling, but no change in $p21^{cip1}$ levels were detected (Fig. 4*a*). These observations indicated that $p27^{kip1}$ was a downstream nuclear of HGF signaling.

To determine if $p27^{kip1}$ mediated cell scattering directly, we treated HepG2 cells with TAT-$p27^{wt/kk/\Delta'}$ proteins, TAT-$Cdk2^{DN}$, TAT-$p16^{wt}$ (refs 15 & 16) or control TAT-TK protein (Fig. 4*b* and *c* and Table 1*a*). Transduction of full-length TAT-$p27^{wt}$ protein into HepG2 cells (Fig. 4*b*, panel f) induced a cell-scattering phenotype near identical to that of HGF-treated cells (Fig. 4*b*, panel c). However, all other TAT fusion proteins and TGF-β failed to induce cell scattering, even though TAT-$p27^{\Delta'}$ and TAT-$Cdk2^{DN}$ proteins retained the ability to elicit a G_1 arrest (Fig. 3*d* and Table 1*a*). Cell migration involves alterations in the actin cytoskeleton[17]. Therefore, we stained actin filaments with rhodamine-conjugated phalloidin from control or HepG2 cells treated with TGF-β, HGF, $p27^{wt/kk/\Delta'}$ proteins, TAT-$Cdk2^{DN}$ and TAT-$p16^{wt}$ proteins (Fig. 4*d* and Table 1*a*). Filopodia only appeared in cells transduced with full-length TAT-$p27^{wt}$ protein (Fig. 4*d*, panels e and f) or treated with HGF (Fig. 4*d*, panel c). Thus, using the method of direct protein transduction into cells, we discovered a previously unknown biological property of $p27^{kip1}$ of mediating cell scattering in hepatocellular carcinoma cells. In addition, we conclude that cyclin E:Cdk2 complexes are not the downstream target of the HGF-$p27^{kip1}$ cell migration signaling pathway; therefore, $p27^{kip1}$ is either targeting an unknown cyclin:Cdk complex or a non-Cdk protein. Furthermore, these observations are consistent with a broadening role of Cdk inhibitors, such as $p21^{cip1}$, in regulating non-cell-cycle cellular processes[18].

Table 1 *In vivo* responses of transduced proteins

a. Induction of biological responses

Treatment/TAT fusion protein	G_1 arrest	Scattering	Filopodia
control	–	–	–
TGF-β	+	–	–
HGF	+	+	+
TAT-$p27^{wt}$	+	+	+
TAT-$p27^{kk}$	–	–	–
TAT-$p27^{\Delta'}$	+	–	–
TAT-$p16^{wt}$	+	–	–
TAT-$Cdk2^{DN}$	+	–	–
TAT-HSV TK	–	–	–

b. Biochemical and biological responses by transduced proteins

TAT fusion protein	*In vivo* biochemical effect	Biological effect
TAT-HPV E7 (18 kDa)[15]	Bind pRB	TCR-AID rescue
TAT-$p16^{ink4a}$ (20 kDa)[15,16]	Bind Cdk6	G_1 arrest
TAT-$p27^{kip1}$ (30 kDa)	Bind Cdk2	Cell migration & G_1 arrest
TAT-CDK2 dom.-neg. (36 kDa)	Bind Cyclin E	G_1 arrest
TAT-CPP32 (32 kDa)[c]	DNA degradation	Apoptosis
TAT-HSV TK (42 kDa) plus Acyclovir[c]	ND[a]	Cell killing
TAT-13S E1A (60 kDa)[b]	Bind pRB	ND[a]
TAT-pRB (115 kDa)[b]	ND[a]	G_1 arrest

[a]Not determined; [b]Unpublished observations; [c]Manuscript submitted

To understand further the efficiencies involved in inducing biological responses by transduction of proteins, we directly compared soluble, correctly folded TAT-$p27^{wt}$ protein with 8 M urea-denatured TAT-$p27^{wt}$ protein for the ability to induce cell migration (Fig. 4*e*). Transduction of denatured TAT-$p27^{wt}$ protein readily induced cell migration at 50 nM, 100 nM or 150 nM concentrations; however, correctly folded TAT-$p27^{wt}$ protein failed to induce cell migration at even the highest concentration. However, this is not a failure of correctly folded TAT-$p27^{wt}$ protein to transduce into cells, it merely represents the inefficiency to

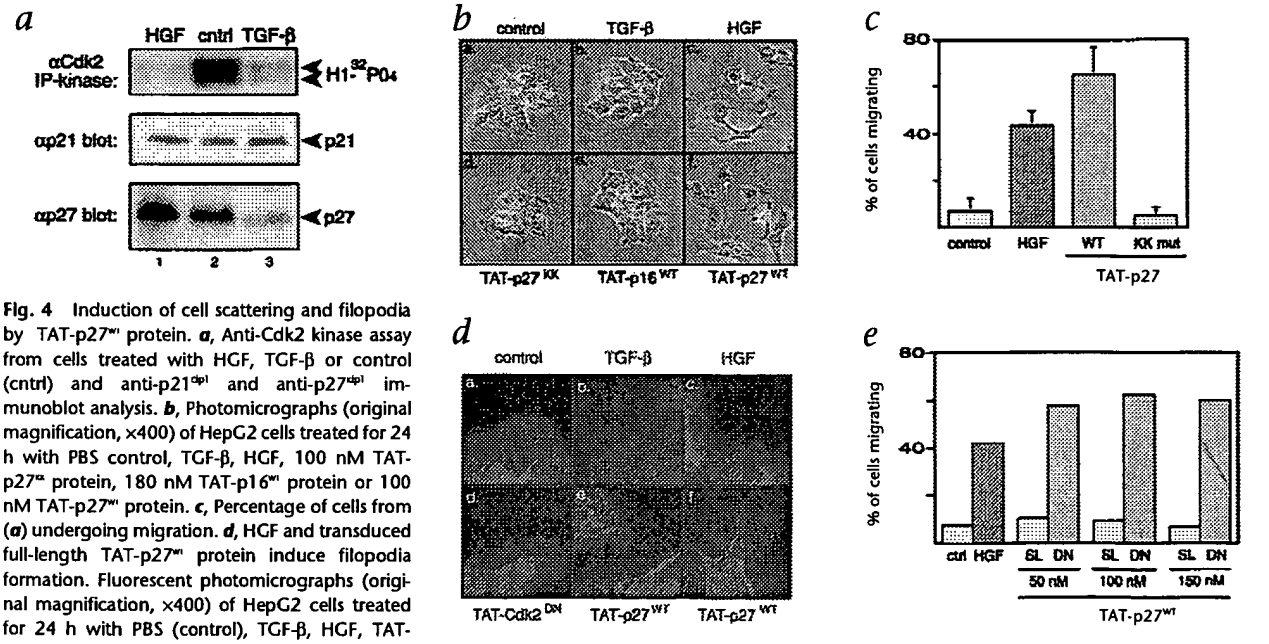

Fig. 4 Induction of cell scattering and filopodia by TAT-$p27^{wt}$ protein. ***a***, Anti-Cdk2 kinase assay from cells treated with HGF, TGF-β or control (cntrl) and anti-$p21^{cip1}$ and anti-$p27^{cip1}$ immunoblot analysis. ***b***, Photomicrographs (original magnification, ×400) of HepG2 cells treated for 24 h with PBS control, TGF-β, HGF, 100 nM TAT-$p27^{kk}$ protein, 180 nM TAT-$p16^{wt}$ protein or 100 nM TAT-$p27^{wt}$ protein. ***c***, Percentage of cells from (***a***) undergoing migration. ***d***, HGF and transduced full-length TAT-$p27^{wt}$ protein induce filopodia formation. Fluorescent photomicrographs (original magnification, ×400) of HepG2 cells treated for 24 h with PBS (control), TGF-β, HGF, TAT-$Cdk2^{DN}$ or TAT-$p27^{wt}$ protein and stained for actin filaments with rhodamine-conjugated phalloidin. ***e***, Direct comparison of soluble (SL), correctly folded TAT-$p27^{wt}$ and denatured (DN) TAT-$p27^{wt}$ protein in their ability to induce cell migration.

Methods

Cell culture, flow cytometry, immunoprecipitations. Human HepG2 hepatocellular carcinoma cells, HaCaT keratinocytes and Jurkat T cells were maintained as described[15,16]. TGF-β (10 ng/ml; R&D Systems, Minneapolis, MN) or HGF/SF (20 ng/ml; Sigma) was added to HepG2 cells for 48 h (5×10^5 cells per 10-cm dish) before analysis of Cdk2 activity and immunoblotting. Contact inhibition of HaCaT keratinocytes done as described[16]. Cell-cycle position was determined by propidium iodide staining and flow cytometry analysis (FACS; Becton Dickinson, San Jose, CA)[15,16]. For filamentous actin staining, treated and control HepG2 cells were grown on cover slips, washed in PBS, fixed in 4% paraformaldehyde, washed in 0.2% Triton-x100/PBS, stained in 0.2 mg/ml rhodamine-conjugated phalloidin (Sigma), rinsed three times in PBS and once in water, and mounted. Photomicrographs of cells were taken under fluorescence at x400 magnification. Uptake of FITC-labeled TAT-$p27^{kip/cip}$, TAT-$Cdk2^{-/-}$, TAT-TK proteins in Jurkats, HepG2 and/or whole blood cells was determined by FACS analysis (10,000 live cells) and by confocal microscopy (×1,000 magnification) of cells fixed in 4% paraformaldehyde. For immunoprecipitations, HepG2 cells were labeled with 250 μCi ^{35}S-methionine (NEN, Boston, MA) in the presence of 100 nM TAT-p27 or TAT-TK proteins for 4 h and immunoprecipitated as described[15,16] using anti-HA antibodies (BAbCO, Richmond, CA), followed by re-immunoprecipitation with polyclonal anti-Cdk2 antibodies (Santa Cruz Biotechnology, Santa Cruz, CA). Anti-Cdk2 immunoprecipitation–kinase reactions were done as described[15,16] and histone H1 as a substrate (Sigma). Immunoblots were done as described[15,16] using polyclonal anti-p21 or anti-p27 antibodies (Santa Cruz).

TAT fusion protein purification. pTAT-HA was constructed by inserting a double-stranded oligomeric nucleotide encoding the 11-amino acid TAT protein transduction domain[3] flanked by glycine residues (GYGRKKRRQRRRG) into pRSET vector (Invitrogen, San Diego, CA) and adding a new polylinker. The pTAT-$p27^{wt}$/^{mt} vectors were constructed by inserting a PCR fragment encompassing the wild-type and KKPV mutant[3] p27 open reading frame flanked by engineered *Nco*I and *Eco*RI sites and inserted into pTAT-HA. The pTAT-$p27^{mt}$ vector was generated by *Nae*I at codon 103 and re-ligation. The vectors pTAT-$Cdk2^{wt}$ and pTAT-HSV TK were generated by subdoning from pCdk2(NFG) vector[15] and HSV TK cDNAs into pTAT-HA. TAT fusion proteins were purified by sonication of high expressing BL21(DE3)pLysS (Novagen, Madison, WI) cells obtained from a 4- to 6-h 1-liter culture inoculated with 100 ml overnight culture, in 10 ml of buffer A (8 M urea/20 mM HEPES [pH 8.0]/100 mM NaCl). Cellular lysates were resolved by centrifugation, loaded onto a 5-ml Ni-NTA column (Qiagen, Valencia, CA) in buffer A plus 10–20 mM imidazole, washed, eluted with imidazole in buffer A 'stepwise' (100, 250 and 500 mM) and applied to a Mono-Q/5 column on an FPLC (Pharmacia, Piscataway, NJ) in 4 M urea/20 mM HEPES (pH 8.0 or 6.5)/50 mM NaCl. TAT fusion proteins were 'shocked' into aqueous buffer by a single urea 'step' from 4 M to 0 M, followed by elution with a single 1 M NaCl 'step', desalted on a PD-10 column into PBS, flash-frozen in 10% glycerol and stored at –80 °C. Soluble TAT-$p27^{wt}$ was produced by sonication of cells in PBS and purified as described above, without urea. FITC-labeled TAT fusion proteins were generated by fluorescein labeling (Pierce, Rockford, IL), followed by gel filtration and added directly to cells in culture media.

achieve the required intracellular threshold level to elicit cell migration. Thus, we conclude that using urea-denatured TAT fusion proteins enhances the ability of transduced proteins to modulate biological processes.

Future directions

Our contribution to advancing protein transduction has been to generate an in-frame TAT bacterial expression vector (pTAT-HA) and to devise a misfolding purification protocol that achieves two goals. First, most bacterially expressed recombinant proteins are insoluble and present in inclusion bodies, and our protocol allows for the purification and use of this material. Second, to traverse the cell membrane, TAT fusion proteins may require partial unfolding. Therefore, the use of energetically unstable (high ΔG), urea-denatured fusion proteins seems to enhance the ability to transduce proteins into cells. Transduced denatured proteins may be refolded by chaperones[11] such as HSP90 (ref. 12).

Because of size constraints, research on therapeutically important proteins has focused on miniaturization of protein-specific functions, such as contact sites. However, large protein domains have been evolutionarily selected to yield high-affinity active sites, protein–protein and protein–DNA contact sites. As an example, in our lab, 300 μM of a 20-amino acid p16 peptidyl mimetic[19] is required to elicit a G_1 phase cell-cycle arrest (D. Gius & S.F.D., unpublished observation); however, only 150 nM of full-length TAT-p16 protein is required[14]. Thus, transduction of full-length p16 protein into cells increases the specificity of the biological response by three orders of magnitude compared with that of a peptidyl mimetic. We conclude that transduction of denatured proteins directly into ~100% of primary or transformed cells has broad implications for regulating intracellular processes in experimental systems and has the potential to allow development of new therapeutic strategies using full-length proteins and protein domains that retain high affinities for their intracellular targets.

Acknowledgments

We thank J. Roberts for wild-type p27 cDNA, J. Massague for $p27^{KPV}$ mutant cDNA; E. Harlow for Cdk2-DN cDNA; M. Dustin for confocal microscopy; and all members of the Dowdy lab for critical input. This work was supported by an NIH-MSTP fellowship (E.L.S.) and the Howard Hughes Medical Institute (S.F.D.).

1. Anderson, W.F. Human gene therapy. *Nature* **392**, 25–30 (1998).
2. Bar-Sagi, D. Mammalian cell microinjection assay. *Meth. Enzymol.* **255**, 436–442 (1995).
3. Green, M. & Loewenstein, P.M. Autonomous functional domains of chemically synthesized human immunodeficiency virus tat trans-activator protein. *Cell* **55**, 1179–1188 (1988).
4. Frankel, A.D. & Pabo, C.O. Cellular uptake of the tat protein from human immunodeficiency virus. *Cell* **55**, 1189–1193 (1988).
5. Fawell, S. *et al.* Tat-mediated delivery of heterologous proteins into cells. *Proc. Natl. Acad. Sci USA* **91**, 664–668 (1994).
6. Vives, E., Brodin, P. & Leblus, B. A truncated Tat basic domain rapidly translocates through the plasma membrane and accumulates in the nucleus. *J. Biol. Chem.* **272**, 16010–16017 (1997).
7. Elliott, G. & O'Hare, P. Intercellular trafficking and protein delivery by a herpesvirus structural protein. *Cell* **88**, 223–233 (1997).
8. Derossi, D., Joliot, A.H., Chassaings, G. & Prochiantz, A. The third helix of the antennapedia homodomain translocates through biological membranes. *J. Biol. Chem.* **269**, 10444–10450 (1994).
9. Luo, Y., Hurwitz, J. & Massague, J. Cell-cycle inhibition by independent CDK and PCNA binding domains in $p21^{cip1}$. *Nature* **375**, 159–161 (1995).
10. Van den Heuvel, S. & Harlow, E. Distinct roles for cyclin-dependent kinases in cell cycle control. *Science* **262**, 2050–2054 (1993).
11. Gottesman, S., Wickmer, S. & Maurizi, M.R. Protein quality control: Triage by chaperones and proteases. *Genes Dev.* **11**, 815–823 (1997).
12. Schneider, C. *et al.* Pharmacologic shifting of a balance between protein refolding and degradation mediated by HSP90. *Proc. Natl. Acad. Sci. USA* **93**, 14536–14541 (1996).
13. Jeffers, M., Rong, S. & Vande Woude, G.F. Hepatocyte growth factor/scatter factor—Met signaling in tumorigenicity and invasion/metastasis. *J. Mol. Med.* **74**, 505–513 (1996).
14. Matsumoto, K. & Nakamura, T. Hepatocyte growth factor: Molecular structure, roles in liver regeneration, and other biological functions. *Crit. Rev. Oncol.* **3**, 27–54 (1992).
15. Lissy, N.A. *et al.* TCR-antigen induced cell death (AID) occurs from a late G_1 phase cell-cycle check point. *Immunity* **8**, 57–65 (1998).
16. Ezhevsky, S.A. *et al.* Hypo-phosphorylation of the retinoblastoma protein by cyclin D:Cdk4/6 complexes results in active pRb. *Proc. Natl. Acad. Sci. USA* **94**, 10699–10704 (1997).
17. Van Aelst, L. & D'Souza-Schorey, C. Rho GTPases and signaling networks. *Genes Dev.* **11**, 2295–2322 (1997).
18. Di Cunto, F. *et al.* Inhibitory function of $p21^{cip1/waf1}$ in differentiation of primary mouse keratinocytes independent of cell cycle control. *Science* **280**, 1069–1072 (1998).
19. Fahraeus, R., Paramio, J.M., Ball, K.L., Lain, S. & Lane, D.P. Inhibition of pRb phosphorylation and cell-cycle progression by a 20-residue peptide derived from p16. *Curr. Biol.* **6**, 84–91 (1996).

STIC-ILL

Fr m: Sullivan, Daniel
Sent: Tuesday, October 22, 2002 2:19 PM
To: STIC-ILL
Subject: Request

Please send the following:

Nat Biotechnol. 1998 Sep;16(9):857-61.

Proc Natl Acad Sci U S A. 1997 Sep 30;94(20):10699-704.

Nat Med. 1998 Dec;4(12):1449-52.

Immunity. 1998 Jan;8(1):57-65.

J Immunol. 1999 May 1;162(9):5205-11.

J Immunol Methods. 1998 Mar 1;212(1):41-8.

Nat Biotechnol. 1998 May;16(5):440-3.

Cell. 1997 Jan 24;88(2):223-33.

Biochem Biophys Res Commun. 1993 Jul 30;194(2):876-84.

Proc Natl Acad Sci U S A. 1994 Jan 18;91(2):664-8.

J Cell Biol. 1995 Mar;128(5):919-27.

FEBS Lett. 1998 May 8;427(2):203-8.

Nat Med. 1999 Jan;5(1):29-33.

Thank you.

Daniel M. Sullivan
Examiner AU 1636
Room: 12D12
Mail Box: 11E12
Tel: 703-305-4448

09937837

Vol. 194, No. 2, 1993 BIOCHEMICAL AND BIOPHYSICAL RESEARCH COMMUNICATIONS
July 30, 1993 Pages 876-884

TUMOR CELL RETENTION OF ANTIBODY FAB FRAGMENTS IS ENHANCED BY AN ATTACHED HIV TAT PROTEIN-DERIVED PEPTIDE

D.C. Anderson, E. Nichols, R. Manger, D. Woodle, M. Barry and A.R. Fritzberg

NeoRx Corporation, 410 West Harrison, Seattle, WA 98119

Received June 17, 1993

Summary: Two peptide analogs of the 37-62 sequence region of the HIV TAT protein bind tightly to the surface of A431 breast carcinoma cells. After conjugation to either of two poorly internalized anti-tumor antibody Fab fragments, the analogs enhanced the in vitro cell surface retention and internalization of the Fab fragments to the level of the whole antibodies. This was at the expense of some binding specificity in the case of 1.6 peptides/NRLU-10 Fab, but not in the case of 1.1 peptides/Fab. Enhanced retention may occur by enhanced bivalent binding of the Fab fragments. The internalized fraction of free peptide, but not of the Fab conjugates, is enhanced by chloroquine. The conjugates which were less specific for tumor cell binding may be useful for enhanced retention/ internalization of specifically acting agents, for use at specific sites of injection, or against pre-separated target cell populations, while the more specific conjugate may be of interest for further development.

Enhancing the cell surface binding or internalization of proteins such as monoclonal antibodies or drug delivery agents may improve certain of their properties, such as the effectiveness of the drug, or their circulatory half life. Poorly internalized monoclonal antibody Fab fragments may be useful for testing such retention enhancers, and improved internalization or retention may be useful for therapeutic monoclonal fragments, such as anti-tumor antibodies used for radiotherapy. Typically, about 0.005% of an injected dose/gram localizes in or at tumor sites. This may need to be increased 10-fold or more for effective therapy (1).

The HIV TAT protein is an 86-102 residue (depending on virus strain) immediate early protein that can transactivate the expression of specific HIV genes. It has a cysteine-rich domain involved in zinc-mediated dimerization (2), an activation domain (3-4) and a highly basic region involved in TAR RNA recognition (5) which contains a nuclear localization sequence. The whole protein is rapidly taken up by HeLa cells (3, 6), and synthetic peptides derived from this basic region, including residues 37-62, can have minimal but clear transactivation activity (4).

Here we examine the effect of residues 35-62 on in vitro tumor retention when covalently attached to Fab fragments of two different poorly internalized mouse antitumor antibodies. These fragments have been used in clinical trials for the imaging of metastatic melanoma (7) and for detection and staging of small cell lung carcinomas (8-9). Fab fragments were chosen as they more rapidly penetrate the tumor than whole antibodies, but are not as easily retained at tumors as are whole antibodies, allowing a ready measure of enhanced retention effects.

0006-291X/93 $4.00

MATERIALS AND METHODS

Peptide Synthesis. Peptides were synthesized on p-methylbenzhydrylamine resin (0.6 meq/g) on an Applied Biosystems 430A peptide synthesizer using standard boc-benzyl cycles. Coupling yields were monit red by ninhydrin using resin collected automatically, and were all above 99.3% for the single-coupled parent peptide:

CGGQVC(Acm)FITKALGISYGRKKRRQRRRPPQGS-amide 1

This peptide includes the sequence from residues 35-62 of the HIV TAT protein in its positions 4-31, a CGG spacer at the N terminus and a cys (S-acetamidomethyl) at position 6 protected to avoid crosslinking at this residue. The 35-62 sequence was selected from references 3 and 10. Other HIV isolates can have somewhat altered sequences in this region (see for example 11-12). The standard N-methylpyrrolidone-dimethylsulfoxide synthesis protocol was modified to include shaking of the coupling vessel during addition of the boc-amino acids. This avoided clumping of the resin observed in trial syntheses when coupling in the lys and arg rich region. The peptide was acetylated at the N-terminus with [^{14}C]-acetic anhydride while on the resin (13), cleaved using the low-high HF protocol (14), extracted with 10% acetic acid, lyophilized, and purified by C4 reversed phase chromatography (13). The final specific radioactivity of pure peptide was 1.8 mCi/mmol.

For retention studies of the free peptide, an additional analog (peptide 2) was synthesized as a control. In this analog, the N terminal sequence was modified to include tyrosines to direct radioiodination to this part of the sequence and less to the tyrosine just before the positively charged region:

CGGYYKYYQVC(Acm)FITKALGISYGRKKRRQRRRPPQGS-amide 2

Peptides were checked by amino acid analysis using in vacuo gas phase hydrolysis (15) and derivatization and chromatography using the Hewlett Packard AminoQuant amino acid analysis system, and by Edman degradation sequencing using a Porton sequencer.

Crosslinked Fab-peptide complexes. [^{14}C]-labeled peptides were crosslinked to Fab fragments of the anti-melanoma antibody NRML-05 (16) and the pan-carcinoma antibody NRLU-10, which binds a 39 kDa cell surface antigen (17), using the heterobifunctional crosslinker sulfosuccinimidyl 4-(N-maleimidomethyl)-cyclohexane-1-carboxylate (sulfo-SMCC) with methodology described in (13). A 10-fold excess of N-ethylmaleiimide was added to react with any remaining free peptide thiols after reaction of peptide with Fab-SMCC, to prevent formation of disulfide-linked peptide dimers which in test runs were difficult to separate from conjugates by gel filtration.

Different matrices were screened for purification of the peptide-Fab complexes. Silicon-based columns or ultrafiltration membranes gave poor recovery of both free peptide and conjugate. This may be due to the stickiness of the peptide. The best results were obtained on carbohydrate-based matrices such as Pharmacia's Superose resin. The recovery of conjugate after final purification on a Pharmacia Superose 12 column (1.5 x 28 cm, 5 pooled injections, flow rate 0.5 ml/min.) was 49%. The peptide-Fab complexes were assayed for covalency of peptide attachment to Fab by incubation in 6M guanidine hydrochloride and 0.1 M dithiothreitol for 1 hour at 26 oC before chromatography on a C4 reversed phase hplc column, as described (13). The stoichiometry of attachment was derived from the peptide specific activity and the counts covalently bound in the conjugate.

Assay for tumor cell retention. Complexes of Fab-SMCC-peptide were radioiodinated using iodobeads (Pierce Chemical Co., Rockford IL) as described (13). The final specific activity of the conjugates was in the range of 0.2-1.1 μCi/μg Fab in different experiments. For the chloroquine experiments (fig. 3), the specific activities (μCi/μg) were: Fab, 0.12; Fab-1.6, 1.09; tat peptide, 0.17. For the experiments in fig. 2 the specific activities were Fab, 0.51; Fab-1.1, 0.23; and Fab-1.6, 0.23. Constant amounts of conjugate (and thus variable counts) were used with the tumor cells. On HT-29 cells, for example, 0.7 μg Fab were cell surface bound at t=0. With the 10^6 cells used in the retention assays, saturating amounts of Fab were

in the range of 5-10 μg, thus the Fab used was well below that required for saturation of surface antigen binding sites.

Assays for the retention of conjugates on FEMX human melanoma cells (for NRML-05) or HT-29 colon carcinoma cells (for NRLU-10) were performed as described (13). The shed cpm indicate c njugate which is n t bound to cells, cell surface cpm indicate conjugate stripped by two pH 2.5-chymopapain treatments after unbound conjugate was separated by centrifugati n, and internalized cpm indicate conjugate remaining after the acid-chymopapain stripping of the cell surface (18).

Attachment to or desorption of free peptide or conjugate from tumor cells was fit to a first order process using the program REDUCEP (19).

ELISA assay of antigen binding. Competition ELISA was used to assay the effect of peptide derivatization on the antigen binding activity of each Fab (13). Briefly, the NRLU-10 antigen extracted from LS174 colon carcinoma cells, or the NRML-05 antigen extracted from A375 met-mix melanoma cells, was used to coat ELISA plates. The test conjugate was then mixed with biotin-labeled whole antibody, varying in concentration from 0.9 to 70 nM, and both were equilibrated in the ELISA wells. After washing, the bound fragment was detected by the loss of whole antibody binding, which was detected with streptavidin-horse radish peroxidase. The apparent inhibition constants were the concentration of conjugate half-inhibiting whole antibody binding.

RESULTS

Characterization of NRLU-10 Fab-peptide 1 conjugates. These conjugates were analyzed by gel filtration chromatography, reversed phase chromatography, and ELISA (Table 1). Unlike the more complex species resulting from derivatization with a negatively charged amphipathic peptide (13), conjugates with peptide 1 gave two separate peaks by gel filtration (data not shown). The higher molecular weight peak ("Fab-1.6"), pooled from 5 preparative runs, contained an average of 1.61 peptides/Fab, while the lower molecular weight peak ("Fab-1.1") contained an average of 1.07 peptides/Fab. The Fab-1.6 conjugate appears to bind antigen three times tighter than Fab-1.1, while the Fab-1.1 conjugate has slightly diminished antigen binding relative to the Fab. Neither binds antigen as well as the whole antibody control, which has an apparent K_i half as large as that of unmodified Fab. The

Table 1. Properties of NRLU-10 Fab, mAb and Peptide 1 Conjugates

	Fab-1.1	Fab-1.6	Fab	whole mAb
MWapp, kDa[a]	50 (n=3)	91 (n=3)	50 (n=1)	150 (n=1)
bound ^{14}C-peptide/Fab	1.07	1.61		
K_i,nM[b]	96+/-9.6 (n=2)	36+/-17 (n=2)	56+/-2.6 (n=3)	20+/-8.5 (n=5)
mole-percent peptide covalently attached	100	99.1		

[a] Obtained by gel filtration on a 1.5 x 28 cm Pharmacia Superose 12 column in phosphate buffered saline, pH 7.4, 22 °C, eluted at 0.5 ml/min. The Fab fragment molecular weight was assumed to be 50 kDa, and the whole IgG_{2b} antibody molecular weight 150 kDa.

[b] Apparent inhibition constant obtained by competition ELISA with the indicated number of replicates.

peptide, essentially entirely covalently bound, appears t cause a higher apparent molecular weight for the Fab-1.6 complex (91 kDa) than for the control Fab (50 kDa) or Fab-1.1 complex (50 kDa).

Retention of free peptides n tumor cells. Figure 1 shows the time-dependence f tumor cell retention f peptides 1 and 2 on NRLU-10 antigen positive HT-29 cells. After 24 hours, ca. 15-20% of peptides 1 and 2 were internalized. About 80% or more of both peptides were cell-surface associated initially, while 45% of peptide 1 and 20% of peptide 2 remained bound to the cell surface after 24 hours. Thus both peptides are significantly bound to the cell surface or internalized.

The loss of peptide from the cell surface is well approximated by a first order process with a rate constant of 0.089 hr^{-1} (peptide 1) or 0.31 hr^{-1} (peptide 2), while the increase of shed counts is described by a first order rate constant of 0.16 hr^{-1} (peptide 1) and 0.14 hr^{-1} (peptide 2). Thus peptide 1 appears to have a slower desorption rate from the cell surface than peptide 2. The similarity of the rate constants for peptide 1 loss from the cell surface and the appearance of shed counts suggests that they may be due to desorption of some of the peptide from the cell surface.

Retention of peptide-NRLU-10 Fab complexes on tumor cells. Figure 2 shows the retention of peptide conjugates of NRLU-10 Fab on antigen-positive and antigen-negative cells. The Fab control appears to be specifically associated with antigen positive cells (5-8% cell-surface bound vs. 2% cell-surface bound on antigen negative M14 cells) over ca. 24 hours while the Fab fragment is internalized nonspecifically and to a very limited extent. The shed component is not shown, but represents the counts left over after the cell surface and internalized counts are plotted.

The Fab-1.1 conjugate exhibits enhanced cell surface retention on antigen positive cells, up to 41% of total conjugate at 1 hour and 22% after 24 hours. This appears to be significantly more than on antigen

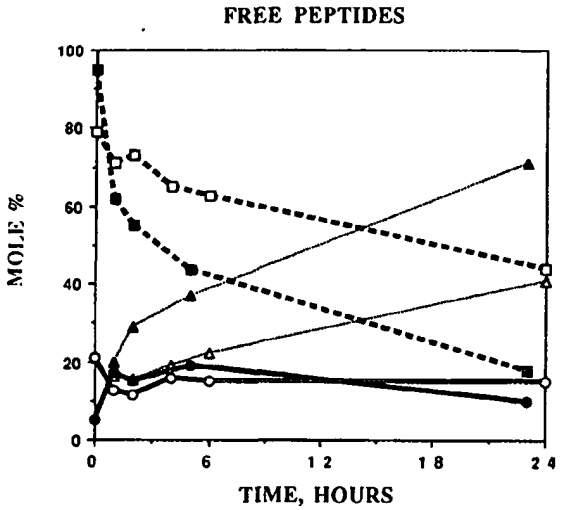

Figure 1. Retention/internalization of [^{125}I]-peptides 1 and 2 on HT-29 colon carcinoma cells over 24 hours. Peptides 1 (open symbols) and 2 (solid symbols) are listed as shed (free in solution; triangles), cell surface bound (squares), or internalized (circles). At t=0, 10800 cpm of peptide 1 were internalized, 40650 were surface bound, and 69500 were shed. The HT-29 cells are antigen positive for NRLU-10 Fab.

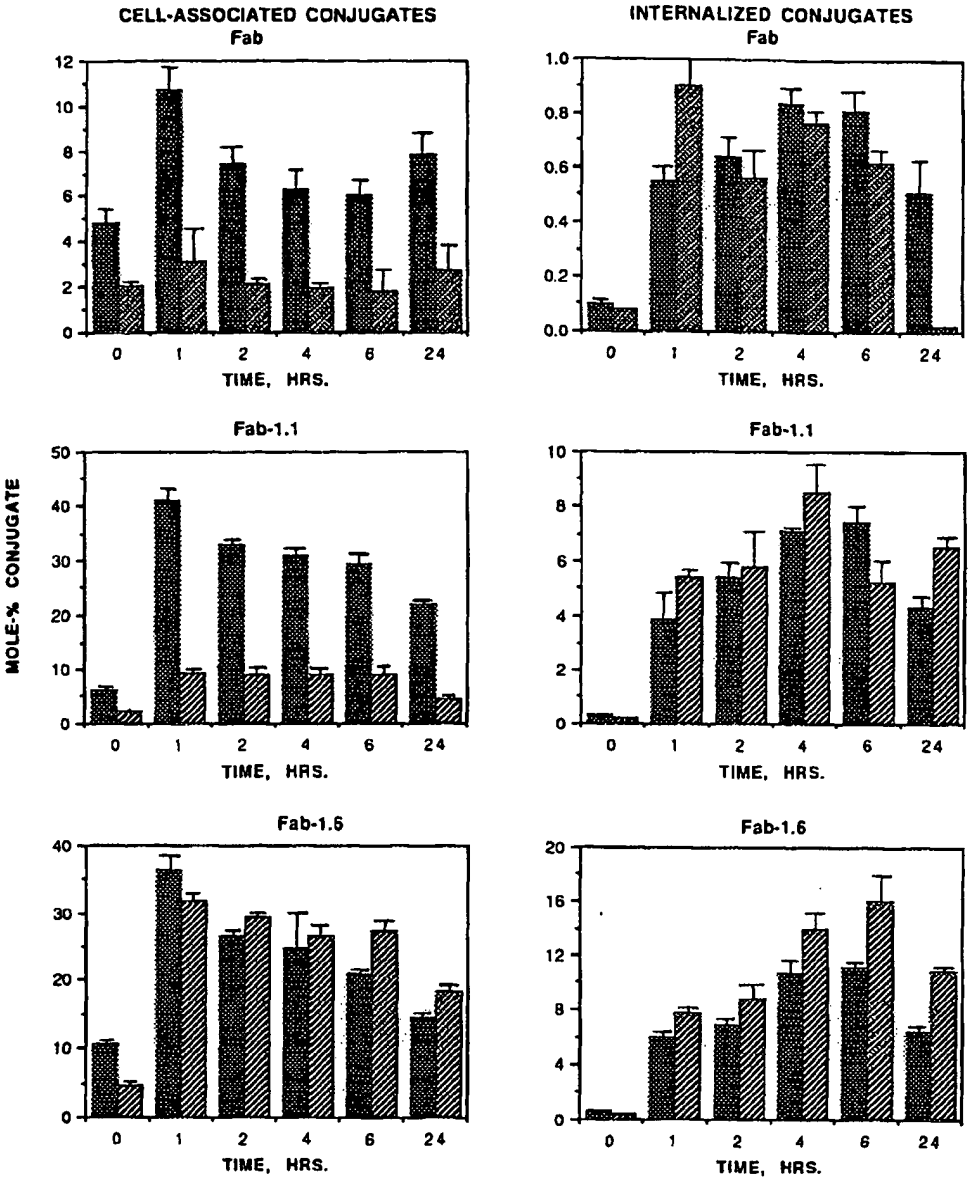

Figure 2. Specificity of cell surface-bound and internalized NRLU-10 Fab and Fab-peptide 1 conjugates on antigen positive cells (HT-29 colon carcinoma cells, solid bars) and antigen negative cells (M14 human melanoma cells, hatched bars). Data were obtained in triplicate for each point, and error bars representing one standard deviation are shown. Shed counts, representing free Fab or conjugate in solution, are not shown. Specific interactions were obtained for Fab and Fab-1.1 binding to antigen positive cells. The mole percent of the total conjugate or Fab is shown on the y-axis.

negative cells, where cell surface conjugate is maximal at about 10% of the total, after 1 hour. The internalized fraction of Fab-1.1 is maximal on antigen positive cells at 7-7.5% at 4-6 hours and decays to 4.3% after 24 hours. Similar values for internalized Fab-1.1 are obtained on antigen negative cells.

The Fab-1.6 conjugate exhibits cell surface retention roughly similar to that of the Fab-1.1 conjugate on antigen positive cells. However the antigen-negative cells also show a similar level of cell surface retention, peaking at 37% and 32% after 1 hour for antigen positive and negative cells, respectively. Internalization, enhanced 10-fold or mor over Fab al ne for both antigen positive and negative cells, reaches levels of 10-15% after 6 hours.

The kinetics of cell surface binding and internalization appear to differ from those of free peptide, reaching a peak after 1 hour with subsequent decay in the case of cell surface binding or reaching a peak after 6 hours with subsequent decay in the case of internalization. This biphasic pattern resembles that of Fab alone.

As a control, the retention of the whole IgG_{2b} antibody NRLU-10 was tested on antigen positive HT-29 cells(Fig. 3). About 7 mole-percent of antibody is internalized after 6 hours, and this diminishes slightly after 24 hours. About 60% of the antibody is cell surface bound after 1 hour, and this slowly decreases to ca. 45% after 24 hours. These results are similar to the retention of the Fab-1.1 and Fab-1.6 peptide conjugates. Since the whole antibody is an IgG, this result suggests that bivalent binding to the cell surface may be responsible for the enhanced peptide conjugate internalization seen above.

Effect of chloroquine on conjugate retention/internalization. Chloroquine has been shown to enhance internalization of the free TAT 86mer protein in HL3T1 cells by 10^3 fold (5). We tested the effect of 100 μM chloroquine on the uptake of free peptide 1 by A431 breast cancer cells(Fig. 4) which

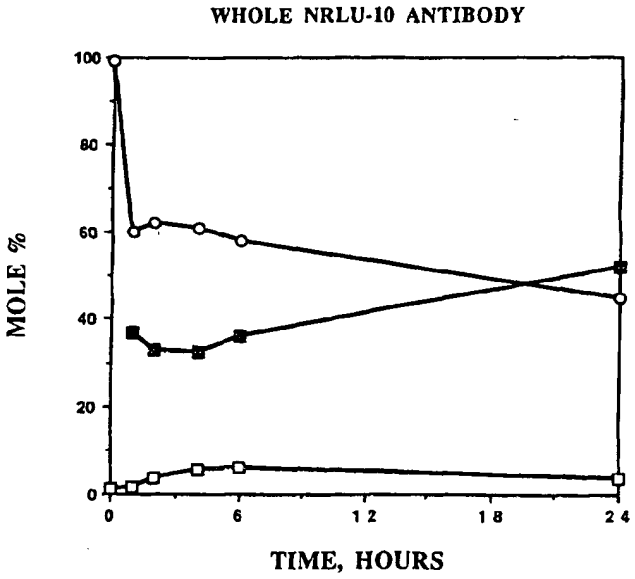

Figure 3. Cell surface binding and internalization of the whole monoclonal antibody NRLU-10 on HT-29 cells. The mole-percent of total antibody is plotted vs. time. The cell surface binding (open circles) and internalized fraction (open squares) appear similar to the Fab-1.1 and Fab-1.6 conjugates. Both are significantly enhanced for this bivalent antibody over its underivatized Fab fragment. Shed counts are represented as closed squares.

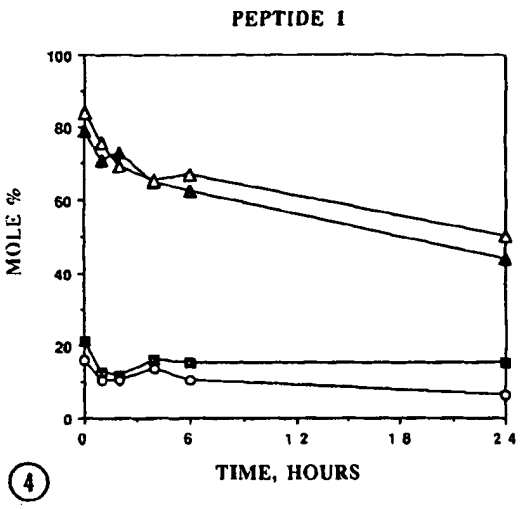

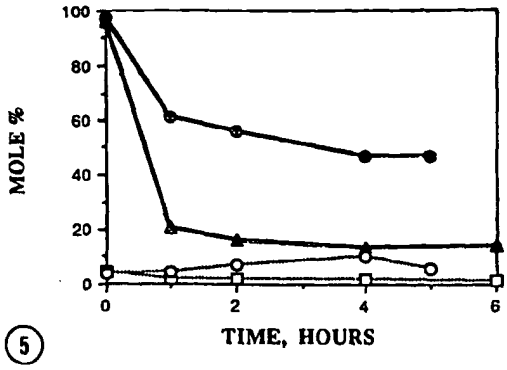

Figure 4. Cell surface binding and internalization of peptide 1 in the presence and absence of pretreatment of HT-29 colon carcinoma cells with 0.1 mM chloroquine. The high level of surface binding of free peptide (solid triangles) is not diminished by chloroquine treatment (open triangles). Internalized free peptide (solid squares) is decreased by up to ca. 60% after 24 hours (open circles) in the presence of chloroquine.

Figure 5. Internalization and cell surface binding of the NRML-05 Fab fragment and a Fab-5.6 peptide 1 conjugate on human FEMX melanoma cells. The cell surface binding of Fab (solid triangles) is more than doubled by attachment of peptide 1 (solid circles) while the very low percentage of Fab which is internalized (open squares) is substantially increased by attachment of peptide 1 (open circles). The y-axis represents the mole percent of the total conjugate which is either internalized or surface bound. Shed counts are not shown.

are antigen-positive for NRLU-10. Chloroquine had no effect on the cell surface bound peptide, as expected since this peptide fraction is not internalized. Chloroquine diminished the internalized peptide by about 50% at 24 hours. Thus some peptide may be internalized into an acidic internal compartment.

For either free Fab or the Fab-1.6 conjugate, chloroquine had essentially no effect on the cell surface conjugate, or on the internalized component (data not shown). Thus peptide 1 when attached to Fab may go to a different intracellular compartment than free peptide. We thus did not see the dramatic increase in internalization reported with the TAT protein into other cells.

Peptide 1-NRML-05 Fab conjugate retention. To test whether peptide 1-mediated increases in Fab retention are antibody-antigen pair specific, as we have observed with an amphipathic negatively charged peptide (13), peptide 1 was conjugated to the Fab fragment of the anti-melanoma antibody NRML-05 (Fig. 5). After reaction and purification by gel filtration as described in the methods section, an average of 5.6 peptides per Fab were attached. Antigen binding as measured by competition ELISA gave apparent inhibition constants of 25 nM (whole antibody), 260 nM (Fab) and 260 nM (Fab-5.6 peptides). This level of derivatization thus does not appear to be deleterious to antigen binding of this Fab, nor does it enhance the Fab's apparent affinity for antigen positive cells.

Results in Fig. 5 show that the cell surface binding to antigen positive FEMX ascites is enhanced by peptide from 15-20% (Fab alone) to over 50% for the conjugate, and that internalization of the Fab

fragment is increased from 2-3% to 8-10% for the conjugate. Thus the enhanced cell surface binding and internalization seen by peptide 1 attachment to Fab fragments is not confined to a single antigen-antibody pair. Chloroquine (100 μM) had no effect n the internalization of this conjugate (data not shown).

DISCUSSION

We have found that attachment of a peptide including residues 37-62 of the HIV TAT protein to two different poorly internalized Fab fragments substantially increased their cell surface binding and entry into cells. A previously examined negatively charged amphipathic peptide (13) increased cell binding and entry for only a single Fab (NRML-05)-antigen pair. Thus the TAT fragment may be more generally useful in this regard. The free peptide analogs appear to be intrinsically sticky, with ca. 45 mole-% of peptide 1 remaining cell surface-bound after 24 hours in vitro.

Attachment of peptide 1 to either NRML-05 or NRLU-10 Fab appears to increase internalization roughly 10-fold, although the levels remain relatively low. This may be a result of increased cell surface binding from 10% to ca. 30% after 1 hour ((NRLU-10 Fab-peptide), and from less than 20% to above 50% after 1 hour ((NRML-05 Fab-peptide). The disappearance of ^{125}I counts from internalized conjugate may be due to catabolism of the labeled Fab fragment with subsequent excretion of ^{125}I from the cell (18). Our results may thus underestimate the internalized conjugate.

The active core of the highly basic TAT protein has been proposed to involve the sequence GRKKR, which is present in both peptides tested here, and which when fused to the N-terminus of beta galactosidase allowed its accumulation in the cell nucleus (10). We have observed that ^{125}I-labeled peptide 1 also accumulates in the nucleus of A431 cells (data not shown), suggesting that the alterations in the sequence of the analog used here may not destroy its nuclear localization. Internalization does not appear to be limited by Fab binding to antigen, since internalized amounts of Fab or conjugate appear similar in antigen positive and negative cells. Although chloroquine modestly increases internalization of free peptide 1, it fails to increase internalized counts of either of the two Fab conjugates. Thus an internal acidic compartment does not appear to be involved in conjugate entry into cells. Poly(L-lysine), previously used as a polycationic drug carrier (20), increases the weak base-sensitive internalization and potency of conjugated antiviral antisense DNA fragments (21). Thus although the TAT-derived peptides used here contain a core of basic residues, their internalization appears different than that of the much larger 14 kDa polylysine conjugate.

It might be expected that attempts to increase the retention of a Fab fragment by addition of a less specific secondary interaction could decrease the specificity of Fab interaction with the tumor cell, as we have observed with a negatively charged amphipathic peptide (13). This is observed, except in the case of the 1:1.07 NRLU-10 Fab-peptide 1 binding to the cell surface of A431 cells. Since the apparent inhibition constant of this conjugate is not decreased in ELISA experiments, the increased apparent retention may be due to a kinetic effect (slower desorption rate) instead of tighter equilibrium binding. Derivatization with 1.6 peptides/Fab appears to abolish the remaining specificity of cell surface binding, but enhances the level of internalization of the conjugate to that of the whole antibody. Thus internalization may be due to the fraction of conjugate which can bivalently or multivalently bind to cells. The fraction which binds specifically to the cell surface may include underivatized Fab. If the derivatives

were binomially distributed am ng 3 states for Fab-1.1, roughly 1/4 would be underivatized, 1/2 w uld be mono-derivatized, and 1/4 would be derivatized with two peptides. Th mono-derivatized Fab may be more specifically attached to the cell but less efficiently internalized. It is also possible that an additional lysin in a hypervariable loop is derivatized at the higher level of modification of Fab-1.6, resulting in a loss of specificity.

Since a conjugate retaining some specificity of cell surface binding with enhanced retention properties can be produced with NRLU-10 Fab, production of site-directed derivatives by cloning and mutagenesis of the Fab fragment to include a unique surface cysteine for attachment might be useful to further explore the effect of the site of peptide derivatization on cell binding specificity. Peptide 1 genetically fused to NRLU-10 Fab, away from the hypervariable loops, might be of interest to separate the properties of Fab with 1 or 2 peptides attached. The lack of specificity of the Fab-1.6 conjugate might restrict its potential use, or that of similar conjugates lacking specificity but possessing improved cellular retention, to delivery of agents which themselves impart specificity of action such as antisense RNA or ribozymes, to injection at specific sites, or to ex vivo use against selected cell populations.

REFERENCES

1. Hnatowich, D.J. (1990). Nucl. Med. Biol. 17, 49-55.
2. Green, M. and Loewenstein, P.M. (1989). Cell 55, 1179.
3. Green, M. Ishino, M. and Loewenstein, P.M. (1989). Cell 58, 215.
4. Weeks, K.M., Ampe, C., Schultz, S.C., Steitz, T.A., and Crothers, D.M. (1990). Science 249, 1281-5.
5. Frankel, A.D. and Pabo, C.O. (1989). Cell 55, 1189-93.
6. Frankel, A.D., Bredt, D.S. and Pabo, C.O. (1988). Science 20, 7073.
7. Abrams, P.G., Carrasquillo, J.A., Schroff, R.W., Eary, J.F., Fritzberg, A.R., Morgan, A.C., Wilbur, D.S., Beaumier, P.L., Larson, S.M. and Nelp, W.B. (1987) in Principles of Cancer Biotherapy (R.K. Oldham, ed.), Raven Press, New York, p. 337 ff.
8. Balaban, E.P., Walker, B.S., Cox, J.V., Tin Sein, A.A., Abrams, P.G., Salk, D., Sheehan, R.G., and Frenkel, E.P. (1991). Clin. Nucl. Med. 16, 732.
9. Friedman, S., Sullivan, K., Salk, D., Nelp, W.B., Griep, R.J., Johnson, D.H., Blend, M.J., Aye, R., Suppers, V. and P.C. Abrams (1990). Hematol./Oncol. Clinics of North America 4, 1069.
10. Ruben, S., Perkins, A., Purcell, R., Joung, K., Sia, R., Burghoff, R., Haseltine, W.A., and C.A. Rosen (1989). J. Virol. 63, 1-8.
11. Kuppuswamy, M., Subramanian, T., Srinivasan, A., and Chinnadurai, G. (1989). Nucleic Acids Res. 17, 3551-61.
12. Garcia, J.A., Harrich, D., Pearson, L., Mitsuyasu, R., and Gaynor, R.B. (1988). EMBO J. 7, 3143-47.
13. Anderson, D.C., Manger, R., Schroeder, J., Woodle, D., Barry, M., Morgan, A., and Fritzberg, A.R. (1993). Bioconj. Chem. 4, 10-18.
14. Tam, J.P., Heath, W.F., and Merrifield, R.B. (1983). J. Am. Chem. Assoc. 105, 6442.
15. Meltzer, N., Tous, G.I., Gruber, S. and Stein, S. (1987). Anal. Biochem. 160, 356.
16. Woodhouse, C., Bordonaro, J., Beaumier, P., and Morgan, A. (1990) in Human Melanoma, from Basic Research to Clinical Application. S. Ferrone, et al., eds. Springer-Verlag, 413-429.
17. Varki, N., Reisfeld, R. and Walker, L. (1984). Antigens associated with a human lung adenocarcinoma defined by monoclonal antibodies. Cancer Res. 44, 681-7.
18. Press, O., Hansen, J.A., Farr, A., and Martin, P.D. (1988). Cancer Res. 48, 2249-2257.
19. REDUCEP v.4.8a was obtained from Koerber Research Company, 818 Narco Road, Encinitas, CA 92024.
20. Ryser, H.J. and Shen, W.C. (1978). Proc. Nat. Acad. Sci. USA 75, 3867-70.
21. Leonetti, J.-P., Degols, G., and Lebleu, B. (1990). Bioconjugate Chem. 1, 149-53.

STIC-ILL

NPL

From: Sullivan, Daniel
Sent: Tuesday, October 22, 2002 2:19 PM
T : STIC-ILL
Subject: Request

Please send the following:

Nat Biotechnol. 1998 Sep;16(9):857-61.

Proc Natl Acad Sci U S A. 1997 Sep 30;94(20):10699-704.

Nat Med. 1998 Dec;4(12):1449-52.

Immunity. 1998 Jan;8(1):57-65.

J Immunol. 1999 May 1;162(9):5205-11.

J Immunol Methods. 1998 Mar 1;212(1):41-8.

Nat Biotechnol. 1998 May;16(5):440-3.

Cell. 1997 Jan 24;88(2):223-33.

Biochem Biophys Res Commun. 1993 Jul 30;194(2):876-84.

Proc Natl Acad Sci U S A. 1994 Jan 18;91(2):664-8.

J Cell Biol. 1995 Mar;128(5):919-27.

FEBS Lett. 1998 May 8;427(2):203-8.

Nat Med. 1999 Jan;5(1):29-33.

Thank you.

Daniel M. Sullivan
Examiner AU 1636
Room: 12D12
Mail Box: 11E12
Tel: 703-305-4448

09937837

Killing HIV-infected cells by transduction with an HIV protease-activated caspase-3 protein

ADITA M. VOCERO-AKBANI[1,2], NANCY VANDER HEYDEN[2], NATALIE A. LISSY[1,2], LEE RATNER[2] & STEVEN F. DOWDY[1,2]

[1]Howard Hughes Medical Institute and [2]Division of Molecular Oncology, Departments of Pathology and Medicine, Washington University School of Medicine, St. Louis, Missouri 63110, USA
Correspondance should be addressed to S.F.D.; email: dowdy@pathology.wustl.edu

At present, treatment of HIV infection uses small inhibitory molecules that target HIV protease; however, the emergence of resistant HIV strains is increasingly problematic. To circumvent this, we report here a new 'Trojan horse' strategy to kill HIV-infected cells by exploiting HIV protease. We engineered a transducing, modified, apoptosis-promoting caspase-3 protein, TAT–Casp3, that substitutes HIV proteolytic cleavage sites for endogenous ones and efficiently transduces about 100% of cells, but remains inactive in uninfected cells. In HIV-infected cells, TAT–Casp3 becomes processed into an active form by HIV protease, resulting in apoptosis of the infected cell. This strategy could also be applied to other pathogens encoding specific proteases, such as hepatitis C virus, cytomegalovirus and malaria.

Production of infectious virions from HIV-infected cells depends on expression of HIV protease for cleavage and maturation of structural Gag and Gag-Pol polyproteins[1–5]. Thus, treatment of HIV infection now uses small molecule protease inhibitors[6]; however, selection for resistant protease proteins, involving single or double mutations, has been widely documented and is increasingly problematic[4,7–9]. Moreover, HIV-infected cells that respond to protease inhibitors show significantly increased longevity[6]. Thus, an alternative approach for treating HIV patients that results in the death or apoptosis of infected cells, thereby limiting or eliminating virus production, while leaving uninfected cells unharmed, would offer a considerable advantage over treatments now available.

Activation of caspase-3 (Casp3) has been shown to be a 'rubicon' of apoptosis by cleavage of the inhibitor of caspase-activated DNAse, resulting in the activation of caspase-activated DNAse and, ultimately, cell death[10–15]. In addition, activated Casp3 can catalyze the activation of inactive Casp3, thereby further amplifying the apoptotic signal. Casp3 zymogen contains an N-terminal Pro domain, followed by a caspase cleavage recognition site, then the p17 domain that contains the catalytic Cys residue, a second caspase cleavage site and finally the p12 domain (Fig. 1*a*). The zymogen form of Casp3 remains inactive; however, during apoptotic signaling, it is cleaved by upstream caspases, such as caspase-8 in T cells[11], resulting in loss of the Pro domain and an active p17:p12 heterotetramer[13].

Rather than attempting to inactivate the viral replication machinery, we report here a new 'Trojan horse' strategy to treat HIV-infected cells that exploits the HIV protease to kill the infected cell while leaving uninfected cells unharmed. To do so, we engineered a modified caspase 3 protein, TAT–Casp3, that transduces about 100% of infected and uninfected cells. However, because of the substitution of endogenous cleavage sites for HIV proteolytic cleavage sites[16], TAT–Casp3 is only specifically activated by HIV protease in infected cells, resulting in apoptosis, whereas in uninfected cells it remains in the inactive zymogen form. By substituting proteolytic cleavage sites, this strategy could be applied to other pathogens encoding specific proteases, such as hepatitis C virus[17], cytomegalovirus[18] and malaria[19].

Results

We first generated a modified Casp3 protein by deleting two residues from the two endogenous caspase cleavage sites (Asp-Ser) on Casp3 and inserting fourteen residues encompassing the HIV p17–p24 gag cleavage site ('A' site) and a p7–p1 cleavage site ('D' site) (ref. 20; Fig. 1*a*). To introduce the modified Casp3 protein into cells, we used our published method of transducing cells directly with full-length proteins[21–24]. Bacterially produced, misfolded fusion proteins containing an in-frame N-terminal protein transduction domain from HIV TAT are capable of transducing, in a rapid and concentration-dependent manner, about 100% of all target cell types, including peripheral blood lymphocytes, all cells present in whole blood, diploid fibroblasts, fibrosarcoma cells, hepatocellular carcinoma cells and leukemic T cells[21–24]. The Pro domain of the modified Casp3 was removed and substituted with the TAT transduction domain, resulting in TAT–Casp3^{WT} fusion protein (Fig. 1*a*). In addition, a catalytically inactive TAT–Casp3 mutant protein was generated by substituting a Met residue for the Casp3 active site Cys^{163} residue (TAT–Casp3^{MUT}).

To test the ability of TAT–Casp3 proteins to transduce cells, TAT–Casp3 proteins were conjugated to fluorescein (FITC), then added directly to the media of Jurkat T cells and analyzed by flow cytometry (FACS) (Fig. 1*b* and *c*). Both TAT–Casp3^{WT} and TAT–Casp3^{MUT} proteins rapidly transduced about 100% of cells, achieving maximum intracellular concentration in less than 20 min. In addition, given the narrow peak width before and after addition of FITC-labeled proteins, individual cells within the population contain nearly identical intracellular concentrations of TAT–Casp3–FITC protein. Confocal microscopic analysis showed the presence of TAT–Casp3–FITC proteins in both cyto-

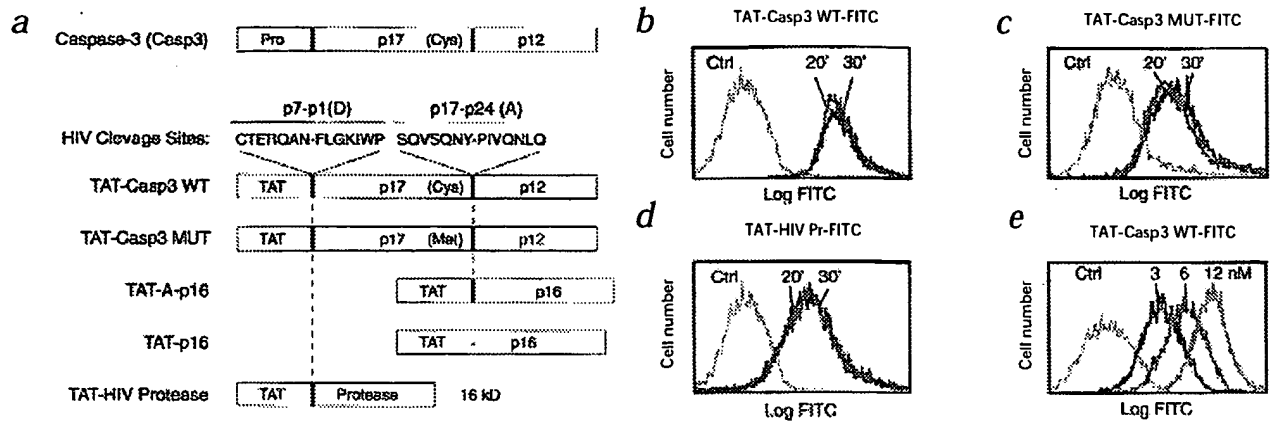

Fig. 1 Generation and transduction with TAT fusion proteins. *a*, HIV cleavage site sequences and domains of TAT fusion proteins. *b–d*, FACS kinetic analysis of fluorescein (FITC)-labeled TAT–Casp3^{WT}, TAT–Casp3^{MUT} and TAT–HIV Pr proteins added to cells at 0 (green), 20 (red) and 30 (purple) min. *e*, FACS dose analysis 1 h after addition 3 (purple), 6 (red) or 12 (blue) nM TAT–Casp3^{WT}–FITC protein to cells. There was rapid, concentration-dependent transduction of about 100% of cells by all FITC-labeled protein and nearly identical intracellular concentrations within the population (as measured by FACS peak width of control (green) compared with transduced cells).

plasmic and nuclear compartments, and not merely attached to the cellular membrane (data not shown). FACS analysis of transduced cells at equilibrium 1 hour after the addition of 3, 6 or 12 nM TAT–Casp3^{WT}–FITC protein demonstrated protein transduction is concentration dependent (Fig. 1*e*). Thus, TAT–Casp3 proteins readily transduce 100% of all cells in a rapid and concentration-dependent fashion.

To test HIV protease cleavage of heterologous substrates after transduction, we devised a model substrate by inserting HIV proteolytic cleavage sites into a TAT–p16 fusion protein[21,22,24]. The HIV A cleavage site was inserted between the TAT and p16 domains, yielding TAT–A–p16 fusion protein (Fig. 1*a*). In addition, we generated a transducing HIV protease (TAT–HIV Pr) (Fig. 1A). FITC-labeled TAT–A–p16 (data not shown), TAT–16 proteins[21,24] and TAT–HIV Pr protein (Fig. 1*d*) also rapidly transduced 100% of cells. To assay for *in vivo* cleavage, p16(-) Jurkat T cells were transduced with 100 nM TAT–A–p16 or control TAT–p16 protein (no HIV cleavage site) alone or in combination with 50 nM TAT–HIV Pr fusion protein for 5 hours and analyzed by anti-p16 immunoblot for *in vivo* cleavage at the HIV A proteolytic cleavage site (Fig. 2*a*). Co-transduction of TAT–A–p16 protein substrate with TAT–HIV Pr resulted in specific substrate cleavage, whereas control TAT–p16 protein (no HIV cleavage site) was not cleaved. Size analysis of the cleaved TAT–A–p16 protein was consistent with retention of the residual HIV half-site present on the N terminus of p16 (Fig. 2*a*, lanes 4 and 5). Moreover, the HIV A site was preferentially cleaved rather than a D site containing TAT–D–p16 protein in this assay (data not shown). We next transduced cells with TAT–Casp3^{MUT} protein in combination with TAT–HIV Pr protein (Fig. 2*b*). Co-transduction with TAT–Casp3 and TAT–HIV Pr resulted in detection of specific cleavage of TAT–Casp3 at the HIV A site between the p17 and p12 domains in an HIV protease-dependent fashion, yielding a TAT–D site–p17–A half-site protein. These observations demonstrate that transduced TAT–A–p16 and TAT–Casp3 proteins containing heterologous HIV cleavage sites can be recognized as substrates by TAT–HIV protease in cell culture.

We next tested the ability of TAT–Casp3 protein to induce

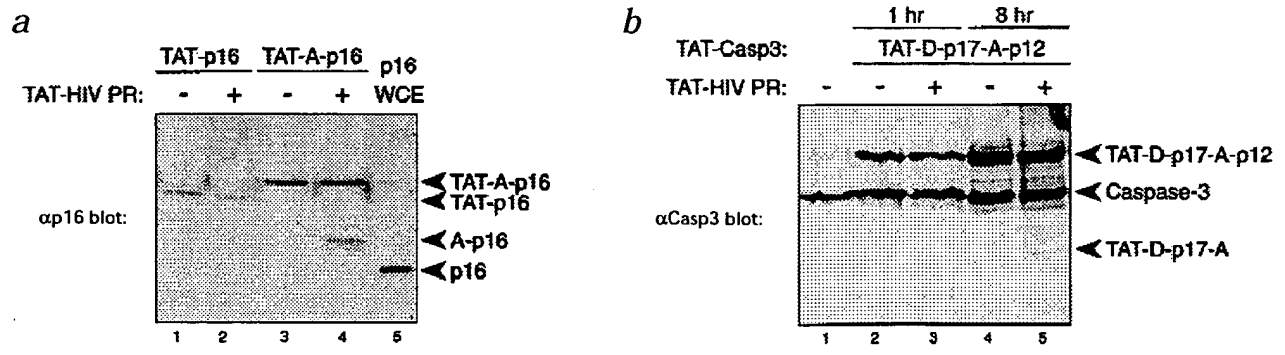

Fig. 2 *In vivo* substrate processing in co-transduced cells. *a*, Cultures of p16(-) Jurkat T cells were transduced with TAT–p16 or TAT–A–p16 substrate proteins in combination with TAT–HIV Pr proteins for 5 h and analyzed by anti-p16 immunoblot. Co-transduction of TAT–A–p16 protein with TAT–HIV Pr protein resulted in specific cleavage at the HIV A site. p16 WCE (far right lane), HepG2 whole-cell lysate containing wild type endogenous p16; A-p16 (right margin of blot), cleaved TAT–A–16 product retaining the HIV half-site on p16. *b*, Cultures of Jurkat T cells were transduced with TAT–Casp3^{MUT} protein (TAT–D site–p17 domain–A site–p12 domain) alone or in combination with TAT–HIV Pr protein and immunoblotted with anti-caspase-3 antibodies specific for the p17 domain. TAT–D–p17–A (right margin of blot), cleaved product of TAT–Casp3 containing the N-terminal HIV A half-site.

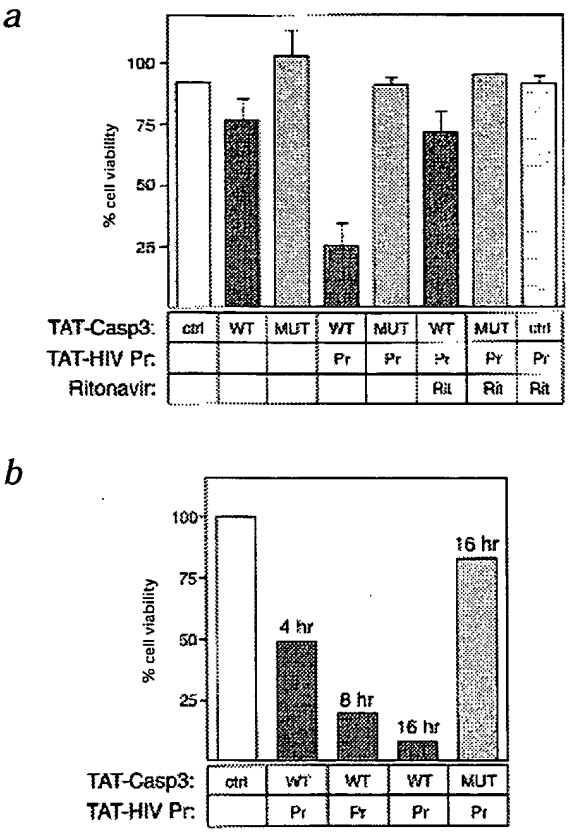

Fig. 3 Activation of TAT-Casp3 and apoptotic induction in co-transduced cells. *a*, Cultures of Jurkat T cells were transduced with combinations of TAT-Casp3^{WT} (WT), TAT-Casp3^{MUT} (MUT) and TAT-HIV protease (Pr) proteins for 16 h and analyzed for cell viability. Co-transduction with TAT-Casp3^{WT} and TAT-HIV Pr protein resulted in specific cytotoxicity, whereas transduction with TAT-Casp3^{MUT} and TAT-HIV Pr did not. Inclusion of HIV protease inhibitor Ritonavir (Rit) blocked activation of the TAT-Casp3^{WT} protein and protected cells from cytotoxic effects. *b*, Cultures of Jurkat T cells were co-transduced with TAT-Casp3^{WT} (WT) or TAT-Casp3^{MUT} (MUT) proteins in combination with TAT-HIV Pr (Pr) protein and analyzed for kinetics of cell viability. Ctrl, control (PBS addition to culture).

apoptosis in cells co-transduced with TAT-HIV Pr protein. Jurkat T cells were treated with 100 nM TAT-Casp3^{WT} or TAT-Casp3^{MUT} proteins alone or in combination with 50 nM TAT-HIV Pr protein and assayed for cell viability 16 hours after treatment (Fig. 3*a*). Transduction of cells with TAT-Casp3^{WT} protein alone demonstrated a small amount of cytotoxicity. However, co-transduction of cells with TAT-Casp3^{WT} and TAT-HIV Pr protein resulted in considerable cytotoxicity. Co-transduction of cells with TAT-Casp3^{MUT} and TAT-HIV Pr protein showed only a small amount of cytotoxicity and also demonstrated an absence of TAT-HIV Pr cytotoxic effects on cells. To further demonstrate the requirement for HIV protease to activate TAT-Casp3 protein, cells were first pretreated with the HIV protease inhibitor Ritonavir (1 μg/ml), then co-transduced with TAT-Casp3^{WT} or TAT-Casp3^{MUT} in combination with TAT-HIV Pr protein (Fig. 3*a*). Pretreatment of cells with Ritonavir resulted in protection from the cytotoxic effects of TAT-Casp3^{WT} protein when co-transduced with TAT-HIV Pr protein. Kinetic analysis of TAT-Casp3-dependent cell death demonstrated a linear killing curve with cellular death detected as early as 4 hours after transduction (Fig. 3*b*). These results demonstrate that cytotoxicity occurs only in the presence of catalytically active TAT-Casp3^{WT} protein and that activation of TAT-Casp3^{WT} specifically requires active HIV protease, consistent with HIV protease cleavage of TAT-Casp3 (Fig. 2*b*).

Activation of endogenous Casp3 results in DNA degradation and apoptosis[10-15]; therefore, we assayed transduced cultures for degraded genomic DNA by TUNEL assay[25], an apoptotic end-marker. Transduction of cells with 100 nM TAT-Casp3^{WT}, 100 nM TAT-Casp3^{MUT} or 50 nM TAT-HIV Pr protein alone showed only background levels of TUNEL-positive cells (Fig. 4*a*). However, co-transduction with TAT-Casp3^{WT} and TAT-HIV Pr protein resulted in a considerable increase in TUNEL-positive cells. Co-transduction with TAT-Casp3^{MUT} and TAT-HIV Pr protein produced only a background level of TUNEL-positive cells (Fig. 4*a*). We also assayed for activation of TAT-Casp3 by assessing its ability to cleave an artificial caspase-3 substrate. Jurkat T cells were treated with 100 nM TAT-Casp3^{WT} or TAT-Casp3^{MUT} proteins alone or in combination with 50 nM TAT-HIV Pr protein for 6 hours and then assayed for cleavage of DEVD-AFC (ref. 26) by release of fluorescent AFC (Fig. 4*b*). Consistent with our TUNEL results, co-transduction with TAT-Casp3^{WT} and TAT-HIV Pr proteins resulted in a substantial increase in caspase activity that was greater than a positive control of cross-linking the pro-apoptotic FAS death receptor with antibodies (αFAS).

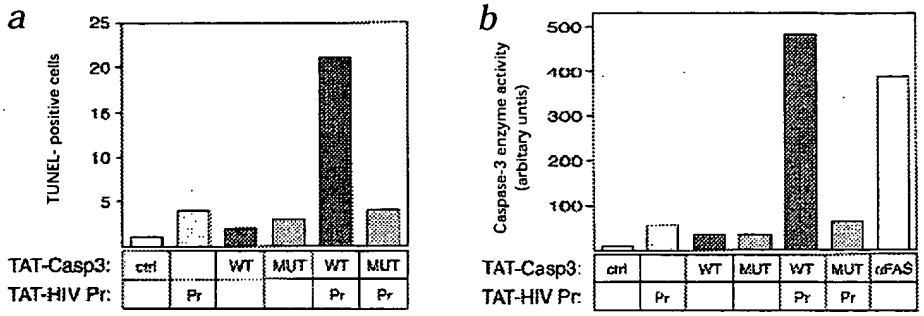

Fig. 4 HIV protease activates TAT-Casp3^{WT} protein. *a*, Cultures of Jurkat T cells co-transduced with TAT-Casp3^{WT} (WT) and TAT-HIV protease (Pr) protein resulted in specific TUNEL-positive cells. However, transduction by TAT-Casp3^{MUT} (MUT) in combination with TAT-HIV Pr protein and transduction by TAT-Casp3^{WT}, TAT-Casp3^{MUT} or TAT-HIV Pr proteins alone produced only background levels of TUNEL-positive cells. Vertical axis, TUNEL-positive cells per high-powered microscopic field; Ctrl, control (addition of PBS to cultures); error bars represent s.d. *b*, Transduction by TAT-Casp3^{WT} (WT) in combination with TAT-HIV protease (Pr) results in specific activation of caspase-3 activity as measured by DEVD-AFC cleavage and AFC fluorescence reported as enzyme activity. Ctrl, control (PBS addition); αFAS crosslinking, positive control.

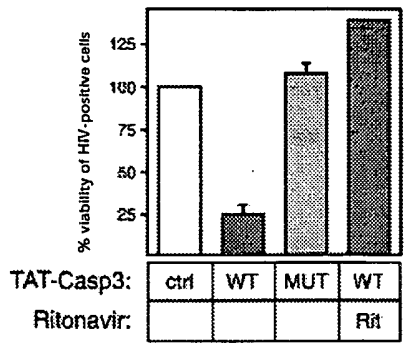

Fig. 5 Specific killing of HIV-infected cells. Jurkat T cells were infected for 7–14 days with HIV strain NLHX, then transduced with TAT-Casp3^{WT} (WT) or TAT-Casp3^{MUT} (MUT) proteins for 16 h and assayed for cell viability. TAT-Casp3^{WT} protein efficiently kills a large percentage of HIV positive cells with a single administration, whereas the catalytically inactive TAT-Casp3^{MUT} proteins has no effect. Pretreatment of HIV-infected cells with the HIV protease inhibitor Ritonavir (Rit) protects infected cells from being killed by TAT-Casp3^{WT} protein. Ctrl, control (addition of PBS to cultures); vertical axis, % viability of HIV positive cells in the population at start of transduction; error bars represent s.d.

Transduction with TAT-Casp3^{WT}, TAT-Casp3^{MUT} or TAT-HIV Pr alone showed only background levels of caspase activity. In addition, we detected the appearance of cells containing <2n DNA content in cells co-transduced with TAT-Casp3 and TAT-HIV Pr (data not shown), a 'hallmark' of caspase-3-induced apoptosis, rather than necrosis[13]. These observations demonstrate that after transduction, TAT-Casp3^{WT} protein remains inactive in cells lacking HIV protease, but becomes specifically activated in cells with active HIV protease inducing of apoptosis and ultimately death.

Because there is not a general animal model for HIV, we sought to determine if TAT-Casp3^{WT} protein could kill cells infected with live HIV in culture. Jurkat T cells were infected for 7–14 days with the NLHX strain[27] of HIV-1 and then examined with a microscope for HIV cytopathic effects. At the beginning of each transduction experiment, approximately 50% of the culture was HIV-positive. HIV-infected cultures were transduced for 16 hours with 100 nM TAT-Casp3^{WT} or TAT-Casp3^{MUT} protein and then assayed for cell viability (Fig. 5). Treatment of HIV-infected cells with TAT-Casp3^{WT} protein resulted in a substantial loss of HIV positive cells from the cultures. We also detected both the appearance of cells containing <2n DNA content and cells with condensed nuclei in cells treated with TAT-Casp3 (data not shown). However, transduction with TAT-Casp3^{MUT} protein produced negligible effects. To determine if apoptosis induced by TAT-Casp3^{WT} was dependent on active HIV protease in the infected cultures, HIV-infected cultures were pretreated with 1 μg/ml Ritonavir and then transduced with 100 nM TAT-Casp3^{WT} protein (Fig. 5). Consistent with the results above, pretreatment of HIV-infected cultures with Ritonavir resulted in protection from apoptosis induced by TAT-Casp3^{WT}. In addition, the observed increased survival of Ritonavir-treated cells is consistent with increased longevity of HIV-infected cells treated with protease inhibitor[6]. These observations demonstrate specific killing of HIV-infected cells by the transducing protein TAT-Casp3^{WT} protein containing active HIV protease and the lack of apoptotic induction in cells devoid of HIV protease activity.

Discussion

We demonstrate here a proof-of-concept for a new strategy to kill HIV-infected cells that harnesses the HIV-encoded protease by using a modified zymogen form of an apoptotic inducer, Casp3, combined with a protein transduction delivery system. Transduction of cells with proteins is a rapid, concentration-dependent process that targets 100% of cells in a receptor-independent manner[21–24], allowing for equally efficient transduction of both infected and uninfected cells with TAT-Casp3^{WT} protein. TAT-Casp3 protein remains inactive in uninfected cells and is specifically activated by HIV protease-dependent cleavage in HIV-infected cells. This degree of specificity indicates that killing HIV-infected cells using such a strategy may result in a high therapeutic index in patients. Future optimization will focus on HIV cleavage site efficiencies and modification of TAT-Casp3 to avoid binding by cellular inhibitor of apoptosis proteins[10–13]. We have also had some success pursuing a strategy of using for transduction an enzyme (TAT-A site-HSV TK protein) that converts a 'pro-drug' (gancyclovir) into a cytotoxic form specifically in HIV-infected cells (unpublished observations). Moreover, construction of additional pro-apoptotic transducing zymogens, such as Bid[28,29] and other non-naturally occurring zymogens, that are activated by specific pathogen proteases may also have therapeutic potential.

The treatment of HIV-infected cells with protease inhibitors results in increased longevity of infected cells[30,31]. In direct contrast to this, TAT-Casp3 protein specifically kills HIV-infected cells. Moreover, selection for mutations that renders HIV protease resistant to a broad spectrum of inhibitors is a continuing and growing problem in combating the HIV epidemic[6–9]. However, by substituting HIV cleavage sites, our approach allows for the continual adaptability of TAT-Casp3 proteins to HIV strain proteolytic cleavage site variance and/or mutation. Furthermore, given that both protease and reverse transcriptase molecules are packaged inside the virion[32], TAT-Casp3 proteins may also be packaged inside the virion and, if so, could either kill the virion after it buds from the cell and/or initiate apoptosis immediately after subsequent infection of a naive cell. In addition to HIV, infectious pathogens such as hepatitis C virus[17], cytomegalovirus[18] and malaria[19] are dependent on pathogen-encoded proteases for their life cycles. Thus, the generation of modified TAT-Casp3 proteins containing these pathogen-specific protease cleavage sites may prove helpful in combating other infectious diseases and human malignancies that have either upregulated cellular proteases or express specific cellular proteases.

Methods

Cell culture. p16(-) Jurkat T cells (ATCC) were grown as described[22]. For *in vivo* substrate cleavage, 1 × 10^6 cells were transduced with 100 nM TAT-p16, TAT-A-p16, TAT-Casp3^{MUT} and/or 50 nM TAT-HIV Pr proteins for 1, 5 or 8 h and analyzed by anti-p16 (Santa Cruz Biotechnology, Santa Cruz, California) or anti-Casp3 (PharMingen, San Diego, California) immunoblot analysis[21]. To determine cytotoxicity of TAT-Casp3 on uninfected cells, 1 × 10^5 cells were transduced with 100 nM TAT-Casp3^{WT}, TAT-Casp3^{MUT} and/or 50 nM TAT-HIV Pr proteins for 16 h and assayed for viability by Trypan Blue exclusion and/or genomic DNA damage by TUNEL assay (Trevigen, Gaithersburg, Maryland). The number of TUNEL-positive cells are reported as 'per high-powered microscopic field' with four fields per experiment averaged. TAT-Casp3 activity was measured by incubation of 20 μg of whole-cell lysate with 50 μM DEVD-AFC and fluorescent AFC formation measured on a FL500 microplate fluorescence reader (Bio-Tek, New York, New York) as described[25]. Cells were preincubated with 1 μg/ml Ritonavir (Abbott, Chicago, Illinois) for 1 h before transduction. To determine cytotoxicity of TAT-Casp3

on infected cells, Jurkat cultures were infected with 100 ng p24 Ag equivalent NLHX HIV-1 strain[26] for 7–14 days, assayed microscopically for cytopathic effects, then replated at 1×10^6 per ml and transduced with 100 nM of TAT–Casp3^{WT} or TAT–Casp3^{MUT} proteins for 16 h followed by exclusionary dye viability analysis. Infected cells were pretreated with 1 μg/ml Ritonavir for 24 h before transduction with TAT–Casp3^{WT} protein. For flow cytometry (FACS) analysis, fluorescein (FITC)-conjugated TAT fusion proteins were added to Jurkat T cell culture media and 1×10^4 cells were analyzed by FACS as described[21].

TAT fusion proteins. The pTAT–A/D–p16 expression vectors were constructed by inserting double-stranded oligomeric nucleotides encoding 14 residues of the HIV p17–p24 ('A')[16,18] cleavage site (SQVSQNY-PIVQNLQ) or the HIV p7-p1 ('D')[16,18] cleavage site (CTERQAN-FLGKIWP) into the *Nco*I site of pTAT–p16 (refs. 23, 24). The pTAT–Casp3^{WT} vector was constructed by independent PCR amplification of the p17 and p12 domains containing engineered HIV A and D cleavage sites (14 residues) into the primers (p17 forward primer: 5'–CGCCTCGAGGGCGGCTGCACCGAACGCCAGGCTAACTTC-CTGGGCAAAATCTGGCCAGGCGGAATATCCCTGGACAACAGTTATAAAATG–3'; p17 reverse primer: 5'–CCGCCCTGCAGGTTCTGCACGATTGGATAGTTCT-GTGACACCTGGGAGCCGCCTGTCTCAATGCCACAGTCCAG–3'; p12 forward primer: 5'–GGCGGCTCCCAGGTGTCACAGAACTATCCAATCGTGCA-GAACCTGCAGGGCGGTGTTGATGATGACATGGCG–3'; p12 reverse primer: 5'–CGAGCTACGCGAATTCTTAGTGATAAAAATAGAGTTC–3') followed by mixing of the PCR products and then PCR amplification using the p17 forward and p12 reverse primers (the p17 reverse and p12 forward primer sequences overlap). The resultant PCR fragment was subcloned into pTAT–HA (refs. 23,24), resulting in a TAT–D–p17–A–p12 configuration (see Fig. 1A). The pTAT–Casp3^{MUT} vector was constructed by inserting a double stranded oligomeric nucleotide (positive strand: 5'–CCATGCGTGGTACCGAACTG-GACTGTGGCATTGAGACAGGCGGCTCCCAGGTGTCACAGAACTATC-CAATCGTGCAGAACCTGCA–3') containing a Met residue for the active site Cys[163] residue into the *Stu*I and *Pst*I sites of pTAT–Casp3^{WT} vector. The pTAT–HIV Pr vector was constructed by PCR cloning the HIV protease gene from HXB2R HIV strain (forward primer: 5'–CGGTCCATGGGCGGCGGCC-CTCAGGTCACTCTTTGGCAACG–3'; reverse primer: 5'–CGGGAATTCT-CAAAAATTTAAAGTGCAACCAATCTG–3') and cloning into pTAT (refs. 23,24). TAT fusion proteins were purified by sonication of high expressing BL21(DE3)pLysS (Novagen, Madison, Wisconsin) cells in 8 M urea, and were then purified over a Ni-NTA column and misfolded on a Mono S column as described[23,24]. FITC-conjugated TAT fusion proteins were generated by fluorescein isothiocyanate labeling (Pierce, Rockford, Illinois), followed by gel purification in PBS on an S-12 column attached to an FPLC (Pharmacia) or PD-10 desalting column (Pharmacia), then were added directly to cells in culture media and analyzed by FACS or microscopy.

Acknowledgments

We thank E.S. Alnemri for the human Casp3 cDNA; K. Wang for help with DEVD-AFC reactions; Abbott Labs for Ritonavir; S. Horning for doing the TUNEL assays; and D. Goldberg, C. Rice, S. Virgin and all the members of the Dowdy and Ratner labs for critical input. This work was supported by the N.I.H. (L.R.) and the Howard Hughes Medical Institute (S.F.D.). S.F.D. is an Assistant Investigator of the Howard Hughes Medical Institute.

RECEIVED 5 AUGUST; ACCEPTED 11 NOVEMBER 1998

1. Lillehoj, E.P. *et al.* Purification and structural characterization of the putative gag-pol protease of human immunodeficiency virus. *J. Virol.* **62**, 3053–3058 (1988).
2. Kohl, N.E. *et al.* Active human immunodeficiency virus protease is required for viral infectivity. *Proc. Natl. Acad. Sci. USA* **85**, 4686–4690 (1988).
3. Göttlinger, H.G., Sodroski, J.G. & Haseltine, W.A. Role of capsid precursor processing and myristoylation in morphogenesis and infectivity of human immunodeficiency virus type 1. *Proc. Natl. Acad. Sci. USA* **86**, 5781–5785 (1989).
4. Kaplan, A.H. *et al.* Selection of multiple human immunodeficiency virus type 1 variants that encode viral proteases with decreased sensitivity to an inhibitor of the viral protease. *Proc. Natl. Acad. Sci. USA* **91**, 5597–5601 (1994).
5. Gatlin, J., Arrigo, S.J. & Schmidt, MG. Regulation of intracellular human immunodeficiency virus type-1 protease activity. *Virology* **244**, 87–96 (1998).
6. Coffin, J.M., Hughes, S.H. & Varmus, H.E. *Retroviruses* (Cold Spring Harbor Press, Cold Spring Harbor, New York, 1997).
7. Condra, J.H. *et al. In vivo* emergence of HIV-1 variants resistant to multiple protease inhibitors. *Nature* **374**, 569–571 (1995).
8. Gulnik, S.V. *et al.* Kinetic characterization and cross-resistance patterns of HIV-1 protease mutants selected under drug pressure. *Biochemistry* **34**, 9282–9287 (1995).
9. Tisdale, M. *et al.* Cross-resistance analysis of human immunodeficiency virus type 1 variants individually selected for resistance to five different protease inhibitors. *Antimicrob. Agents Chemother.* **39**, 1704–1710 (1995).
10. Salvesen, G.S. & Dixit, V.M. caspases: intracellular signaling by proteolysis. *Cell* **91**, 443–446 (1997).
11. Henkart, P.A. ICE family proteases: mediators of all apoptotic cell death? *Immunity* **4**, 195–201 (1996).
12. Cohen, G.M. caspases: the executioners of apoptosis. *J. Biochem.* **326**, 1–16 (1997).
13. Woo, M. *et al.* Essential contribution of caspase 3/Casp3 to apoptosis and its associated nuclear changes. *Genes Dev.* **12**, 806–819 (1998).
14. Enari, M. *et al.* A caspase-activated DNase that degrades DNA during apoptosis, and its inhibitor ICAD. *Nature* **391**, 43–50 (1998).
15. Liu, X. *et al.* DFF40 induces DNA fragmentation and chromatin condensation during apoptosis. *Proc. Natl. Acad. Sci. USA* **15**, 8461–8466 (1998).
16. Ratner, L. *et al.* Complete nucleotide sequence of the AIDS virus, HTLV-III. *Nature* **313**, 277–284 (1985).
17. Rice, C.M. in *Fields Virology* (eds. Fields, B.N., Knipe, D.M. & Howley, P.M.) 931–960 (Lippincott-Raven, Philadelphia, 1996).
18. Welch, A.R., Woods, A.S., McNally, L.M., Cotter, R.J. & Gibson, W. A. Herpesvirus maturational protease, assemblin: identification of its gene, putative active site domain, and cleavage site. *Proc. Natl. Acad. Sci . USA* **88**, 10792–10796 (1991).
19. Francis, S.E., Sullivan, D.J. Jr. & Goldberg, D.E. Hemoglobin metabolism in the malaria parasite Plasmodium falciparum. *Annu. Rev. Microbiol.* **51**, 97–123 (1997).
20. Barrie, K.A. *et al.* Natural variation in HIV-1 protease, gag p7 and p6, and protease cleavage sites within gag/pol polyproteins: amino acid substitutions in the absence of protease inhibitors in mothers and children infected by human immunodeficiency virus type 1. *Virology* **219**, 407–416 (1996).
21. Ezhevsky, S.A. *et al.* Hypo-phosphorylation of the retinoblastoma protein by cyclin D:Cdk4/6 complexes results in active pRb. *Proc. Natl. Acad. Sci. USA* **94**, 10699–10704 (1997).
22. Lissy, N.A. *et al.* TCR-antigen induced cell death (AID) occurs from a late G_1 phase cell cycle check point. *Immunity* **8**, 57–65 (1998).
23. Nagahara, H. *et al.* Highly efficient transduction of full length TAT fusion proteins directly into mammalian cells: p27^{Kip1} mediates cell migration. *Nature Med.* **4**, 1449–1452 (1998).
24. Vocero-Akbani, A. *et al.* Transduction of full length TAT fusion proteins directly into mammalian cells:analysis of TCR-activation induced cell death (AID) in *Methods in Enzymology* (ed. Reed, J.C.) (Academic, San Diego, in the press).
25. Coates, P.J. Molecular methods for the identification of apoptosis in tissues. *J. Histotechnol.* **17**, 261–267 (1994).
26. Xiang, J., Chao, D.T. & Korsmeyer, S.J. Bax-induced cell death may not require interleukin 1B-converting enzyme-like proteases. *Proc. Natl. Acad. Sci. USA* **93**, 14559–14563 (1996).
27. Westervelt, P., Genedelman, H.E. & Ratner, L. Identification of a determinant within the HIV-1 surface envelope glycoprotein critical for productive infection of cultured primary monocytes. *Proc. Natl. Acad. Sci USA* **88**, 3097–3101 (1991).
28. Lou, X., Budihardjo, I., Zou, H., Slaughter, C. & Wang, X. Bid, a Bcl2 interacting protein, mediates cytochrome c release from mitochondria in response to activation of cell surface death receptors. *Cell* **94**, 481–490 (1998).
29. Li, H., Zhu, C.-j. & Yuan, J. Cleavage of BID by caspase 8 mediates the mitochonrial damage in Fas pathway of apoptosis. *Cell* **95**, 491–501 (1998).
30. Wong, J.K. *et al.* Recovery of replication-competent HIV despite prolonged suppression of plasma viremia. *Science* **278**, 1291–1295 (1997).
31. Finzi, D. *et al.* Identification of a reservior for HIV-1 patients on highly active antiretroviral therapy. *Science* **278**, 1295–1300 (1997).
32. Wu, X. *et al.* Functional RT and IN incorporated into HIV-1 particles independently of the Gag/Pol precursor protein. *EMBO J.* **16**, 5113–5122 (1997).

STIC-ILL

MPC
Q11.N26

From: Sullivan, Daniel
Sent: Tuesday, October 22, 2002 2:19 PM
To: STIC-ILL
Subject: Request

Please send the following:

Nat Biotechnol. 1998 Sep;16(9):857-61.

Proc Natl Acad Sci U S A. 1997 Sep 30;94(20):10699-704.

Nat Med. 1998 Dec;4(12):1449-52.

Immunity. 1998 Jan;8(1):57-65.

J Immunol. 1999 May 1;162(9):5205-11.

J Immunol Methods. 1998 Mar 1;212(1):41-8.

Nat Biotechnol. 1998 May;16(5):440-3.

Cell. 1997 Jan 24;88(2):223-33.

Biochem Biophys Res Commun. 1993 Jul 30;194(2):876-84.

Proc Natl Acad Sci U S A. 1994 Jan 18;91(2):664-8.

J Cell Biol. 1995 Mar;128(5):919-27.

FEBS Lett. 1998 May 8;427(2):203-8.

Nat Med. 1999 Jan;5(1):29-33.

Thank you.

Daniel M. Sullivan
Examiner AU 1636
Room: 12D12
Mail Box: 11E12
Tel: 703-305-4448

09937837

Proc. Natl. Acad. Sci. USA
Vol. 91, pp. 664–668, January 1994
Cell Biology

Tat-mediated delivery f heterol gous proteins int cells

STEPHEN FAWELL, JOE SEERY, YASMIN DAIKH, CLAIRE MOORE, LING LING CHEN, BLAKE PEPINSKY, AND JAMES BARSOUM

Biogen Inc., 14 Cambridge Center, Cambridge, MA 02142

Communicated by Phillip A. Sharp, October 7, 1993

ABSTRACT **The Tat protein of human immunodeficiency virus 1 (HIV-1) can enter cells efficiently when added exogenously in tissue culture. To assess if Tat can carry other molecules into cells, we chemically cross-linked Tat peptides (residues 1–72 or 37–72) to β-galactosidase, horseradish peroxidase, RNase A, and domain III of *Pseudomonas* exotoxin A (PE) and monitored uptake colorimetrically or by cytotoxicity. The Tat chimeras were effective on all cell types tested, with staining showing uptake into all cells in each experiment. In mice, treatment with Tat–β-galactosidase chimeras resulted in delivery to several tissues, with high levels in heart, liver, and spleen, low-to-moderate levels in lung and skeletal muscle, and little or no activity in kidney and brain. The primary target within these tissues was the cells surrounding the blood vessels, suggesting endothelial cells, Kupffer cells, and/or splenic macrophages. Tat-mediated uptake may allow the therapeutic delivery of macromolecules previously thought to be impermeable to living cells.**

The potential for intracellular therapeutic use of proteins, peptides, and oligonucleotides has been limited by the impermeable nature of the cell membrane to these compounds. A wide variety of methods have been proposed for the delivery of proteins and other macromolecules into living cells for either experimental or therapeutic uses, including microinjection, scrape loading, electroporation, liposomes (1–7), bacterial toxins (8–10), and receptor-mediated endocytosis (11–16). Most of these methods are either inefficient or time-consuming, cause appreciable cell death, or result in uptake into intracellular vesicles without efficient cytoplasmic delivery. Several approaches (15–18) rely on binding of macromolecules to the cell surface, followed by internalization via the endocytic route. However, since proteins that have entered this pathway remain enclosed within lipid vesicles, they do not have access to the cell cytoplasm, most typically the target environment. It seems reasonable to assume that the escape from endocytic vesicles is the rate-limiting step in achieving true cellular delivery, yet many assays fail to measure this.

Recently the Tat protein from human immunodeficiency virus 1 (HIV-1) was shown to enter cells when added exogenously (19, 20). Tat protein can simply be added to medium at concentrations as low as 1 nM, and biological responses can be detected. Since the assay for this process was the transactivation of a transfected reporter gene, activity reflects those molecules that had been targeted to the nucleus, presumably after cytoplasmic delivery. The mechanism by which Tat traverses a membrane and the precise intracellular location of this event remain unclear. However, Tat binds efficiently to cells, with $>10^7$ sites per cell and then is internalized by an adsorptive endocytosis process (20). In characterizing the uptake process using iodinated Tat, Mann and Frankel (20) observed that only 3% of the Tat became cell-associated. In contrast, using Tat that was metabolically labeled with [^{35}S]methionine, we found that >60% of the Tat became cell-associated. The added radioactivity was rapidly converted into a trypsin-insensitive form, indicating that it had been internalized. We estimate that it is possible to deliver 10^7 molecules per cell into a trypsin-insensitive form.

Experiments in our laboratory and from Frankel's group have shown that fluorescently tagged Tat protein becomes cell surface-associated and is internalized into punctate structures that resemble endosomes/lysosomes; eventually label becomes apparent both cytoplasmically and in the nucleus (20). The basic RNA binding domain of Tat has been implicated in mediating at least the cell surface binding of Tat; indeed, uptake/activation can be blocked by incubation with soluble polyanions, including heparin and dextran sulfate (20). To obtain optimal Tat-dependent transactivation, Frankel and Pabo (19) added the lysosomotropic agent chloroquine and showed subsequently that this treatment reduced degradation of the Tat protein.

The apparent efficiency with which Tat is able to enter cells raised the possibility of utilizing Tat to deliver heterologous macromolecules into cells. Here we show that Tat peptides conjugated to heterologous proteins can confer cellular delivery to these "cargo" proteins. Delivery is independent of cell type, has been successfully applied to four different cargo proteins, and has been shown unambiguously to mediate cytoplasmic delivery. Preliminary *in vivo* experiments confirm that this system may allow the therapeutic use of proteins/peptides with intracellular targets.

MATERIALS AND METHODS

Preparation of Tat Peptides. Tat-(1–72) was expressed in *Escherichia coli* by using a T7 expression vector (21) and was purified by sequential chromatography steps on Q-Sepharose (Pharmacia), gel filtration on an A.5M agarose column in 6.0 M guanidine hydrochloride, and reverse-phase HPLC on a C_4 column (Vydac). The product was >95% pure as judged by analysis by SDS/PAGE. Tat-(37–72) (CFITKALGISYGRKKRRQRRRPPQGSQTHQVSLSKQ in single-letter amino acid code) was synthesized on an Applied Biosystems 430A synthesizer following the manufacturer's recommended procedures and purified by reverse-phase HPLC; integrity was verified by mass spectrometry.

Chemical Conjugation. β-Galactosidase (Sigma) was dissolved in phosphate-buffered saline (PBS) at 25 mg/ml and treated with iodoacetamide (final concentration, 0.37 mg/ml) for 60 min at 23°C. The product was desalted on a G-25 column (Pharmacia) in PBS and concentrated to 32 mg/ml in a Centricon 10 concentrator (Amicon). 4-(Maleimidomethyl)-cyclohexanecarboxylic acid *N*-hydroxysuccinimide ester (SMCC; Pierce) at 1.2 mg/ml in dimethylformamide was added to 60 μg/ml, and after 30 min at room temperature the

The publication costs of this article were defrayed in part by page charge payment. This article must therefore be hereby marked "*advertisement*" in accordance with 18 U.S.C. §1734 solely to indicate this fact.

Abbreviations: HIV-1, human immunodeficiency virus 1; SMCC, 4-(maleimidomethyl)cyclohexanecarboxylic acid *N*-hydroxysuccinimide ester; HRP, horseradish peroxidase; BMV, brome mosaic virus.

reaction mix was desalted on a G-25 c lumn in 100 mM Na_2HPO_4 (pH 7.5). Tat peptide (100 μg) was added to 2 mg f the β-galactosidase-SMCC adduct (7 mg/ml) and st red vernight at 4°C. The cross-linked conjugate was isolated by S-200HR gel filtrati n in PBS and analyzed by SDS/PAGE, Western immunobl tting with anti-Tat antisera, and assay for β-galactosidase activity. Typical preparations had a ratio of one or two Tat peptides per β-galactosidase tetramer and retained >50% of the β-galactosidase enzyme activity. β-Galactosidase activity of conjugates and of cell extracts was measured by using *o*-nitrophenyl β-D-galactopyranoside as a substrate, incubating in 0.1 M sodium phosphate buffer, pH 7.5/1 mM $MgCl_2$ at 37°C for 30 min, stopping the reaction with sodium carbonate (0.625 M final concentration), and reading the absorbance at 420 nm.

To prepare Tat-HRP (horseradish peroxidase) conjugates, we used a commercially available maleimide-activated HRP (Pierce) that is selective for free sulfhydryl groups. Tat peptides (0.5 mg/ml) were incubated with maleimide-conjugated HRP (5 mg/ml) in triethanolamine at pH 8.2 for 80 min at 23°C. The conjugates were analyzed by SDS/PAGE.

PE(III). a fragment (residues 381–613) of *Pseudomonas* exotoxin A (PE) comprising 19 residues of domain Ib and all of domain III of PE, was cloned into a phage T7 expression vector (21) by using the naturally occurring *Apa* I site in the PE sequence to generate a construct encoding the sequence NH_2-Met-Glu-Pro-Val-Val-Ser-Leu-Ser-[PE-(381–613)]-COOH and was expressed in *E. coli* BL21. This portion of PE has no cell-binding or translocation activity. Cells were lysed in a French press and purified from the soluble fraction by ion-exchange chromatography on Q-Sepharose followed by gel filtration on a Superdex 75 fast protein liquid chromatography (FPLC) column. PE(III) and RNase A (Sigma no. R5500) were treated with sulfo-SMCC (Pierce), desalted, and then added to Tat peptides. The resultant preparations were analyzed by SDS/PAGE and shown to consist of 90% conjugated material with an approximately equal ratio of single and double peptide addition.

Animal Studies. Six-month-old BALB/c mice were injected intravenously via the tail vein with 200 μg of Tat-β-galactosidase conjugate or β-galactosidase control in 0.2 ml of PBS. After 20 min the animals were sacrificed by CO_2 intoxication, and various organs and tissues were removed. Tissue was immediately frozen in liquid nitrogen and stored at −80°C. Thin frozen sections (5.0 μm) were cut on a cryomicrotome at −20°C; sections were mounted on coverslips, fixed, and processed for histology as described below.

Histological Staining. HeLa cells were cultured by standard techniques in Dulbecco's minimal essential medium/10% (vol/vol) donor calf serum. Cells were plated at ≈30–50% confluency into six-well dishes or onto sterile coverslips that had been coated with poly(L-lysine), were allowed to attach, and then were incubated (0–18 hr) with control. SMCC-activated, or activated conjugated enzyme preparations diluted in medium at the concentrations indicated. After washing three times with PBS, cells were fixed with 2.0% formaldehyde/0.2% glutaraldehyde in PBS, washed again with PBS/2 mM $MgCl_2$, and then developed with the appropriate chromogenic substrate. For β-galactosidase staining, the fixed cells were incubated in 1 mg of X-Gal (5-bromo-4-chloro-3-indolyl β-galactoside) per ml/5 mM $K_3Fe(CN)_6$/5 mM $K_4Fe(CN)_6$/2 mM $MgCl_2$. For HRP, cells were incubated with diaminobenzidine (Sigma) and H_2O_2 according to the manufacturer's instructi ns. When the desired degree of staining intensity was reached, the reaction was terminated by washing in distilled water.

Cytotoxicity Assay. The cytotoxicity of PE(III) and RNase was assessed by the ability to inhibit protein synthesis, measured by [^{35}S]methionine incorporati n into CCl_3COOH-insoluble material. Cells were plated into either 24- or 48-well dishes at ≈50% confluence and allowed to attach. Protein conjugates or controls were added in 100 μl of PBS at the concentrati ns indicated and incubated for 1 hr at 37°C, after which medium was added t 0.5 ml. After a further 3–18 hr f incubation, the medium was rem ved, and cells were washed in PBS and then incubated with 1.0 μCi (37 kBq) of [^{35}S]methionine per well in either PBS or methionine-deficient minimal essential medium. After 2 hr the medium was removed, and the cells were washed three times with cold 5.0% CCl_3COOH, washed once with PBS, and then extracted with 0.1 ml of 0.5 M NaOH. The CCl_3COOH-precipitable material was quantified by liquid scintillation counting.

***In Vitro* Assays.** The activity of expressed/purified PE(III) was determined by the inhibition of translation of brome mosaic virus (BMV) RNA in a rabbit reticulocyte lysate following the manufacturer's protocols (Promega). Translations were carried out with [^{35}S]methionine and analyzed by SDS/PAGE and autoradiography; the BMV-encoded bands were quantified with a Molecular Dynamics densitometer. RNase A activity was assessed by conversion of a tRNA substrate from CCl_3COOH-insoluble to soluble material.

RESULTS AND DISCUSSION

Since the Tat protein from HIV-1 can enter cells when added extracellularly, we decided to test if Tat could be used as a carrier to deliver heterologous molecules into cells. Chemically crosslinked conjugates of the enzymes β-galactosidase and HRP were prepared with either Tat-(1–72) or Tat-(37–72). Truncated Tat-(37–72) was selected because it retains the basic domain implicated in binding/uptake and lacks the cysteine-rich region of Tat (residues 22–37) that has complicated the handling and analysis of peptides/conjugates (B.P., unpublished results). Tat-(37–72) retains the cellular delivery function of Tat-(1–72) (see below). The degree of conjugation was monitored by SDS/PAGE and adjusted so that only one or two peptides per β-galactosidase tetramer or one peptide per HRP molecule was incorporated. Under these conditions the conjugates were shown to retain essentially full enzymatic activity.

Samples were then applied to cells under standard tissue culture conditions and evaluated for uptake by histology using chromogenic enzyme substrates. Even at the highest concentration tested (20 μg/ml) there was no staining with either control enzyme lacking the Tat peptides (Fig. 1 *a* and *d*). HRP has been used by others as a fluid-phase uptake marker, but in these experiments very high concentrations (>200 μg/ml) have typically been used (22), and in our hands similar experiments result in staining levels considerably lower than those described below. Separate addition of the enzyme with noncovalently linked Tat peptides did not result in cell staining (data not shown). Cells treated with Tat conjugates consistently revealed intense cellular staining (Fig. 1 *b*, *c*, *e*, and *f*). Staining was predominantly surface-associated after short, 0- to 20-min incubation periods with progressive accumulation in intracellular staining over 30 min to 6 hr. Incubations of 18 hr yielded highest levels of staining, and subsequent chase periods of up to 24 or 48 hr without conjugate still resulted in detectable intracellular activity with a concomitent decrease in surface staining. A large proportion of the intracellular staining appeared to be punctate, even at late tim points, suggestive of endosomes/lysosomes, but there was significant diffuse cytoplasmic, nuclear, and nucleolar staining in all experiments, specially at higher doses and later time points (Fig. 1 *c* and *f*). The nuclear/nucleolar localization (Fig. 1 *c*, *h*, and *i*) is consistent with studies of fluorescently labeled free Tat (ref. 20; S.F., unpublished data) and probably results from the nuclear localization sequence and RNA binding activity of Tat pro-

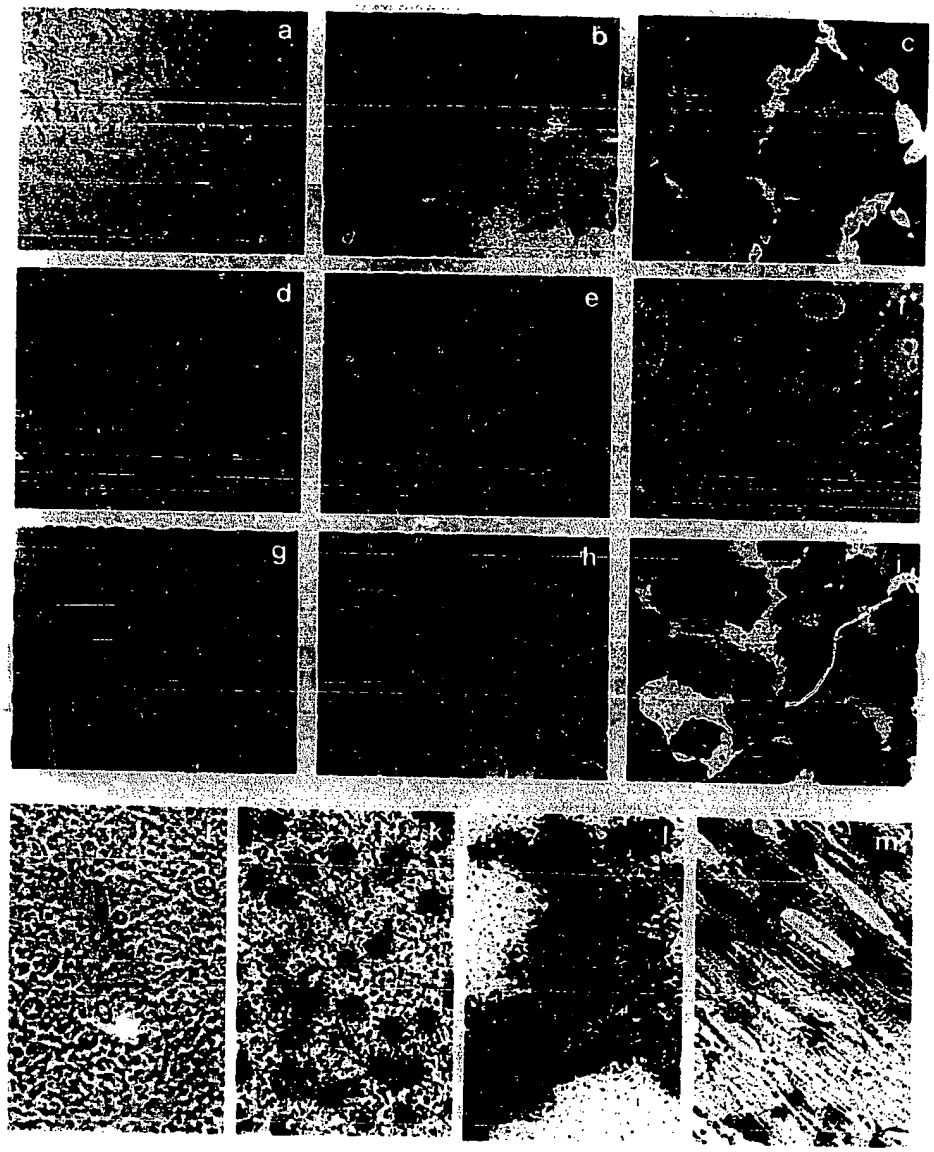

FIG. 1. Tat-mediated delivery of β-galactosidase and HRP in tissue culture and mouse models. HeLa cells (*a–i*) were grown under standard tissue culture conditions and then incubated with control SMCC-activated β-galactosidase (*a*) or HRP (*d*) or with Tat-β-galactosidase (*b*, *c*, and *g–i*) or Tat-HRP (*e* and *f*) conjugates. Incubations were with 20 μg of test compound per ml of Dulbecco's modified Eagle's medium containing 10% serum for 18 hr. All data are in the absence of added chloroquine with the exception of *g*, which shows cotreatment with 80 μM chloroquine. Tat conjugates used were prepared with Tat-(37–72) peptide with the exception of *i* in which Tat-(1–72) was used. Mice were injected intravenously with 200 μg of Tat-(37–72)-β-galactosidase (*j–m*) and sacrificed 20 min later; thin frozen sections of major organs were prepared. (*j*) Kidney. (*k*) Liver. (*l*) Spleen. (*m*) Heart. Cells and sections were fixed prior to development of enzyme chromogenic substrates as described and then photographed with a Zeiss Axiovert 405M photomicroscope. [×75 (*a*, *b*, *d*, *e*, and *g*), ×150 (*h*, *i*, and *j–m*), and ×500 (*c* and *f*).]

tein (23, 24). Similar results were obtained with Tat-enzyme conjugates with either Tat-(1–72) (Fig. 1*i*) or Tat-(37–72) (Fig. 1*c*), although the reagents prepared with the latter peptide typically possessed improved solubility and storage characteristics. Repeated washing of treated cells before fixation did not reduce the cell-associated enzyme activity, but mild trypsinization abolished the surface staining.

β-Galactosidase activity was also measured quantitatively by using the substrate *o*-nitrophenyl β-D-galactopyranoside. After overnight incubation with the Tat-β-galactosidase conjugate (40 μg/ml), cells were trypsinized, and trypsin sensitive and -insensitive activities were determined. Typically 5×10^6 molecules of enzyme were bound per cell, and of this material at least 20% was internalized as judged by resistance to trypsin treatment—i.e., 10^6 molecules per cell. A striking feature of the enzyme delivery was that all cells in each experiment were stained and that uptake could be demonstrated in all cells tested (including HeLa, COS-1, Chinese hamster ovary, H9, NIH 3T3, and primary human keratinocytes and umbilical vein endothelial cells).

Experiments with enzyme conjugates prepared with either poly(L-lysine) or poly(L-arginine) in place of Tat resulted in surface-associated staining that was mostly trypsin accessible, with little obvious intracellular activity (data not shown). In these experiments the development times of the chromogenic substrates for Tat-β-galactosidase were minutes to a few hours. When a β-galactosidase cDNA driven from a simian virus 40 promoter was transfected into cells, expression levels required several hours or overnight development, and staining never reached the levels reported here. This difference must reflect the relatively large levels of conjugate delivered into cells.

Since optimal uptake/long terminal repeat (LTR) activation of Tat required the presence of the lysosomotropic agent chloroquine to reduce protein degradation (19), enzyme conjugate uptake was examined in the presence or absence of chloroquine. Equivalent staining patterns and intensities were observed over a range of chloroquine concentrations (Fig. 1 *b* and *g*), and quantitative analysis of β-galactosidase activity in treated cells showed no more than a 2-fold increase in activity with chloroquine (data not shown). This is in comparison to Tat activation of the HIV-1 LTR, where chloroquine induction is 500- to 5000-fold.

To examine the *in vivo* biodistribution and potential delivery activity of this method, we injected Tat-β-galactosidase intravenously into mice. After various time periods, animals were

sacrificed, tissues were harvested, and thin frozen secti ns were prepared for analysis. Hist logical staining sh wed very high tissue-associated activity in the liver (Fig. 1*k*), spleen (Fig. 1*l*), and heart (Fig. 1*m*). Low but detectable staining was seen in skeletal muscle and lung, little r n staining was seen in the kidney, and n ne was seen in the brain. Analysis f stained sections showed that cells surrounding the blood vessels were labeled, with some penetration into surrounding cells and tissues visible. The red pulp in spleen was heavily stained, and there was evidence of Kupffer cells in liver and muscle cells in heart being labeled on examination 30 min after injection. The reasons for the tissue distribution observed are not clear but cannot reflect simply blood flow, given the relatively low level of staining seen in the lung/skeletal muscle, and may reflect qualitative or quantitative differences, or both, in the endothelium of these organs. With the control β-galactosidase, essentially no tissue staining was seen, with only trace levels evident in the spleen. When radiolabeled Tat-(1–72) peptide was administered intravenously, a tissue profile similar to that of Tat-β-galactosidase was seen, except for very high levels in the kidney and a much shorter serum half-life for the peptide, presumably reflecting renal clearance (S.F., unpublished data).

Since histological analysis is complicated by the presence f active enzyme on the cell surface and within intracellular vesicular structures, we decided to use reporter cargo molecules whose activity would be translocation dependent. The toxin momordin has been used by Leamon and Low (15) as a reporter molecule to examine cellular uptake that was mediated by folate conjugation and utilized the folate receptor (16). However, by analogy to ricin A chain (25), it is not clear whether this molecule is nontoxic when added to cells simply because it lacks binding activity and whether it may retain a translocation function. This idea is supported by the cytotoxicity of momordin immunotoxins (26). In contrast, the structure/function of PE has been studied in great detail (27, 28), and the translocation activity of the native toxin has been localized to domain II. Therefore, we selected domain III of PE and also RNase A, since both are nontoxic when applied to cells and neither has any known binding or delivery activities. RNase is presumably toxic to cells because of nonspecific degradation of cellular RNA, while PE is known to ADP-ribosylate elongation factor 2, thus inactivating protein synthesis (27). Neither molecule should have any effect upon entry into the endocytic pathway and should only be effective if delivered to the cytoplasm.

Tat conjugates were prepared by using RNase A and purified PE(III), and the relative activity of these enzymes was tested by either an *in vitro* RNA degradation assay or by inhibition of protein translation in a rabbit reticulocyte lysate, respectively (see *Materials and Methods*). At the degree of modification used, one or two Tat peptides per molecule of either RNase or PE(III) (Figs. 2*A* and 3*A*), there was little or no detectable decrease in enzyme activity (Figs. 2*B* and 3*B*). These conjugates were then applied to HeLa cells in tissue culture and tested for the ability to inhibit protein synthesis. IC_{50} ([^{35}S]methionine incorporation) values of 15 μg/ml for Tat-RNase and 7 μg/ml for Tat-PE(III) (Figs. 2*C* and 3*C*) were obtained. The conjugates were visibly cytotoxic, with cells rounding-up and detaching from the plastic surface at either the highest doses or with extended incubation. As was described for the enzyme conjugates above, all cells in a culture suffered morphological effects after conjugate administration, implying delivery to the entire cell population. The control nonconjugated preparations or coaddition of nonlinked Tat peptides with RNase/PE(III) showed n cyt toxicity at equivalent concentrations (Figs. 2*C* and 3*C*). Similar results were obtained with a number f ther cell lines including NIH 3T3 and SAOS-2. While Tat-PE(III) cytotoxicity is less potent than nativ PE, the activity of the PE(III) constructs were also low when tested *in vitro*, perhaps due to

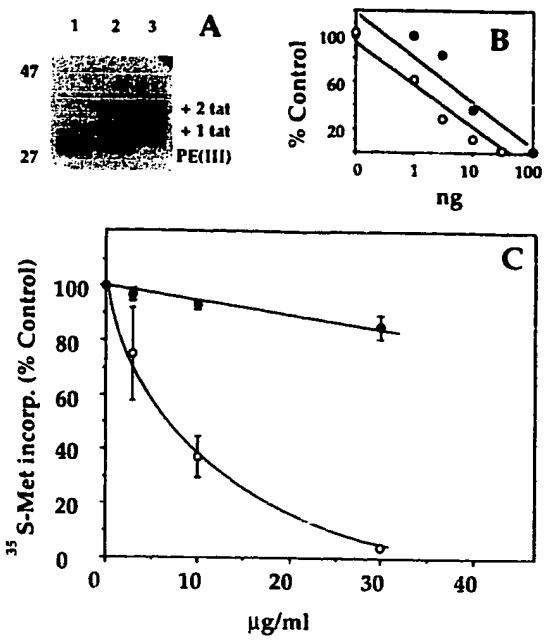

FIG. 2. Tat-mediated delivery of PE(III). PE(III) w. s expressed in bacteria and purified as described. Tat-(37–72) peptide was coupled by using the heterobifunctional cross-linker SMCC, and the control and coupled material were examined by SDS/PAGE. (*A*) Coomassie-blue stained gel. The position of the unconjugated (lane 1) and increasingly conjugated (lanes 2 and 3) complexes and molecular mass standards are indicated. (*B*) Activity *in vitro* of the PE(III) control (●) and Tat-(37–72)-PE(III) (○) was measured by inhibition of protein synthesis of BMV message in a rabbit reticulocyte lysate. Translations were carried out in the presence of [^{35}S]methionine and analyzed by SDS/PAGE and autoradiography. Relative levels of BMV-encoded proteins were determined by densitometry and shown as arbitrary units. (*C*) Cytotoxicity was measured by the inhibition of [^{35}S]methionine incorporation into CCl_3COOH-insoluble material. Cells were incubated with PE(III) control (●) and Tat-(37–72)-PE(III) (○) at the concentrations indicated and as described in text. Experiments were carried out in triplicate, and the results show the average of three independent experiments ± SEM.

the expressio: method used. The lower potency could also reflect decreased binding affinity and/or a lower efficiency of translocation compared with the native full-length toxin. The PE(III) conjugate was equally active in either the presence or absence of chloroquine, whereas 80 μM chloroquine was required to see inhibition with the Tat-RNase conjugate. This concentration of chloroquine alone had little or no effect on cell viability but slightly reduced the protein synthetic rate in cells. Consequently all data shown for RNase is normalized to the appropriate chloroquine-treated control.

In addition to studies with Tat-(37–72), we also analyzed protein delivery with shorter varients [Tat-(37–58) and Tat-(47–58)] conjugated to PE, RNase, and β-galactosidase via cysteine residues at either the N or C terminus of the peptides. All peptides retaining the basic domain of Tat promoted uptake, although there were variations in efficiency that were cargo dependent. In general we have found Tat-(37–72) to be the most consistently successful. Since the basic region of Tat contains a nuclear localization signal (NLS), we tested a basic sequence c nstituting the NLS from simian virus 40 large T antigen. No uptake activity was seen with this peptide conjugated to β-galactosidase (Y.D. and J.S., unpublished data).

The role, if any, of the uptake activity of Tat in the physiology of HIV-1 is not understood. Tat has been suggested to play a role (*i*) in activation of latent proviral LTR activity

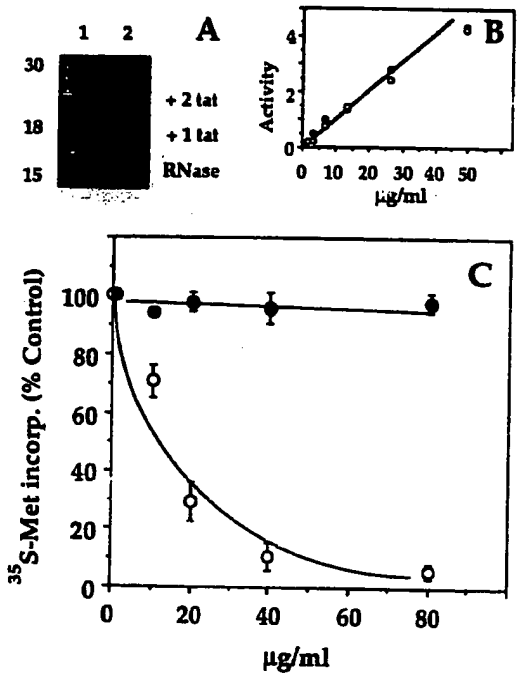

FIG. 3. Tat-mediated delivery of RNase. RNase A was coupled to Tat-(37–72) as described and then examined by SDS/PAGE (*A*). The position of the unconjugated (lane 1) and conjugated complexes (lane 2) and molecular weight standards are indicated. Activity *in vitro* (*B*) and in tissue culture (*C*) of the RNase control (●) or Tat-(37–72)-RNase (○) was determined as described. Experiments were carried out in triplicate, and the results show the average of three independent experiments ± SEM.

and (*ii*) as either a growth factor for Kaposi's sarcoma-derived cells (29) or in the development of this cancer (30). There are also several reports in the literature concerning the intracellular activity or localization, or both, of a number of growth factors including basic and acidic FGF, int2, and interleukin 1 (31–34). These factors either lack a recognizable signal sequence and yet can be secreted or, in some instances, are found in intracellular/nuclear locations. This raises the possibility that a family of factors, including the HIV-1 Tat protein, have gained the ability to enter/exit intact cells and that this function is part of their normal physiological action.

Recently, two laboratories have demonstrated that Tat binds to specific cell surface proteins, raising the possibility that delivery is receptor-mediated (35, 36). Whether these specific interactions are involved in uptake of Tat remains to be determined.

In summary, we have shown that addition of sequences from the HIV-1 Tat protein can confer cellular delivery on at least four diverse heterologous proteins. Histological analysis shows that conjugates bind to the cell surface, are internalized via the endocytic pathway, and must then be able to cross/disrupt a lipid bilayer to gain access to the cytoplasm. Conjugation can be achieved by chemical cross-linking and also gene fusion (J.B., unpublished data), with protein function/delivery retained. Cytotoxicity of Tat-RNase and Tat-PE(III) unambiguously demonstrates cytoplasmic delivery activity by the Tat peptides. Furthermore, we have shown that conjugates gain access to all cell types tested in tissue culture and cells *in vivo*. The chloroquine dependence described for Tat protein was only seen with the RNase conjugate and may reflect the sensitivity of the "cargo" protein to cellular degradati n. However, it is not obligatory for the uptake proces..

This system presents the pportunity to use macromolecular reagents t treat intact living cells and thus access the intracellular environment. Potential uses could include the delivery of peptide/protein inhibitors of intracellular enzymes or transcription factors or the delivery of peptide epitopes to stimulate class I major histocompatibility complex responses.

We thank Richard Tizard for DNA sequencing the various expression vectors used; Sandhya Kalkunte for peptide synthesis; and Alan Frankel, James Rothman, and Fred Taylor for constructive advice and suggestions.

1. Foldvari, M., Mezei, C. & Mezei, M. (1991) *J. Pharm. Sci.* **80**, 1020–1028.
2. Chakrabarti, R., Wylie, D. E. & Schuster, S. M. (1989) *J. Biol. Chem.* **264**, 15494–15500.
3. Connor, J. & Huang, L. (1985) *J. Cell Biol.* **101**, 582–589.
4. Ortiz, D., Baldwin, M. M. & Lucas, J. J. (1987) *Mol. Cell. Biol.* **7**, 3012–3017.
5. McNeil, P. L., Murphy, R. F., Lanni, F. & Taylor, D. (1984) *J. Cell Biol.* **98**, 1556–1564.
6. Renneisen, K., Leserman, L., Matthes, E., Schroder, H. C. & Muller, W. E. (1990) *J. Biol. Chem.* **265**, 16337–16342.
7. Wu, G. Y. & Wu, C. H. (1991) *Biotherapy* **3**, 67–95.
8. Prior, T. I., Fitzgerald, D. J. & Pastan, I. (1992) *Biochemistry* **31**, 3555–3559.
9. Prior, T. I., Fitzgerald, D. J. & Pastan, I. (1991) *Cell* **64**, 1017–1023.
10. Stenmark, H., Moskaug, J. O., Madshus, I. H., Sandvig, K. & Olsnes, S. (1991) *J. Cell Biol.* **113**, 1025–1032.
11. Ishihara, H., Hara, T., Aramaki, Y., Tsuchiya, S. & Hosoi, K. (1990) *Pharm. Res.* **7**, 542–546.
12. Basu, S. K. (1990) *Biochem. Pharmacol.* **40**, 1941–1946.
13. Wu, G. Y. & Wu, C. H. (1988) *Biochemistry* **27**, 887–892.
14. Wilson, J. M., Grossman, M., Wu, C. H., Chowdhury, N. R., Wu, G. Y. & Chowdhury, J. R. (1992) *J. Biol. Chem.* **267**, 963–967.
15. Leamon, C. P. & Low, P. S. (1992) *J. Biol. Chem.* **267**, 1–6.
16. Leamon, C. P. & Low, P. S. (1991) *Proc. Natl. Acad. Sci. USA* **88**, 5572–5576.
17. Wu, G. Y., Wilson, J. M., Shalaby, F., Grossman, M., Shafritz, D. A. & Wu, C. H. (1991) *J. Biol. Chem.* **266**, 14338–14342.
18. Kumagai, A. K., Eisenberg, J. B. & Pardridge, W. M. (1987) *J. Biol. Chem.* **262**, 15214–15219.
19. Frankel, A. D. & Pabo, C. O. (1988) *Cell* **55**, 1189–1193.
20. Mann, D. A. & Frankel, A. D. (1991) *EMBO J.* **10**, 1733–1739.
21. Studier, F. W., Rosenberg, A. H., Dunn, J. J. & Dubendorff, J. W. (1990) *Methods Enzymol.* **185**, 60–89.
22. Melby, E. L., Prydz, K., Olsnes, S. & Sandvig, K. (1991) *J. Cell. Biochem.* **47**, 251–260.
23. Dang, C. V. & Lee, W. M. (1989) *J. Biol. Chem.* **264**, 18019–18023.
24. Calnan, B. J., Biancalana, S., Hudson, D. & Frankel, A. D. (1991) *Genes Dev.* **5**, 201–210.
25. Lord, J. M., Hartley, M. R. & Roberts, L. M. (1991) *Semin. Cell Biol.* **2**, 15–22.
26. Stirpe, F., Wawrzynczak, E. J., Brown, A. N., Knyba, R. E., Watson, G. J., Barbieri, L. & Thorpe, P. E. (1988) *Br. J. Cancer* **58**, 558–561.
27. Fitzgerald, D. & Pastan, I. (1991) *Semin. Cell Biol.* **2**, 31–37.
28. Hwang, J., Fitzgerald, D. J., Adhya, S. & Pastan, I. (1987) *Cell* **48**, 129–136.
29. Ensoli, B., Barillari, G., Salahuddin, S. Z., Gallo, R. C. & Wong, S. F. (1990) *Nature (London)* **345**, 84–86.
30. Vogel, J., Hinrichs, S. H., Reynolds, R. K., Luciw, P. A. & Jay, G. (1988) *Nature (London)* **335**, 606–611.
31. Jaye, M., Howk, R., Burgess, W., Ricca, G. A., Chiu, I.-M., Ravera, M. W., O'Brien, S. J., Modi, W. S., Maciag, T. & Drohan, W. N. (1986) *Science* **233**, 541–545.
32. Auron, P. E., Webb, A. C., Rosenwasser, L. J., Mucci, S. F., Rich, A., Wolff, S. M. & Dinarello, C. A. (1984) *Proc. Natl. Acad. Sci. USA* **81**, 7907–7911.
33. Acland, P., Dixon, M., Peters, G. & Dickson, C. (1990) *Nature (London)* **343**, 662–665.
34. Abraham, J. A., Mergia, A., Whang, J. L., Tumolo, A., Friedman, J., Hjerrild, K. A., Gospodarowicz, D. & Fiddes, J. C. (1986) *Science* **233**, 545–548.
35. Weeks, B., Desai, K., Loewenstein, P. M., Klotman, M. E., Klotman, P. E., Green, M. & Kleinman, K. (1993) *J. Biol. Chem.* **268**, 5279–5284.
36. Vogel, B. E., Lee, S.-J., Hildebrand, A., Craig, W., Pierschbacher, M. D., Wong-Staal, F. & Ruoslahti, E. (1993) *J. Cell Biol.* **121**, 461–468.